

1 **This is a pre-print of**

2 **Barnes S-J. and Ripley, E.M., 2016.** Highly siderophile and strongly chalcophile elements in
3 magmatic ore deposits. In: HIGHLY SIDEROPHILE AND STRONGLY CHALCOPHILE
4 ELEMENTS IN HIGH TEMPERATURE GEOCHEMISTRY AND COSMOCHEMISTRY.
5 Editors J. Havey and J.M. Day Reviews in Mineralogy and Geochemistry 81: 725-
6 774. Available at <http://ring.geoscienceworld.org/content/81/1/725.short>

7 Or upon request directly from me.

8 |
9 **Highly siderophile and strongly chalcophile elements in magmatic ore deposits**

10
11
12
13 **Sarah-Jane Barnes**

14
15 *Sciences de la Terre*
16 *Université du Québec à Chicoutimi*
17 *Chicoutimi, Québec, G7H 2B1 Canada*

18
19 **Edward M. Ripley**

20
21 *Department of Geological Sciences*
22 *Indiana University*
23 *Bloomington Indiana, 47405 USA*

24
25
26
27 **INTRODUCTION**

28 An ore deposit by definition must be economically viable, that is to say it must contain
29 sufficient material at high enough grade to make it possible to mine and process it at a profit
30 (Bates and Jackson 1987). This requires the elements to be collected and concentrated by some
31 phase and for them to be deposited close to the surface of the earth. At the oxygen fugacities
32 found in the crust native Fe is not normally stable and thus the highly siderophile elements
33 (defined as Ru, Rh, Pd, Re, Os, Ir, Pt and Au) cannot behave as siderophile elements except in
34 rare cases such as on Disko Island (Klöck et al. 1986) where the magma is sufficiently reduced
35 for native Fe to be present. However, if mafic magmas become saturated in a base-metal-sulfide
36 liquid the highly siderophile elements behave as highly chalcophile elements (Table 1). Thus
37 these elements are generally found in association with base-metal-sulfide minerals which
38 crystallized from a magmatic sulfide liquid, namely pyrrhotite, pentlandite, chalcopyrite,
39 cubanite +/-pyrite. An exception to this is Au. Although Au is strongly chalcophile and is
40 produced as a by-product from many platinum-group element (PGE) deposits (Table 2) most
41 primary Au deposits consist of native Au (Groves et al. 1998). These will not be discussed in
42 this chapter.

43 There are many PGE-deposits (i.e., accumulations of PGE minerals and base metal
44 sulfides containing PGE; Bates and Jackson,1987) around the world, but most of these do not
45 constitute PGE **ore** deposits because they are either too small or their grade is too low, or other
46 political or infrastructure factors prevent the economic exploitation of the deposit (Bates and
47 Jackson,1987) For the purpose of this work we have defined PGE ore deposits as those which
48 have significant production (>2% of the annual world production) of Pt or Pd (Fig. 1, data from
49 Cowley 2013 and Mudd 2012). Aside from these deposits Pt and Pd are also produced as by-
50 products from many magmatic Ni-deposits. But the amount from each deposit is small, and in
51 total for all deposits is ~ 2 % of annual world production (Fig. 1). They will not be discussed
52 further, but the behavior of the PGE in these types of deposits is similar to their behavior in the
53 Noril'sk and Sudbury deposits and more details on them can be found in Naldrett (2011).
54 Platinum deposits in zoned complexes, also known as Alaskan or Uralian complexes are not
55 currently mined and will not be covered here. Information on these types of deposits is provided
56 by Augé et al. (2005) and Anikina et al. (2014). Finally a small quantity of Pt (~ 2%, Cowley
57 2013) is produced from alluvial deposits, information on these can be found in Weiser (2002)
58 Tolstykh et al. (2004).

59 The majority of the World's Pt and much of its Pd are produced from the Bushveld
60 Complex of South Africa (Figs.1 and 2). These resources are present in three deposits; the UG2
61 reef, the Merensky reef and the Platreef (Table 2). The next most important source of Pd and Pt
62 (Fig. 1) is as a by-product of nickel mining in the Noril'sk area of Russia. These Ni deposits
63 occur in three sub-volcanic intrusions; Noril'sk 1, Talnakh and Kharaelakh (Fig. 3). In fact the
64 Noril'sk deposits produce most of the World's Pd, although that the actual Pd resources are less
65 than those of the Bushveld Complex (Fig. 1, Table 2).

66 In addition to the Bushveld Complex there are three intrusions that are primary producers
67 of Pt and Pd; the Great Dyke of Zimbabwe, the Stillwater Complex of United States and the Lac
68 des Iles Complex of Canada (Figs. 4, 5, 6). The ore deposits in these intrusions are the Main
69 Sulphide Zone, the JM reef and the Roby and Offset Zones respectively (Table 2).

70 In the past the Sudbury Igneous Complex, Canada, (Fig. 7) produced a significant amount
71 of Pt and Pd as a by-product of Ni mining (Table 2). The Sudbury Igneous Complex (Fig. 7) is a
72 unique structure formed as a result of a meteorite impact, which flash melted a mixture of
73 Archean and early Proterozoic crust (Dietz 1964). However, current production is low (Fig. 1)
74 and these resources are now largely mined out. Nonetheless an example of the Sudbury ores will
75 be discussed because in terms of resources it originally represented a major source of PGE
76 (Table 2).

77

78 **CLASSIFICATION OF THE DEPOSITS**

79 Broadly speaking the deposits may be classified based on their location in an intrusion
80 and the amount of base metal sulfide minerals (BMS) present. There are three broad groups;
81 stratiform or reef deposits, contact deposits and Ni-sulfide deposits.

82 **Reef or stratiform deposits**

83 Most primary PGE-deposits (the UG2, the Merensky, the JM reefs and the Main Sulphide
 84 Zone) take the form of laterally extensive narrow (stratiform) layers, of 1 to 3 m thickness, that
 85 contain 3-15 ppm ($1 \mu\text{g g}^{-1}$) Pt+ Pd and occur within the Bushveld, Stillwater and Great Dyke
 86 layered intrusions respectively (Fig. 8). (Workers on economic deposits express the grade of a
 87 deposit in g tonne^{-1} or as ppm: $1 \text{ g tonne}^{-1} = 1 \text{ ppm} = 1 \mu\text{g g}^{-1}$, this chapter will use ppm). In
 88 some places the PGE enriched layer widens to 10-20 m in structures which are termed pot-holes
 89 at the Bushveld reef (Viljoen 1999) and ballrooms in the JM reef (Zientek et al. 2002). With the
 90 notable exception of the UG2 reef, the reefs contain a small amount (0.5-3 wt %) of BMS. Base
 91 metal sulfides are present in the UG2 reef, but the amount is so low ($<0.1 \text{ wt } \%$) that there are no
 92 visible BMS in hand specimen. The reefs are present in a variety of rock types. In the case of
 93 the UG2 the host is a massive chromitite with interstitial orthopyroxene and plagioclase (Barnes
 94 and Maier 2002a, Mathez and May 2005). The rock types in the Merensky reef vary from thin
 95 chromitite seams, through coarse grained melanorite to anorthosite (Kruger and Marsh 1985;
 96 Barnes and Maier 2002b). The JM reef comprises troctolite, olivine gabbro and
 97 anorthosite (Barnes and Naldrett 1985; Zientek et al. 2002; Godel and Barnes 2008). The host
 98 rock of the Main Sulphide Zone is described as a plagioclase orthopyroxenite or bronzitite
 99 (Oberthür 2002; Wilson and Brown, 2005).

100 **Contact deposits.**

102 The term contact deposit has been used to refer to deposits of variable width that are
 103 composed of disseminated BMS found at the margins of intrusions. The Platreef, which occurs
 104 along the northern edge of the Bushveld Complex (Figs. 2 and 8), falls into this group. Strictly
 105 speaking the deposit should not be referred to as a reef because it is not a narrow zone but rather
 106 50 to 100 m thick with variable distribution of PGE across the zone. There is a great deal of
 107 variation in the rock types from pyroxenite to gabbro with minor anorthosite and
 108 peridotites and included in these are xenoliths of the country rocks (Kinnaird 2005; Maier et al.
 109 2008; McDonald and Holwell 2011). The combination of extreme variations in grain size and
 110 textures, the mixture of rock types, and presence of xenoliths with reaction rims around them,
 111 produced a heterogeneous zone referred to as varitextured.

112 Eckstrand (2005) suggested that the Roby Zone of the Lac des Iles Complex should be
 113 classified with the Platreef. The Roby, Offset and Twilight zones consist of varitextured
 114 gabbro containing disseminated BMS and they occur at the contact between the margins of
 115 the intrusion and the homogeneous east gabbro (Fig. 6). Other authors classify the Lac des Iles
 116 deposits as a magmatic breccia e.g., Lavigne and Michaud (2001).

117 **Ni-sulfide deposits**

118 In the Noril'sk area the ores take a number of forms; disseminated BMS, massive BMS,
 119 vein/ breccia/ cupriferous BMS, and low-S-high-Pd-Pt ore (Distler 1994; Torgashin 1994;
 120 Sluzhenikin et al. 2014). Each type will now be briefly described. The disseminated ore is the
 121 main ore type of the Noril'sk 1 intrusion (Sluzhenikin et al. 2014). It occurs in the lower parts of
 122 the intrusion (Fig. 9a) in a varitextured gabbro. Russian geologists use the term taxitic for
 123 this type of texture. The BMS occur both as interstitial amorphous patches and as globules
 124 (referred to as droplet ore). The droplets are 1-4 cm in size and zoned with pyrrhotite-rich bases
 125 and chalcopyrite or cubanite (CuFe_2S_3) rich tops (Czamanske et al. 1992; Barnes et al. 2006) (Fig
 126 10).

127 The main ore type in the Talnakh and Kharaelakh intrusions is massive BMS which
 128 occurs at the lower contact between the intrusions and the country rock (Fig.9b). In many cases
 129 there is a narrow zone of hornfels between the massive BMS and the intrusion. The massive
 130 BMS show a mineralogical zonation similar to that observed in the droplet ore (Fig.9b). The
 131 lower parts and the margins are rich in pyrrhotite and the top or central parts are rich in a number
 132 of Cu-rich sulfide minerals from chalcopyrite to talnakhite [Cu₉(Fe, Ni)₈S₁₆] (Torgashin 1994).

133 Vein/breccia/cupriferous ore occurs in the country rock both above and below the
 134 intrusions and it also occurs cross-cutting the intrusions (Fig. 9b, Torgashin 1994; Sluzhenikin et
 135 al. 2014). The vein ore consists mainly of Cu-rich BMS and takes two forms. In some cases it
 136 consists of veins 2 to 10 cm wide containing massive BMS with sharp contacts with the host
 137 rock. In other cases, such as at the Oktrabr'ysk deposit (Fig.9b), the vein ore occurs towards the
 138 top of the intrusion and in the overlying country rocks as a network of fine anastomosing veins.
 139 This ore is referred to as breccia or cupriferous ore.

140 The low-S-high-Pd-Pt ore is not common. It occurs as narrow discontinuous layers
 141 towards the top of some intrusions (Distler 1994; Sluzhenikin 2011; Sluzhenikin et al. 2014).
 142 The host rock type is gabbro-norite with disseminated chromite (Fig.9a). Generally the rocks
 143 contain ~ 1 wt % BMS.

144 The traditionally the Sudbury ores have been divided into contact ores and offset ores
 145 (Ames et al. 2007; Farrow and Lightfoot 2002). The contact ores consist of massive BMS and
 146 disseminated BMS found at the contact between the intrusion and the country rocks and include
 147 the chalcopyrite-rich massive BMS veins which occur in fractures immediately beneath the
 148 contact ores. The offset ores are found in quartz diorite dikes (Grant and Bite 1984; Lightfoot et
 149 al. 1997). These dikes are 50 to 100 m wide and extend for several kilometers into the country
 150 rocks. The dikes are thought to represent injections of the differentiated impact melt into the
 151 country rocks. Massive BMS occur both at the center and on the margins of the dikes, and occur
 152 where the dikes widen. More recently a new category of deposits has been described in the
 153 country rocks; these are low-S-high-Pd-Pt deposits (Pentek et al. 2008; Tuba et al. 2014).

154 MINERALS HOSTING THE PLATINUM-GROUP ELEMENTS

155 Base metal sulfides

156 The highly chalcophile nature of the PGE suggests that they should partition into a
 157 sulfide liquid and therefore could be present in the BMS (pyrrhotite, pentlandite, chalcopyrite,
 158 pyrite) formed from this liquid. It has long been established that Pd, Rh and Ru can be present in
 159 pentlandite (Cabri 1992 and references therein). However, until the advent of laser ablation ICP-
 160 MS analysis it was difficult to obtain in situ concentrations of all the PGE in BMS. As discussed
 161 below there is now rapidly growing literature on PGE contents of the BMS. We have chosen to
 162 represent examples where both whole rock and mineral analyses are available from the same
 163 samples. This section is not intended as a complete inventory of all the analyses available.

164 In order to facilitate comparison of the mineral data with the whole rock data the mineral
 165 data will be presented in the same fashion as the whole rock PGE data, namely normalized to
 166 primitive mantle and plotted in order of compatibility. More details on the reason for this choice
 167 of this are outlined below in the section on whole rock geochemistry.

168 Pentlandite is the BMS with the highest PGE and Re contents (Table 3). All of the pentlandites
 169 show similar patterns with an increase in concentration from Re to Pd and strong negative Pt
 170 anomalies (Fig.11). Pentlandites from the JM reef are richest in all of the PGE. The other reefs
 171 and Noril'sk pentlandites contain an order of magnitude less PGE. Pentlandites from McCreedy
 172 East and the Roby Zone contain 3 orders of magnitude less Os, Ir, Ru and Rh than the JM reef
 173 pentlandites (Fig. 11, Table 3). The whole rock concentrations of these elements are low at
 174 McCreedy and Roby Zone (Table 4). The magmas that formed the Sudbury deposits and Roby
 175 Zone are thought to have been andesitic in composition and thus contained less Os, Ir, Ru and Rh
 176 than the picritic to basaltic magmas that formed the other deposits. Thus there are less of these
 177 elements in the sulfides. Pyrrhotite is the next most important host of PGE and Re. Pyrrhotites
 178 from the reefs and Noril'sk 1 have higher concentrations of all the PGE than those from
 179 McCreedy East or Roby Zone and once again reflect the difference in whole rock concentrations
 180 (Table 4, Fig.12). Rhenium, Os, Ir, Ru and Rh are present at approximately similar mantle
 181 normalized concentrations and these decrease for Pt and Pd (except at the JM reef where the
 182 pyrrhotite appears to contain some Pd). McCreedy East and Roby Zone pyrrhotites have similar
 183 mantle normalized patterns but at lower levels. The concentrations of all of the PGE are low in
 184 all of the chalcopyrite and the patterns are approximately flat. Complete PGE analyses are
 185 available for pyrite from McCreedy East and in the Roby Zone. It occurs in two forms; in
 186 essentially igneous assemblages, where it makes up less than 5% of the BMS, and in altered
 187 assemblages where it appears to have replaced pyrrhotite and is the most common sulfide present
 188 (Dare et al. 2011; Djon and Barnes 2012). The pyrites show similar patterns to the pyrrhotite
 189 patterns both in level and shape (Fig.11), except that the pyrites from the unaltered assemblage at
 190 McCreedy East are richer in Ir, Os and Ru and Rh than the pyrrhotite. Pyrite is present in the
 191 Main Sulfide Zone and the Platreef and is known to contain PGE (Oberthür et al. 1997) however
 192 complete PGE analyses are not available at present.

193

194 **Platinum-group minerals**

195 A detailed list of the 109 known platinum-group minerals (PGM) may be found in Cabri
 196 (2002) and PGM are also described in another chapter of this publication (O'Driscoll and
 197 González-Jiménez 2015). Here only a brief mention of the main types of PGM found in PGE
 198 deposits will be presented. For the Merensky and UG2 reefs reviews of the PGM are provided
 199 by Kinloch (1982), McLaren and de Villiers (1982) and Cawthorn et al. (2002). Platinum and Pd
 200 are mainly hosted by Pt and Pd sulfides (cooperite and braggite), the next most common hosts of
 201 Pd and Pt are bismuthotellurides (merenskyite, kotulskite, michenerite, moncheite). Arsenides
 202 and stannides (sperrylite and rustenburgite) are minor hosts of Pt. Close to the potholes the
 203 mineralogy is different with FePt alloys being common and sulfides less common (Kinloch
 204 1982; Cawthorn et al. 2002). In the case of the Platreef the mineralogy is similar, but
 205 bismuthotellurides are more common than sulfides (Holwell and McDonald 2007). The common
 206 PGM of Rh and Ir are sulfarsenides (hollowingworthite-irarsite series). In the UG2 reef Junge et
 207 al. (2014) found that Os and Ru are mainly found in laurite, Pt is present in Pt-Fe alloy and
 208 cooperite-braggite whereas Pd, Rh and Ir are largely present in pentlandite. In contrast Penberthy
 209 et al. (2000) in their study of the reef report Rh and Ir occur as sulfides in combination with Cu
 210 and Pt in malantite-cuprorhodosite.

211 In the JM reef of the Stillwater complex the PGM mineralogy is similar to that of the
 212 Merensky reef consisting of Pd and Pt sulfides followed by Pd-Pt bismuthotellurides (Zientek et
 213 al. 2002; Godel and Barnes 2008). In contrast the Pd and Pt PGM of the Main Sulfide Zone of
 214 the Great Dyke are largely bismuthotellurides with sulfide making up <13% of the PGM.
 215 Arsenides of Pt, Rh and Ir are common throughout the complex, but are more common in the
 216 southern part of the Dyke than the northern part (Oberthür 2002).

217 There is a large literature on PGM of the Noril'sk-Talnakh ores. Kozyrev et al. (2002)
 218 gives an overview and Sluzhenikin et al. (2011) an update. The PGM present are similar to those
 219 reported from the PGE reef deposits. The main PGM from the ores of the Noril'sk 1 intrusion
 220 are Pt and Pd stannides (rustenburgite and atokite), FePt alloys (isoferroplatinum), Pt, Rh, and
 221 Ir arsenides, (sperrylite and hollingworthite). The composition of the PGM in the massive ores
 222 varies with the type of ore. The pyrrhotite (Cu-poor ore) contains mainly FePt alloy and
 223 sperrylite. The Cu-rich ore contains a wider variety of PGM, mainly Pt sulfide, Pt arsenide, Pt
 224 stannide (rustenburgite and niggliite), FePt alloy, Pd stannides (atokite and paolovite) and Pd
 225 bismuthide (sobolevskite).

226 Farrow and Lighfoot (2002) summarize the PGM mineralogy at Sudbury as follows. The
 227 PGM assemblage at Sudbury is dominated by Pt and Pd bismuthotellurides. The next most
 228 common group of Pd minerals is antinomides (sudburyite and mertierite). Apart from the
 229 bismuthotellurides Pt is hosted mainly by sperrylite in deposits on the south side of the Sudbury
 230 intrusion and by the stannide niggliite in deposits from the north side of the intrusion. Rhodium
 231 and Ir occur as hollingworthite and irarsite in deposits from the south side of the intrusion.

232 **Chromite**

233 Experimental work has shown that Os, Ir, Ru and Rh are compatible in both magnetite
 234 and chromite whereas Pd, Pt and Re are not (Capobianco et al. 1994; Righter et al. 2004; Brenan
 235 et al. 2012). Laser ablation work has shown that in volcanic rocks the IPGE and Rh are present in
 236 chromite phenocrysts in solid solution (Locmelis et al. 2011; Pagé et al. 2012; Park et al. 2012)
 237 whereas the concentrations of Pd, Pt and Re are less than detection levels. Furthermore
 238 chromites in the marginal rocks of the Bushveld contain IPGE and Rh apparently in solid
 239 solution (Pagé and Barnes 2013). All of the volcanic chromites contain 5 to 100 ppb (ng g^{-1})
 240 each of Os, Ir and Rh and 100 to 500 ppb Ru and thus could be a significant host for these
 241 elements in ore deposits. However we have analyzed the chromites from the UG2 and
 242 Merensky reefs and they contain less than detection levels of all the PGE and Re (Godel 2007)
 243 and do not appear to host the IPGE and Rh.
 244

245 **Mass Balance**

246 The proportion of each element in each mineral is important both for petrogenetic studies
 247 and for metallurgical work. Petrogenetic studies concentrate on how each element came to be
 248 hosted in each mineral. These studies require textural information and are necessarily concerned
 249 with individual hand-specimen sized samples. Metallurgical studies consider the mill feed and
 250 report on large bulk samples and focus on maximizing the recovery of the economically
 251 important elements (mainly Pt and Pd). The methodology required to optimize the results is
 252 different for the different types of study. This chapter is concerned with the petrogenesis and will
 253 consider the results based on individual samples and their textures.

254 Although to date the petrogenetic studies have been based on small sample sets they do
 255 show similar trends (Fig.13). Rhenium, Os, Ir, Ru and Rh are hosted in large part by a
 256 combination of pentlandite and pyrrhotite in the unaltered ores and by pyrite and pentlandite in
 257 altered ores. Pentlandite is the only base metal sulfide mineral to host significant amounts of Pd.
 258 The amount of Pd hosted by the pentlandite versus the amount of Pd in PGM is variable, at some
 259 deposits (Noril'sk 1, Merensky and JM reefs) most of the Pd is in the pentlandite. In contrast in
 260 the Roby Zone most of the Pd is in PGM. In all cases that have been examined so far very little
 261 of the Pt and Au are present in BMS. In most cases the Pt is present in platinum-group minerals.
 262 Detailed studies of Au minerals were only made at McCreedy East and Noril'sk and in these
 263 cases Au was found to be present largely as native Au (Dare et al. 2011, 2014; Sluzhenikin 2011)
 264 with minor amount as electrum.

265 GEOCHEMISTRY

266 Introduction

267 The grade of Pt and Pd in the PGE dominated deposits are in the 2 to 15 ppm range with
 268 Ni and Cu values of ~ 1000 ppm (Table 2). The concentrations of Au and the remaining PGE
 269 are generally at the 0.01 to 0.5 ppm level (Tables 2 and 4). Within the deposits the concentrations
 270 may vary considerably. In Ni sulfide deposits the combined Ni and Cu concentrations are
 271 generally around 2 wt % (Table 2). The Pd and Pt contents can vary from quite low values such
 272 as those found at Sudbury, <1 ppm to the high values found in the Noril'sk deposits, 4 ppm
 273 Pd+Pt.

274 Normalization to mantle or chondrite?

275 The PGE data are generally presented on a line graph where the metals have been divided
 276 by mantle or chondrite values. Traditionally the order of the elements is from relatively
 277 compatible elements on the left side (Ni, Os, Ir, Ru, Rh) to relatively incompatible on the right
 278 side (Pt, Pd, Au, Cu). This is in contrast to the practice in lithophile element geochemistry where
 279 the incompatible elements are plotted on left side and compatible on the right. The choice of
 280 whether to normalize to chondrite or mantle values depends on the specific application of the
 281 diagram. During separation of the earth's core from the mantle, PGE partitioned preferentially
 282 into the Fe-Ni core, leaving the mantle depleted in PGEs relative to Ni and Cu (Walker 2009).
 283 Therefore, the patterns for all mantle-derived magmas normalized to chondrite values tend to be
 284 depleted in PGEs relative to Ni and Cu. Consequently, normalizing the data to chondrite values
 285 always produces trough patterns depleted in PGE.

286 Nickel and PGE deposits are thought to form when a sulfide liquid segregates from
 287 mantle derived magma (Naldrett 2004). Therefore normalization to primitive mantle values is
 288 more useful in deducing the history of the formation of a deposit. The PGEs have much higher
 289 partition coefficients between silicate and sulfide liquid than Ni or Cu (Table 1). Therefore, the
 290 first sulfide liquid to segregate from a magma will be rich in PGE, and if normalized to mantle
 291 values, will have normalized Ni values approximately in line with Os and Ir, and normalized Pd
 292 values in line with Cu (e.g., disseminated BMS from the Kharaelakh and Talnakh intrusions,
 293 Fig.13). The silicate liquid from which this sulfide liquid segregated will be PGE-depleted and
 294 any sulfide liquid that subsequently forms from it will also have a PGE-depleted pattern and not
 295 be capable of forming a PGE ore deposit. In order to avoid confusion between depletion due to

296 core separation and depletion due to sulfide segregation we normalize data to primitive mantle
297 values (Lyubetskaya and Korenaga 2007).

298 **Recalculation to 100 % Sulfides or whole rock.**

299 On mantle-normalized diagrams, metal values can be plotted as whole-rock values,
300 however in Ni-deposits the sulfide contents vary from 1 to 90 %. Therefore in order to compare
301 rocks with different sulfide contents many authors recalculate the metal abundances to 100
302 percent sulfide (i.e., the metal tenor of the sulfide). The mineralogy observed in a magmatic
303 sulfide under crustal conditions is essentially pyrrhotite, pentlandite, and chalcopyrite (+/- minor
304 pyrite +/- cubanite). In rocks where the bulk of the BMS are pyrrhotite, pentlandite, and
305 chalcopyrite, the concentration of an element in the sulfide fraction maybe calculated using the
306 formula

$$307 \quad C_{(100 \text{ percent sul})} = C_{wr} * 100 / [2.527 * S + 0.3408 * Cu + 0.4715 * (Ni - Ni_{sil})] \quad (1)$$

308 Where $C_{(100 \text{ percent sul})}$ = concentration of an element in 100 percent sulfide; C_{wr} = concentration of
309 the element in the whole rock; S, Cu, and Ni = concentration of these elements in the whole
310 rock, in weight percent, Ni_{sil} = Ni in silicates and oxides.

311 This calculation is useful for Ni-deposits and for the Ni-deposits the mantle normalized
312 whole rock values have been recalculated to 100 % sulfides. However, its application to PGE
313 dominated deposits with their low S content is questionable because at many localities the
314 presence of metal alloys or abundant millerite and bornite or the alteration of pyrrhotite and
315 pentlandite (e.g. in the UG2 and Merensky reef, Li et al. 2004; High Grade Zone Lac des Iles,
316 Djon and Barnes 2012) suggest that the assemblages do not represent primary igneous BMS.
317 Furthermore, the S content of reef rocks are very low thus the recalculation factors are large
318 which magnifies errors. Therefore we will not recalculate data from PGE dominated deposits to
319 100 % BMS.

320 ***Mantle normalized plots of reef type deposits.*** The mantle normalized metal patterns of the
321 Merensky, the UG2 and the Main Sulfide Zone show strong enrichment in all of the PGE relative
322 to Ni and Cu (Figs. 14a and b) with Pt and Pd (Pd-group PGE, PPGE) 10 to 100 times higher
323 than Cu and Os, Ir and Ru (Ir-group PGE, IPGE) approximately 10 to 100 times higher than Ni
324 giving the overall the patterns an arch shape. Furthermore the PPGE are enriched over the IPGE,
325 with Pd/Ir of 5 to 35 (Figs. 15a and b). There appears to be a relationship with the amount of
326 chromite present and the IPGE plus Rh content of the reefs, with the UG2 reef containing higher
327 levels of IPGE and Rh than the other reefs (Table 4, Fig. 14b) and within the Merensky reef the
328 chromite rich layers are richer in IPGE and Rh than the reef as a whole (Figs. 14a, b). The shape
329 of the JM reef mantle normalized pattern is slightly different (Fig. 14c). It is enriched in PGE
330 relative to Ni and Cu as in the case of other reefs, but is much more enriched in PPGE than IPGE
331 with higher Pd/Ir (660).

332 Concentrations of the PGE vary across the reefs. In the UG2, the Merensky and the JM
333 reefs the highest PGE concentration tend to be found at towards the upper and lower parts of the
334 reefs (Cawthorn et al. 2002; Maier and Barnes 2008; Zientek et al. 2002). In the Great Dyke the
335 lowest parts of the reef are richest in Pt, followed by Pd, followed by Ni and Cu (Oberthür 2002;
336 Wilson and Brown 2005).

337 ***Mantle normalized plots of contact type deposits.*** The grade and shape of patterns from the
 338 Platreef vary along strike, with most deposits not being economic (Kinnaird 2005; Maier et al.
 339 2008). The highest grade mineralization at surface in the Platreef is found at Sandsloot,
 340 Overysel and Zwartfontein, and here the shape of the PGE patterns is similar to that of the
 341 Merensky reef (Fig.14a), with enrichment of Pd over Cu and the IPGE over Ni. Some workers
 342 have suggested that the Platreef grades into the Merensky reef down dip and into the intrusion
 343 (Maier et al. 2008 2013) and thus the similarity in the shape of the patterns is reasonable.

344 Despite some similarities in the outcrop and textures the metal patterns of the Roby and
 345 Twilight Zone of the Lac des Iles Complex do not resemble those of the Platreef (Figs. 14a and
 346 c). The Lac des Iles ore zones show a strong enrichment of Pd over Cu, similar to the JM reef of
 347 the Stillwater complex and an enrichment of Pd over Pt. The ores are even more depleted in
 348 IPGE and Rh than the JM reef resulting in very high (7500) Pd/Ir and Ni is enriched relative to
 349 the IPGE (Fig.14c).

350 ***Mantle normalized plots of Ni-deposits.*** The mantle normalized plots for the disseminated BMS
 351 from the Noril'sk area are fairly steep (Fig.12) with high Pd/Ir (220-350). The concentrations of
 352 the metals in the disseminated BMS of the Talnakh and Kharaelakh intrusions and the PGE are
 353 not enriched relative to Cu and Ni with Pd approximately in line with Cu and Ir approximately in
 354 line with Ni. In contrast the Noril'sk 1 disseminated BMS are richer in PGE than the Talnakh
 355 and Kharaelakh BMS by an order of magnitude and show a strong enrichment of Pd over Cu
 356 (Fig.12). The mantle normalized metal patterns for the Sudbury disseminated BMS is similar to
 357 the Talnakh and Kharaelakh BMS from Ni to Rh, but not as rich in Pd, Pt and Cu and
 358 consequently has lower Pd/Ir (54).

359 The composition of the massive sulfides at both Noril'sk and Sudbury reflects variations
 360 observed in the mineralogy with the ores with high concentrations of chalcopyrite and cubanite
 361 being Cu-rich and those rich in pyrrhotite being Cu-poor. The Cu-poor ore is the more common
 362 type and is poorer in Pt, Pd and Au (Table 4). Therefore the Cu-poor massive sulfide have flatter
 363 mantle normalized metal patterns than the disseminated BMS with Pd/Ir of 30 to 150 and slight
 364 negative Pt anomalies (Fig.12). The Cu-rich massive BMS from both Noril'sk and Sudbury are
 365 depleted in IPGE and Rh and enriched in Pt, Pd and Au, consequently the patterns are extremely
 366 steep (Fig.12), with Pd/Ir that exceed 17 000. The vein/breccia samples from the Kharaelakh
 367 intrusion have similar compositions to the Cu-rich massive BMS and show extremely steep
 368 patterns similar to the Cu-rich massive ores (Fig.12).

369

370 **Other chalcophile elements.**

371 Platinum-group minerals host most of the Pt and a substantial amount of the other PGE in
 372 all the deposits (Fig.13; Distler et al. 1994; Barnes et al. 2006; Godel et al. 2007; Barnes et al.
 373 2008; Godel and Barnes 2008; Holwell and McDonald 2007; Dare et al. 2011; Rose et al. 2011;
 374 Djon and Barnes 2012; Sluzhenikin et al. 2014). The common PGM contain Te, As, Bi, Sb and
 375 Sn (TABS) as major elements and thus may play an important role in collecting PGE. All of
 376 these elements are chalcophile, but only Te may be described as strongly chalcophile (Table 1).
 377 For the PGE dominated deposits there is very little data available for these elements because of
 378 the difficulty in determining them in silicate rocks (They are present only at very low levels,

379 which requires that the analyses are carried out by solution work; but they are volatile, which
 380 means the dissolution must be done at moderate to low temperatures to prevent loss of these
 381 elements). There has been a large study at the JM reef (Zientek et al. 1990) which gave values in
 382 the 0.01 to 2 ppm range. For the Merensky reef, the UG2, the Platreef and Roby Zone there is a
 383 little data available and these values are also in the 0.1 to 2 ppm range (Table 5). For the Main
 384 Sulfide Zone no data there is no data available. When the elements are normalized to mantle
 385 and plotted in order of compatibility with MORB (Fig. 15a) the patterns increase from
 386 approximately twice mantle at Sn and Sb to around one hundred times mantle at Te. (Fig.15b).

387 In the massive BMS the concentrations of TABS are higher than in the PGE dominated
 388 deposits and are in the 1 to 100 ppm range (Table 5). As in the case of the PGE there is a
 389 variation in concentrations with ore type - the Cu-rich ores contain higher concentrations of
 390 TABS than the Cu-poor ores. Furthermore, the Cu-rich ores have steep TABS patterns than the
 391 Cu-poor ores (Figs. 15c and d).

392 INTERPRETATION

393 Composition of the silicate melt

394 It is generally accepted that the Ni-sulfide ore deposits are formed by collection of the
 395 metals from a mafic or ultramafic magma by a su

396 lfide liquid (Naldrett 2004). This model can also be applied to PGE dominated deposits,
 397 although there is a school of thought (e.g. Boudreau and Meurer 1999) that suggests that in the
 398 case of PGE dominated deposits the PGE partition into a late magmatic fluid and that the BMS
 399 and PGM currently found in the deposits precipitate from this fluid. In either case the question
 400 arises as to whether the magmas which formed the deposits were exceptionally enriched in PGE
 401 when compared with most mafic magmas.

402 The Noril'sk deposits are found in sub-volcanic intrusions of the Siberian flood basalts
 403 and the concentrations of the PGE in Siberian basalts (squares on Fig.16a) are similar to the
 404 concentrations reported for basalts and komatiites from the literature (circles Fig.16). For the
 405 Bushveld there are a series of dykes and sills found around the intrusion that are thought to
 406 represent the initial magmas (Sharpe and Hulbert 1985; Barnes et al. 2010). There is a long
 407 standing unresolved debate as to how much crustal contamination these magmas have
 408 experienced versus how much the sub-continental lithosphere has contributed to the magmas
 409 (Kruger 1994; Harmer and Sharpe 1985; Harris et al. 2005; Richardson and Shirey 2008). The
 410 magmas (stars and crosses on Fig.16b) appear to have Pd contents similar to most basalts and
 411 komatiites. The Pt contents, however, are slightly higher than most basalts and komatiites. The
 412 composition of the sills and dikes associated with Stillwater complex are similar to the Bushveld
 413 magmas in terms of major elements (Helz 1995). Unfortunately many of the samples contain a
 414 large amount of BMS and are thus not suitable for estimating the initial PGE content of the
 415 magmas. Samples with S contents less than 3000 ppm (these include all of the magma types
 416 thought to have formed the Stillwater Complex, Zientek et al. 1986)) have Pt and Pd values in
 417 the 1 to 20 ppb range (crosses on Fig.16c) similar to basalts and komatiites. There are no PGE
 418 analyses of chill rocks for the Great Dyke or Lac des Iles complexes. It has been suggested that
 419 the composition of the Great Dyke magma was komatiite (Wilson and Brown 2005) and the
 420 magma of the Roby Zone was andesitic (Barnes and Gomwe 2011). To summarize, for the
 421 intrusions where data is available there is no evidence that the magmas were particularly

422 enriched in PGE, although the Bushveld parental magma is slightly richer in Pt than most
423 magmas.

424 The composition of the magmas thought to have formed the intrusions that host the PGE
425 and Ni-deposits range from komatiitic to andesitic. Whereas the Pt and Pd contents of these
426 magmas are fairly similar (1 to 20 ppb, Fig.16a) the IPGE and Rh contents might be expected to
427 be very different because these elements tend to be moderately compatible. Variations in the
428 IPGE and Rh contents of the magmas may explain, in part, the different shapes of the metal
429 patterns from PGE deposits. Komatiites generally have Ir contents in the 1 to 2 ppb range
430 whereas basalts and andesites have much lower contents in the 0.01 to 0.1 range (Fig.16d). Thus
431 komatiitic magmas have Pd/Ir of around 10 and andesitic magmas ratios of 100 to 1000. The
432 BMS that segregate from a komatiitic magma should thus be expected to have a much lower
433 Pd/Ir than the BMS formed from an andesitic magma. This may in part explain why the Great
434 Dyke reef has Pd/Ir of 25 whereas the Lac des Iles deposits have a ratio of ~7000.

435 Although differences in magma compositions can explain some differences in the metal
436 patterns they are unlikely to explain the enrichment in Os, Ir, Ru and Rh in the chromitite layers
437 of the Merensky reef relative to the silicate parts of the reef because one would expect that the
438 magma composition was similar through-out the reef. The majority of the Os, Ir and Ru in the
439 chromitite are found in laurite (Prichard et al. 2004; Godel et al. 2007; Junge et al. 2014). Many
440 authors suggest that the laurite crystallized from the magma before sulfide saturation occurred
441 and was included in the chromite thereby enriching the chromite layers in these elements (e.g.
442 Merkle 1992). However, the laurite in the Merensky reef is not enclosed in chromite; it is
443 associated with BMS and thus does not support this model (Prichard et al. 2004).

444 **Saturation of the magma in a sulfide liquid**

445 Once the magma has been emplaced into the crust it must become saturated in a sulfide
446 liquid (dominantly FeS) in order for it to collect the PGE. Li and Ripley (2009) reviewed the
447 published work on the factors leading to the saturation of magmas in a sulfide liquid. In
448 summary, the factors that lead to the saturation include: i) a rise in pressure, ii) a fall in
449 temperature, iii) a change in magma composition (in particular a drop in Fe-content or an
450 increase in SiO₂), iv) an increase in fO_2 , and v) a decrease in fS_2 . Li and Ripley (2009)
451 developed an empirical equation to estimate the S concentration of a magma saturated in sulfide
452 liquid,

453 $\ln X_s =$

$$454 \quad -1.76-0.474*(10^4/T)-0.021*P+5.559*X_{FeO}+2.565X_{TiO_2}+2.709*X_{CaO} -3.192*X_{SiO_2}-3.049*X_{H_2O} \quad (2)$$

455 where X = the mole fraction of an element, T = temperature in Kelvin, P = pressure in Kb. Li
456 and Ripley (2009) did not find it necessary to include terms for fO_2 and fS_2 because in terrestrial
457 mafic magmas, fO_2 controls the fS_2 , and fO_2 is in turn controlled by FeO and temperature. Thus,
458 by including FeO and temperature in equation 2 the effects of changes in fO_2 and fS_2 are taken
459 into account.

460 Based on recent experimental work Fortein et al. (2015) developed a new equation

461 $\ln S \text{ ppm} = 34.784 - 5772.3/T - 346.54 * P/T - 17.275 * X_{FeO} - 18.344 * X_{TiO2} - 20.378 * X_{CaO}$
 462 $- 25.499 * X_{SiO2} - 20.393 * X_{H2O} - 27.381 * X_{Al2O3} - 22.398 * X_{MgO} - 18.954 * X_{Na2O} - 32.194 * X_{K2O} \quad (3)$

463 The symbols are the same as for equation 2, but pressure is expressed in GPa. This equation
 464 includes more variables for the composition of the magma but both equations give estimates for
 465 the concentration of S required to attain sulfide saturation in komatiitic and basaltic magmas.

466 An important point to note is that S solubility decreases with increased pressure
 467 (Mavrogenes and O'Neil 1999). Thus, although a primary magma might be saturated in
 468 sulfide liquid when it formed in the mantle, as the magma rises and the pressure decreases the
 469 amount of S required to bring about saturation rises, thus primary magmas when they are
 470 emplaced in the crust are S undersaturated. Therefore, in order to bring about saturation either
 471 the temperature of the magma must drop and/or the composition of the magma must change. As
 472 pointed out in Barnes and Lightfoot (2005) ~ 40 % crystallization would be required to bring a
 473 picrite to sulfide saturation and Barnes et al. (2009) calculate that ~17 % crystallization would be
 474 required to saturate the initial Bushveld magmas. Li and Ripley (2009) and Ripley and Li (2013)
 475 provide detailed calculations on this approach and its implications. The main conclusion are that
 476 considerable crystal fractionation would be required and this would lower the amount of Ni
 477 available in the magma thus making the formation of Ni-rich magmatic BMS difficult. [The
 478 Platinova reef of the Skaergaard intrusions may be examples of Ni-poor PGE reef formed from
 479 evolved magma (Andersen 2006)]. If we consider intrusions such as the Noril'sk 1 as closed
 480 systems the total amount of S in the magma is too low to produce the amount of S observed in
 481 the deposit. Therefore, the systems must have been open and/or S addition must have occurred.

482 It has long been suggested that reefs in reef type deposits form when the incoming
 483 magma mixes with the resident magma. This abruptly changes the composition and temperature
 484 of the magma, resulting in sulfide saturation (Naldrett et al. 1986). This model was very popular,
 485 being supported by an abrupt change in Sr isotopes and magma composition associated with the
 486 Merensky Reef and to some extent the UG2 reef (Kruger 1994). However, it requires that both
 487 magmas be very close to S-saturation and it is questionable whether magmas have enough S to
 488 generate the reef (Ripley and Li 2013).

489 To form a magmatic Ni-sulfide deposit contamination of the magma by melts of S-rich
 490 crustal rock has long been the accepted model (e.g., Grinenko, 1985; Thériault and Barnes 1998;
 491 Leshner and Burnham 2001; Ripley and Li 2003), although, not all authors are in agreement with
 492 this (Seat et al. 2009). The contamination model is supported by the S isotopic composition of
 493 the ores that indicate the S was derived largely from the crustal rocks (e.g., Noril'sk, Grinenko
 494 1985; Platreef, Holwell et al. 2007; Penniston-Dorland et al. 2008). Assimilation of S-rich
 495 crustal rocks will lower the temperature of the magma and increase the S concentrations, thus
 496 bringing about S saturation.

497 It is not possible to examine the process whereby S from the country rock is transferred to
 498 the mafic magmas at most ore deposits because, as will be outlined below, after contamination
 499 the sulfide liquid is transported from the site of contamination to the site of deposition. The
 500 marginal zones of the Duluth Complex have preserved some examples where there are
 501 convincing examples of in situ assimilation of black shale, leading to local sulfide saturation
 502 (Ripley and Al-Jassar 1987; Thériault and Barnes 1998; Quefferus and Barnes 2015). The
 503 mechanism for this assimilation appears to have involved stopping of country rock. The country

504 rock xenoliths are subsequently heated by magma, causing partial melting and formation of
 505 granitic melt veins (Thériault and Barnes 1998). The exact mechanism for the transfer of S to
 506 the melt is still being investigated, but we speculate that the sulfide minerals in the xenolith melt
 507 and are transferred to the mafic magma by the granitic melt as sulfide droplets. In addition to
 508 lowering the temperature of the magma and adding S, mixing of the granitic melt into the
 509 basaltic magma would lower the FeO and raise the SiO₂ and H₂O content of the melt, thus aiding
 510 sulfide saturation (see equation 2). The addition of melts of crustal rocks, in particular black
 511 shale, to the magma could also add some TABS elements as black shales are rich in these
 512 elements compared with mafic magmas (Table 5, Fig. 15a). Depending on the exact nature of
 513 the assimilant different elements may be enriched in the sulfide liquid and eventually influence
 514 exactly which PGM forms. For example it has long been observed that the PGM from ore
 515 deposits on the south side of the Sudbury Intrusion are rich in As, whereas ore deposits from the
 516 north side contain PGM rich in Sn (Ames and Farrow 2007). In the south there are Proterozoic
 517 sediments present, which are rich in As. In the north the host rocks are Archean granite, which
 518 should contain more Sn than As. The addition of TABS elements from the country rock of the
 519 Platreef has been used to explain variations in PGM assemblages (Hutchinson and Kinnaird
 520 2005).

521 Osmium isotopes are particularly useful for investigating the role of crustal
 522 contamination. More details on the Os isotopic evidence may be found in the Os isotope section
 523 below.

524 **Upgrading of the Sulfides**

525 Various equations have been used to model the composition of a sulfide liquid segregated
 526 from a silicate liquid. The one most commonly used is that of Campbell and Naldrett (1979)
 527 where the concentration of a metal in a sulfide liquid (C_S) is controlled by the concentration of
 528 the metal in the silicate liquid (C_L), the partition coefficient between the sulfide and silicate
 529 liquids (D), and the mass of silicate magma from which the sulfide collects the metal, expressed
 530 as R (mass ratio of silicate to sulfide liquid).

$$531 \quad C_S = C_L D(R+1)/(R+D) \quad (4)$$

532 This equation considers a closed system but as pointed out by Brüggmann et al. (1993) in many
 533 cases, such as where sulfide droplets sink through a magma column or where the silicate magma
 534 is replenished, a variation of the zone refining equation would be more appropriate to model the
 535 sulfide liquid composition

$$536 \quad C_S = C_L(D-(D-1)e^{-(1/DN)}) \quad (5)$$

537 where N = number of volumes of magma with which the sulfide liquid interacted. The results
 538 are similar using either equation, but the zone refining equation produces slightly higher results
 539 for elements with high partition coefficients because the liquid does not become depleted in the
 540 elements.

541 Leshner and Burham (2001) pointed out that when sulfide saturation occurs due to the
 542 mixing of the magma with an external source e.g. addition of country rock equation 3 needs to be
 543 modified and should be

544
$$C_S = D(C_L R + C_A) / (R + D) \quad (6)$$

545 where C_A is the initial concentration of the element in the assimilated material. Leshner and
 546 Burham (2001) also provide equations for cases where more complex processes have occurred
 547 and the reader is referred to this article for such modelling.

548 One difficulty in modelling PGE behavior is that partition coefficients between sulfide
 549 and silicate liquids for these elements are not well established. Whereas it is clear from
 550 empirical work that the partition coefficients are greater than 10 000, experimental work has
 551 yielded mixed results. Early experimental work (e.g. Crocket et al 1992; Fleet et al. 1999) gave
 552 values in the 1 000 to 100 000 range, but these experiments suffered from the presence of PGM
 553 nuggets in silicate glass. The exact composition of the silicate glass could not be reliably
 554 determined due to a lack of analytical techniques that could determine the PGE concentrations in
 555 situ in the glass. Consequently, experimentalists began to estimate the partition coefficients
 556 based on the solubilities of the PGE in haplobasalts. These estimates gave very high partition
 557 coefficients $> 10^7$ e.g. Pruseth and Palme (2004), Fonseca et al. (2011). Recently this approach
 558 has been questioned because the haplobasalts did not contain S and Fe. In experiments where S
 559 and Fe were added the solubility of the PGE changed (Laurenz et al. 2013) thus making the
 560 partition coefficients determined in Fe- and S-free glasses questionable. The latest experiments,
 561 which attempt to address some of these problems (Mungall and Brenan 2014) still produce a
 562 wide range in partition coefficients, for instance the partition coefficient for Pd varies from 57
 563 000 to 536 000 (Table 1). More details on recent experiments can be found in Brenan et al.
 564 (2015)

565 Some workers suggest that PGE are not dissolved in the silicate magmas but rather are
 566 present in “clusters” of PGE and semi-metals or S (Tredoux et al. 1995). When a sulfide liquid
 567 forms the whole cluster could be included in this liquid and the PGE concentrations of the sulfide
 568 liquid will appear be high, although the PGE are still thought to be present in the sulfide liquid as
 569 PGE semi-metal clusters. Therefore in the opinion of these authors it is not possible to reliably
 570 determine partition coefficients for PGE between silicate and sulfide liquid. Possible clusters of
 571 PtAs have been observed in experimental sulfide liquids (Helmy et al. 2013a) and some PGM
 572 found within the BMS of the Merensky reef are interpreted as clusters (Wirth et al. 2013). The
 573 presence of clusters has also been demonstrated in other areas of geology and their effect on
 574 partitioning and crystallization is an active area of research (Teng 2013). At this time a
 575 theoretical framework to quantitatively describe the behavior of clusters has yet to be established
 576 (Teng 2013). Indeed clusters may simply represent the first stage of nucleation of a phase
 577 (Baumgartner et al. 2013). According to Teng (2013) clusters may not represent a paradigm
 578 shift, but rather a deeper understanding of how phases form. Therefore, although clusters of
 579 PGE and semi-metals may very well exist we do not necessarily think that they negate partition
 580 coefficients; presumably with further study just as the effects of S and Fe on PGE solubility have
 581 to be investigated the effects of the various semi-metals will be established.

582 Empirical determinations of PGE partition coefficients based on determinations of PGE
 583 concentrations in droplets of BMS from MORB and glass were initially carried out by Peach et
 584 al. (1990) and yielded results $>12\ 000$ for Ir and >23000 for Pd. Roy-Barman et al. (1998) report
 585 $\sim 48\ 000$ for Os. Patten et al. (2013) used LA-ICP-MS to determine partition coefficients for all
 586 the PGE and calculated minimum partition coefficients in the range of 12 000 to 37 300. In

587 summary, at this time it is not possible to say exactly what partition coefficients of the PGE are
588 beyond observing that they are very high and probably >20 000.

589 Partition coefficients determined by experimental work show that values for Ni and Cu
590 vary between ~ 200 and 2000 depending on magma composition, temperature and fO_2 (Table 1).
591 For the purposes of modelling we shall use empirically determined partition coefficients
592 determined from MORB sulfide droplets (Patten et al. 2013) of 776 and 1334.

593 The flood basalts of the Noril'sk area contain ~100 ppm each of Ni and Cu and ~ 10 ppb
594 Pt and Pd (Lightfoot and Keays 2005). The disseminated BMS recalculated to 100 % sulfides
595 contain between 12 and 15 % Cu and between 5 and 8 % Ni and 30 to 300 ppm Pd (Table 4).
596 These values show that the enrichment factors (C_S/C_L) in the BMS are between 500 and 800 for
597 Ni and 1200 and 1500 for Cu and 3 000 to 18 000 for Pd. The variation in enrichment factors for
598 the different elements indicates that high R-factors are required to produce the ores. At low R-
599 factors e.g. 100 all of the metals are equally enriched at approximately 100 times (Fig.17).
600 Nickel has the lowest partition coefficient and thus can only be enriched to a maximum ~800
601 times (i.e., its partition coefficient). In contrast, Pd with a very high partition coefficient can be
602 enriched to a greater degree provided that the R-factor is high enough, for example an
603 enrichment factor of ~ 3000 is required to model the disseminated BMS of the Talnakh and
604 Kharaelakh intrusions. The Noril'sk 1 intrusion disseminated BMS require an R-factor of at
605 least 30 000 (Fig.17).

606 Modelling of the Sudbury sulfide liquid is a little more difficult because the nature of the
607 silicate liquid is not well constrained. Osmium isotopic work (Walker et al. 1991; Dicken et al.
608 1992) indicates that a large percentage of the melt was continental crust. Assuming that the
609 initial liquid had the composition proposed by Keays and Lightfoot (2004) of ~ 60 ppm Ni and
610 Cu and ~ 4 ppb Pd and Pt, the enrichment factors would be ~1000 for the PGE, 605 for Ni and
611 Cu requiring an R-factor of ~1000.

612 Difference in the partition coefficient of Pd and Cu into a sulfide liquid may be used to
613 deduce the R-factor of magma from which a sulfide segregated (Barnes et al. 1993). Assuming a
614 partition coefficient for Cu of 1 400 and for Pd of 500 000, for $R < 3000$, Cu and Pd will be
615 enriched in the liquid almost equally (Fig.17) and the Cu/Pd of the sulfide will be similar in the
616 silicate thus the mantle normalized patterns will not show an enrichment of Pd over Cu, e.g. the
617 BMS from Talnakh and Sudbury (Fig.12). For $R > 3000$, Pd will be enriched more than Cu, and
618 the mantle-normalized metal patterns will show enrichment in Pd relative to Cu (e.g., Noril'sk 1
619 disseminated BMS Fig.12).

620 Recalculating the composition of the PGE-reef deposits to 100 % BMS may lead to errors
621 due to the mobility of S, however we can use the different Cu/Pd to estimate the R-factors that
622 would be required to form the deposits assuming that neither element has been mobilized. This
623 approach is illustrated in Fig.18. The initial silicate magma is assumed to have contained Cu and
624 Pd contents similar to the B-1 liquid of the Bushveld. When a sulfide liquid segregates from a
625 silicate liquid the Cu/Pd of the sulfide liquid will depend on the R factor, with low R-factor BMS
626 having Cu/Pd similar to the silicate liquid, and BMS with R factors $> 3 000$ having Cu/Pd less
627 than mantle values. Tie lines have been drawn between the composition of the sulfide liquid at
628 $R=100, 1000, 10 000, 100 000$ and a cumulate containing 10 % silicate liquid fraction and 90%
629 cumulate consisting of silicate and oxide minerals, assuming these contain no Cu or Pd, (Fig.18).

630 The Cu/Pd of the Platreef (asterisk) ranges from 1 000 to approximately 3 000 suggesting R-
 631 factors of 1 000 to 10 000. The Pd content of the rocks ranges from 500 to 1100 ppb.
 632 Combining the Cu/Pd with Pd values gives a sulfide content of around 1 % for the Platreef,
 633 which is consistent with the amount of BMS observed in the rocks. The Merensky reef (crosses),
 634 the Main Sulfide Zone (solid stars) and the Roby Zone (open crosses) all have similar Cu/Pd
 635 and Pd contents and plot between R-factors of 10 000 and 100 000, with Pd contents indicating
 636 around 1 % BMS. The amount of BMS indicated in each case is consistent with observed
 637 amount of BMS in the rocks. For the UG2 and JM reefs the position of the UG2 (Y) suggests
 638 sulfide contents of 0.01 to 0.1 % and the JM reef approximately 1 % BMS, consistent with
 639 observations, however they would require extreme R-factors of 1 000 000.

640 The Cu/Pd diagram can also be used for Ni-deposits; sulfide bearing samples from
 641 Talnakh and Kharaelakh intrusions (triangles and circles on Fig.19) plot close to the R=1,000
 642 line and can be modeled as a mixture of silicate cumulate and ~1 to 100% sulfide liquids formed
 643 at an R-factor slightly above 1 000 (Fig.19). The samples from the Noril'sk 1 intrusion
 644 (diamonds) have lower Cu/Pd and plot around the R-factor 10,000 mixing line. These
 645 observations are consistent with the amount of sulfide present in the rock and did not require that
 646 the analyses be recalculated to 100 % BMS. Many of the basalts overlying the intrusions
 647 (squares) have Cu/Pd higher than mantle values (7 000) and are depleted in Pd. They plot along
 648 the model line (dashed) for a silicate liquid that has segregated co-tectic proportions of sulfide
 649 liquid, suggesting that these could be the liquids from which the BMS segregated.

650 The calculations indicate that if sulfide liquid is the collector of PGE and if the
 651 composition of the magmas is similar to normal basalts (an assumption that seems reasonable
 652 because the chills and basalts away from the ore deposits resemble normal basalts) then the
 653 sulfide liquid must interact with a very large volume of silicate magma. This requirement raises a
 654 problem for closed system models. Applying either the Li and Ripley (2009) or Fortin et al.
 655 (2015) equation to the average Noril'sk basalt composition indicates that the basalts attained
 656 sulfide saturation at ~ 1000 ppm S . If this sulfide segregates from the magma in situ then the R-
 657 factor will be ~ 350 (S content at saturation/S content of the sulfide liquid) and yet most deposits
 658 require R-factors of >3 000.

659 The mechanism generally invoked to attain a high R-factor is to argue for an extremely
 660 dynamic system. In the case of Noril'sk 1, Talnakh and Kharaelakh, the intrusions that
 661 contained the BMS can be thought of as conduits through which many pulses of magma may
 662 have been transported. In addition the sulfide droplets themselves may have been formed in a
 663 lower chamber and been transported; during transport they could have collected some metals
 664 from the transporting magma. They could also have been kept in suspension after they were
 665 emplaced and collected some metals from the various pulses of magma that passed through the
 666 system. Rice and Moore (2001) carried out finite element modelling to demonstrate how sulfide
 667 droplets can be held in suspension above an embayment in the footwall of an intrusion.

668 In the case of the Platreef it is argued that sulfide saturation took place at depth and the
 669 BMS liquid were entrained in the magma and emplaced at the margins of the Bushveld Complex
 670 (McDonald and Holwell 2007). During transport BMS could have interacted with large volumes
 671 of magma. Some authors (Maier et al. 202013 and references therein) suggest that the Platreef
 672 changes character down dip and into the intrusion and merges with the Merensky reef away from
 673 the margins of the intrusion. We suggest that possibly the magma with entrained sulfide droplets

674 froze rapidly to form the Platreef at the margins of the intrusion, however further into the
 675 intrusion the incoming magma with entrained droplets had more time to interact with the resident
 676 magma and thus the sulfide droplets had the opportunity to collect more PGE and thus the
 677 Merensky reef has a higher PGE grade than the Platreef.

678 The UG2 and JM reef both present a challenge to a simple sulfide collection model. Both
 679 require extreme R-factors in the 10^5 to 10^6 range (Fig. 18) which one of the authors (ER) regards
 680 as unreasonable. One possible solution is that the sulfide droplets come into contact with sulfide
 681 undersaturated magma and partly dissolve (Kerr and Leitch 2005). The sulfides could for
 682 example form at the top of intrusion and settle downwards into sulfide undersaturated magma
 683 (Holwell and Keays 2014). Due to their very high partition coefficients into sulfide liquid the
 684 PGE would be preferentially retained in the sulfide liquid. Other processes that could have
 685 affected the JM and UG2 reefs are considered in the crystallization of sulfide liquids and sub
 686 solidus sections below.

687

688 **Crystallization of a sulfide liquid**

689 Experimental work has shown that the first phase to crystallize from a sulfide liquid is an
 690 Fe-rich monosulfide solid solution (MSS) and the remaining sulfide liquid becomes enriched in
 691 Cu (Kullerud et al. 1969; Dutrizac 1976; Ebel and Naldrett 1997; Sinyakova and Kosyakov
 692 2009). When the temperature decreases sufficiently ($<900^\circ\text{C}$), the Cu-rich liquid crystallizes as
 693 intermediate solid solution (ISS). The partition coefficient of Ni between MSS and sulfide liquid
 694 is dependent on temperature and fS_2 of the system (Li et al. 1996; Barnes et al. 1997a;
 695 Makovicky 2002; Lui and Brenan 2015). At fS_2 reflecting crustal conditions the partition
 696 coefficient increases from ~ 0.2 at 1100°C to ~ 1 at 900°C . Thus the evolved MSS is richer in
 697 Ni than the first MSS.

698 Natural examples of the crystallization history of sulfide liquids can be observed in
 699 sulfide droplets from MORB. Some have chilled sufficiently rapidly for a quench texture of the
 700 BMS to be preserved showing an intergrowth of MSS and ISS, with a Ni-rich phase between the
 701 MSS and ISS (Fig. 20a). If the crystallization of the liquid proceeds more slowly, then the Cu-
 702 rich liquid separates from MSS in some cases. Indeed both in MORB droplets and at Noril'sk 1
 703 there are sulfide droplets with Cu-rich tops and Cu-poor bottoms preserving the crystallization
 704 history of the sulfide liquid (Figs. 10 and 20b). In the case of some of the massive ores, after
 705 initial crystallization of Fe-rich MSS the Cu-rich fractionated liquid migrates away either into the
 706 footwall or into the overlying rocks as seen in the veins surrounding both the Noril'sk Intrusions
 707 and the Sudbury Igneous Complex. This fractionated liquid crystallizes as an ISS cumulates and
 708 can be seen in some MORB droplets (Fig. 20c).

709 Rhenium, Os, Ir, Ru, and Rh substitute into MSS whereas most other elements do not
 710 (Table 1). Thus, the MSS cumulates (Cu-poor massive sulfides) are enriched in IPGE and Re
 711 relative to the original sulfide liquid and have flatter mantle normalized metal patterns than the
 712 disseminated sulfides (Fig. 12b). These elements are also concentrated in the lower parts of the
 713 Noril'sk sulfide droplets (Fig. 10). Most of the elements aside from Cu, Cd and Zn are also
 714 incompatible with the ISS (Table 1) therefore Pd, Pt and TABS partition into the last liquid.
 715 Because the major elements have all been consumed there is very little of the late liquid and it is

716 generally trapped in the ISS cumulate (Cu-rich ore). Consequently the Cu-rich ores are normally
 717 enriched in; Pt, Pd and TABS and have mantle normalized metal patterns that are much steeper
 718 than the disseminated ore (Figs.12b and c and Figs 15c and d). The fractionated interstitial liquid
 719 will be enriched in Pt, Pd and TABS. It is possible that the liquid becomes saturated in Pd and Pt
 720 bismuthotellurides, antinomides and stannides. Composite rounded grains of mixtures of
 721 bismuthotellurides and stannides are found interstitial to chalcopyrite in the Cu-rich ore at
 722 McCreedy East (Figs.21 a and b). The composite nature of these grains suggests that they cannot
 723 be exsolutions and they have been interpreted as the product of crystallization from the late
 724 liquid (Dare et al. 2014).

725 In some cases the late liquid escapes the ISS cumulate producing a Cu-rich ore depleted in PGE
 726 and TABS and Pd-Pt-TABS-rich liquid. This Pd-Pt-TABS-rich liquid could potentially migrate
 727 into the rocks around the sulfide deposits and form low-S-high-Pd-Pt deposits such as those
 728 found around the Sudbury intrusion (Pentek et al. 2008; Tuba et al. 2014) and in the upper parts
 729 of the Noril'sk intrusions (Sluzhenikin 2011). The Pd-Pt bismuthotellurides which could
 730 crystallize from these liquids solidify at fairly low temperatures (<600 °C, Elliott 1965; Hoffman
 731 and MacLean 1976; Savitsky et al. 1978; Moffatt 1979 a, b). Therefore when there is a structural
 732 adjustment of a cooling cumulate (or possibly even during later metamorphism) the
 733 bismuthotellurides could be readily mobilized and move into fractures and faults and may occur
 734 as isolated grains as seen in the Creighton deposit, Sudbury (Dare et al. 2010 and Fig.21e).
 735 Possibly an extremely fractionated liquid also formed the High Grade zone at Lac des Iles (Djon
 736 and Barnes 2012). One could even suggest that addition of Pd-Pt-TABS liquid to a pre-existing
 737 disseminated sulfide layer formed the JM reef, thus account for the extremely low Cu/Pd ratio
 738 observed in the JM reef, by addition of Pd.

739 **Late magmatic fluids**

740 A number of authors (Boudreau et al. 1986; Boudreau et al. 2014; Pentek et al. 2008;
 741 Tuba et al. 2013) favor a role for late magmatic fluids in the formation of PGE-reefs, the Lac des
 742 Iles deposits and the low-S-high-Pd-Pt deposits. In this model late magmatic fluid partly
 743 dissolves magmatic BMS which have already crystallized. Palladium, and to a lesser extent Pt
 744 dissolve into the fluid. The fluid migrates away from the residual BMS and when the physio-
 745 chemical conditions change the fluid deposits the Pd and Pd. In some case the deposition is in
 746 stratiform layers within the intrusion, these are reefs. In some case the Pd and Pt are transported
 747 out of the intrusion and may form low-S-high-Pd-Pt zones surrounding the intrusions. Boudreau
 748 and Meurer (1999) Hanley et al. (2008) Godel and Barnes, (2008) have suggested that Pd and to
 749 a lesser extent Pt have been added to the JM reef by late fluids. Pentek et al. (2008) Tuba et al.
 750 (2013) argue that the low-S-high-Pd-Pt zones formed around the Sudbury deposits formed in this
 751 way.

752 Fluids derived from late cooling or metamorphism also result in a change in the BMS
 753 present. At Lac des Iles pyrrhotite and pentlandite are replaced with pyrite and millerite (Djon
 754 and Barnes 2012). The pyrite inherits the PGE that were present in the pyrrhotite and thus
 755 contains Re, IPGE and Rh (Fig.11). Millerite contains some IPGE but does not accept the Pd
 756 thus Pd combines with Te, As and Sb to form isolated PGM grains (Fig.21d). Similar
 757 replacements have been observed in Grasvalley prospect in the Bushveld Complex (Smith et al.
 758 2014). In the case of the Platreef the PGM assemblage in the altered ores is richer in arsenides
 759 and antinomides (Hutchinson and Kinnaird 2005).

760 **Subsolidus events**

761 At temperatures $<600^{\circ}\text{C}$, MSS exsolves to form pyrrhotite and pentlandite +/- pyrite and
 762 ISS exsolves to form chalcopyrite, +/- cubanite +/-pyrite. The sulfide minerals that exsolve from
 763 MSS (pyrrhotite and pentlandite) inherit the IPGE and Re which were in the MSS (Fig.11) and
 764 thus the mass balance indicates that these elements are concentrated in pyrrhotite and pentlandite
 765 (Fig., 13). All of the PGE, Re and Au are incompatible with ISS (Table 1) and thus the
 766 chalcopyrite and cubanite which exsolve from the ISS are poor in highly siderophile elements
 767 (Fig.11).

768 Significant amounts of Pd are found in pentlandite, which at first glance is surprising because the
 769 partition coefficient of Pd into MSS is 0.1-0.2 (Table 1) and thus one would not expect
 770 pentlandite which is derived from MSS to contain Pd. None the less some Pd will partition pre
 771 into MSS. Dare et al. (2010) postulated that during exsolution of MSS to pentlandite and
 772 pyrrhotite the Pd diffuses along with the Ni into pentlandite. Dare et al. (2010) and Piña et al.
 773 (2012) showed large granular pentlandites, which from at high temperatures, contain more Pd
 774 than small flame pentlandites. They interprets their observation to be the result of the larger
 775 grains, which formed at higher temperature, as having depleting the MSS in Pd before the flame
 776 pentlandite formed. The pentlandite hosts much of the Pd in massive ores because these are
 777 MSS cumulate and thus the contribution of Pd from the Cu-liquid is limited to the trapped liquid
 778 fraction. Consider for example the case where the original sulfide liquid contains 10 ppm Pd,
 779 then the MSS should contain 1ppm. A MSS cumulate with 90 % MSS will then contain 2 ppm
 780 Pd. One ppm of this in the MSS and 1 ppm in the trapped liquid fraction. The Pd in the MSS will
 781 diffuse into pentlandite during exsolution of the MSS and thus 50% of the Pd will be present in
 782 pentlandite.

783 The diffusion of Pd into pentlandite during exsolution could explain the high Pd content
 784 of the pentlandites formed in MSS cumulates, but it will not explain the tendency for almost 100
 785 % of Pd to be present in pentlandite in BMS thought to represent the sulfide liquid compositions
 786 such as the Noril'sk 1 sulfide droplets (Fig.14),. In this case the pentlandite should contain only
 787 10 to 20 % of the Pd. It is possible that not all pentlandite forms by exsolution. Coarse grained
 788 pentlandite occurs between the pyrrhotite and chalcopyrite or cubanite in the droplets (Fig.10).
 789 Makovicky (2002) describes experiments reported by Distler (1977) where the texture was
 790 reproduced in experiments by cooling a sulfide liquid. The "pentlandite" formed by peritectic
 791 reaction between the fractionated liquid and the MSS. They referred to the pentlandite as "high-
 792 temperature" pentlandite. If this is the origin of the coarse pentlandite in the droplets then Pd
 793 could have partitioned into the "high temperature" pentlandite when it formed from the
 794 fractionated liquid.

795 Not all of the PGE are present in BMS (Fig.13). During cooling and exsolution of the
 796 MSS the solubility of the PGE in the sulfide minerals decreases due the fall in temperature and
 797 the change in S content of the BMS (Makovicky et al.1986; Li et al. 1996) therefore, as the BMS
 798 cool PGM exsolve forming elongate grains within the BMS. For example CuRhPtS exsolutions
 799 develops in pyrrhotite and pentlandite from the Merensky reef (Fig.21c). The formation of PGM
 800 can be enhanced by the circulation of late magmatic fluids or metamorphic fluids which
 801 dissolves some S resulting in a further fall in PGE solubility in the BMS especially at the grain
 802 boundaries (Godel et al. 2007)

803 Subsolidus processes have also been called upon to explain the low S and Cu contents of
 804 the UG2 reef (Naldrett 2011). Naldrett (2011) proposed that originally more BMS were present
 805 than are now observed and as the cumulates cooled there was a diffusion of Fe from the BMS
 806 into chromite which destabilized the sulfide minerals and resulted in S and Cu loss from the
 807 assemblage and in exsolution of laurite from the BMS (Junge et al. 2014). The postcumulate
 808 loss of Cu from the UG2 reef could provide a more reasonable explanation for the low Cu/Pd
 809 than the very high R-factors suggested by a simple sulfide collection model. Prichard et al.
 810 (2004) also suggest S loss explains the PGM mineralogy in the chromite layers of the Merensky
 811 reef.

812

813 **UTILIZATION OF THE Re-Os ISOTOPE SYSTEM IN STUDIES OF MAGMATIC Ni-** 814 **Cu-PGE ORE GENESIS**

815 **Background**

816 Rhenium and osmium may both be concentrated in magmatic sulfide liquids, sulfide
 817 minerals or minerals that are strongly associated with sulfides (e.g. arsenides, bismuthinides,
 818 tellurides), and hence the Re-Os isotope system has been extensively utilized in studies of
 819 sulfide ore genesis. Deposits studied include relatively low-temperature black shale-hosted Ni-
 820 and base metal deposits (e.g. Horan et al. 1994; Pasava et al., 2010), hydrothermal Au and
 821 related sulfide mineralization (e.g., Selby and Zhao 2012), higher-T porphyry Cu-Mo systems
 822 (e.g., Drobe et al. 2013; Barra et al. 2003) and magmatic Ni-Cu-PGE deposits (see reviews by
 823 Lambert et al., 1998 a, b; 1999a). We will briefly review the application of the Re-Os system to
 824 magmatic Ni-Cu-PGE deposits, but stress that the system has applicability far beyond the high-
 825 T realm covered here.

826 All aspects of the Re-Os system that are of importance for geochronology have been
 827 covered in other chapters of this book and will not be repeated here (Day and Harvey, 2015;
 828 Harvey et al. 2015). The direct dating of molybdenite using the Re-Os system is reviewed by
 829 Stein et al. (2001). We will review geochronological applications for several deposits, as
 830 appropriate, below. Our emphasis will be on the application of Re-Os isotope measurements as
 831 indicators of the source of Os in magmatic ore deposits and the degree of crustal contamination
 832 that source magmas have undergone. To this end it is important to review the partitioning
 833 behavior of Re and Os into sulfide and silicate melts, silicate and oxide minerals and metallic
 834 alloys. One of the basic tenets of the Re-Os system is that during partial melting of the mantle
 835 Re is strongly partitioned into the melt, whereas Os is retained in the mantle (e.g., Morgan et al.
 836 1981; Hauri 2002). The high Re/Os ratios developed in the partial melts lead to the production
 837 of radiogenic Os in the crust, and much higher $^{187}\text{Os}/^{188}\text{Os}$ ratios than in the residual mantle.
 838 Mantle-derived magmas that then interact with crust during or after emplacement may be
 839 characterized by elevated $^{187}\text{Os}/^{188}\text{Os}$ ratios. Although the distribution of Re and Os appears to
 840 be well-constrained, the carriers of Re and Os in the mantle remain controversial. Within the
 841 mantle both Re and Os appear to be largely controlled by chalcophile tendencies. Studies by
 842 Mallmann and O'Neill (2007), Brenan et al. (2003), and Righter and Hauri (1998), indicate that
 843 Re may be partitioned into silicate and oxide minerals, but is much more strongly partitioned
 844 into sulfide. Experimental studies by Brenan (2008) and Fonseca et al. (2011) indicate that
 845 $D_{\text{Os}}(\text{sulfide melt-silicate melt})$ is on the order of $10^4 - 10^5$, and $D_{\text{Re}}(\text{sulfide melt-silicate melt})$

846 for basaltic systems is between ~ 400 and 800 (see also Brenan et al. 2015). If sulfide minerals
 847 in the mantle are exhausted during partial melting the high Re/Os values of partial melts can
 848 only be explained if Os is retained in the mantle in residual phases such as Os-Ir alloys (e.g.,
 849 Fonseca et al. 2011). If sulfide minerals are retained, then the results of Brenan (2008) suggest
 850 that Os may be considerably more compatible than Re in residual sulfide, and observed Re/Os
 851 ratios in basaltic partial melts can be produced. Additional studies are needed to better constrain
 852 the sites of Re and Os in the mantle, and particularly the partitioning of Os into residual phases
 853 such as alloys during high degree partial melting of the mantle where sulfide minerals are
 854 completely dissolved in the partial melt. Many studies of magmatic Ni-Cu-PGE deposits are
 855 consistent with Re-enrichment in the crust. Whether this is completely a function of melting
 856 where sulfide is retained in the mantle, the retention of Os in alloys, or local interaction between
 857 mantle magmas and crustal sedimentary rocks where Re may be strongly enriched over Os (e.g.
 858 organic -rich shales) must be determined on a deposit to deposit basis.

859 Examples of the application of the Re-Os isotope system to several Ni-Cu-PGE deposits
 860 are presented below. However, we first review the basic tenets of how the system has been
 861 applied in the evaluation of contamination of mafic and ultramafic magmas. The γ_{Os}
 862 terminology has been defined in other chapters (Harvey et al. 2015), but in brief is the deviation
 863 in $^{187}Os/^{188}Os$ from Bulk Silicate Earth (BSE), taken as either Primitive Mantle or Chondrite, at
 864 the time of interest; $\gamma_{Os} = ((^{187}Os/^{188}Os(\text{sample}) - ^{187}Os/^{188}Os(\text{PM or CH})) / ^{187}Os/^{188}Os(\text{PM or CH}) - 1) * 100$ (see Shirey and Walker 1998 and Carlson 2005). When isochronous behavior is
 865 demonstrated the initial $^{187}Os/^{188}Os$ value is utilized in the γ_{Os} calculation. Gamma Os values
 866 that show significant deviation from 0 typically result from either crustal contamination or
 867 hydrothermal processes involving the transport of Re, Os or both. Derivation of magma from
 868 recycled crust in the mantle or metasomatically enriched lithosphere may also produce negative
 869 or positive deviation from 0, although the number of intrusions with γ_{Os} values near those of
 870 BSE suggests that processes occurring in the crust are of more significance in controlling γ_{Os} .
 871 An isochron diagram is useful for illustrating the effects of these processes. Figure 22 shows a
 872 mantle-derived magma with a low $^{187}Re/^{188}Os$ ratio (mafic magmas may have a wide range of
 873 Re/Os ratios but here we take a value less than 150 as being representative of basaltic magmas),
 874 which interacts with a crustal sedimentary rock with an elevated $^{187}Re/^{188}Os$ ratio. We utilize a
 875 sedimentary contaminant with an age of 1.85 Ga, and mixing between the mantle magma and
 876 the sedimentary contaminant at 1.1 Ga. The choice of initial $^{187}Os/^{188}Os$ ratio is arbitrary, but
 877 we use a chondritic initial for both the mantle-derived magma and the sedimentary contaminant
 878 (e.g. mantle-derived detritus, or seawater controlled by leaching of chondritic oceanic crust).
 879 The isochron which represents growth of the sedimentary rock from 1.85 Ga until 1.1 Ga is
 880 shown for reference, as is the isochron for uncontaminated mantle. At 1.1 Ga a mantle-derived
 881 magma is emplaced and is contaminated with Os derived from the sedimentary rock (point M).
 882 Crystallization of the contaminated magma and decay from the time of mixing (1.1 Ga) until the
 883 present will produce an isochron yielding the age of the mixing event with an elevated initial 187
 884 $Os/^{188}Os$, and an elevated γ_{Os} value. If multiple pulses of magma are involved that may have
 885 interacted to different degrees with the sedimentary country rocks (different f values), then a
 886 knowledge of the age of the intrusion (e.g. from U-Pb isotope measurements) is required to
 887 assess the range of γ_{Os} values. The two-component isotopic mixing equation has the form:

$$\begin{aligned}
& ({}^{187}\text{Os}/{}^{188}\text{Os})_{\text{mix},o} = ((C_{Os}^s)(f)/(C_{Os}^s)(f) + (C_{Os}^c)(1-f))(({}^{187}\text{Os}/{}^{188}\text{Os})_{s,o} + \\
& ({}^{187}\text{Re}/{}^{188}\text{Os})_{s,t2}(e^{\lambda T} - e^{\lambda \tau 2})) \\
& + ((C_{Os}^c)(1-f)/(C_{Os}^s)(f) + (C_{Os}^c)(1-f))(({}^{187}\text{Os}/{}^{188}\text{Os})_{c,o} + ({}^{187}\text{Re}/{}^{188}\text{Os})_{c,t2}(e^{\lambda \tau 1} - e^{\lambda \tau 2}))
\end{aligned}$$

Where f = mass fraction of the mantle-derived source magma, C_{Os}^s and C_{Os}^c = concentration of Os in the source magma and contaminant, respectively, subscripts (mix,o), (s,o) and (c,o) refer to the initial ${}^{187}\text{Os}/{}^{188}\text{Os}$ ratio of the mixture, source magma, and contaminant, subscripts ($c,t2$) and ($s,t2$) refer to the ${}^{187}\text{Re}/{}^{188}\text{Os}$ ratios of contaminant and source magma at the time of mixing, $T = 4.557 \times 10^9$, $t1$ = age of the contaminant, and $t2$ = time of mixing

We illustrate in Figure 23 that in addition to multiple magma pulses and variable degrees of contamination, a suite of non-linear ${}^{187}\text{Os}/{}^{188}\text{Os}$ values may also indicate either Re loss/gain or Os gain/loss via lower-temperature interaction with fluids. Xiong and Wood (2001) have shown that Re may be soluble as a hydroxyl species in low $-T$ fluids, and recent studies by Foustoukos et al. (2014) further quantify the extent to which Re and Os may be transported via hydrothermal fluids. Figure 23 illustrates a case of crystallization from 1.1 Ga until 0.5 Ga, when hydrothermal alteration changed the Re/Os ratio of the system. In the case of Re loss or Os gain the resultant ${}^{187}\text{Os}/{}^{188}\text{Os}$ values will plot above the isochron for the uncontaminated system and these points may be difficult to distinguish from those produced by variable degrees of crustal contamination of multiple pulses of magma. Sampling at small spatial intervals may be required to resolve the interpretation; evidence of high degrees of hydrothermal alteration would be expected. In the case of Re gain or Os loss the resultant ${}^{187}\text{Os}/{}^{188}\text{Os}$ values will fall below the expected isochron for uncontaminated mantle and will produce negative γ_{Os} values. Scatter in ${}^{187}\text{Os}/{}^{188}\text{Os}$ values must be carefully evaluated as it may not be indicative of contamination of mantle-derived magma, but perturbation of the Re-Os system by interaction between igneous rock and low-temperature fluids.

913

914 The “R-factor” and its application to Re-Os isotopes

915

The “R-Factor” (ratio of sulfide liquid to silicate magma) has been discussed above, and is often mentioned in conjunction with Re-Os isotope studies (e.g., Lambert et al. 1998a, b, 1999a). If S in the ore-forming system has been primarily derived from country rocks, and contamination has involved only S, then the R-factor directly relates to f values where $f(\text{silicate}) = R/(1+R)$. In the more general case where a sulfide-undersaturated magma assimilates country rock, including S, utilization of the “R-factor” is appropriate after the separation of immiscible sulfide liquid. Although both Re and Os may be strongly partitioned into the sulfide liquid (see above), no isotopic fractionation accompanies this process. If Os is more strongly partitioned into the sulfide liquid than is Re, then the Re/Os ratio of the sulfide liquid may be lower than that of the coexisting silicate magma, but crystallization products of both liquids should lie along the same isochron provided closed system conditions have prevailed. This is an important point in the evaluation of massive sulfides that are suspected of separating from a parent liquid that is now represented by a silicate assemblage that contains only disseminated sulfides. If the systems share a common origin then they should fall along the same isochron.

929

930

931

932 **Examples of the application of the Re-Os isotope system to magmatic ore deposits**

933 *The Sudbury Igneous Complex.* The Sudbury Igneous Complex (SIC) was the world's largest
 934 producer of Ni, with significant production of PGEs as by-products. Walker et al. (1991)
 935 presented results of one of the earliest applications of the Re-Os system to magmatic ore
 936 deposits, in this case the Ni-Cu ores of the SIC. The work by Walker et al. (1991) was followed
 937 by studies by Dickin et al. (1992) and Morgan et al. (2002) who obtained greater precision in
 938 measurements using negative thermal ionization mass spectrometry. All of these studies
 939 confirmed the presence of crustal Os in the ores. Samples collected from the McCreedy West and
 940 Falconbridge mines produced isochrons of 1835 ± 70 Ma and 1825 ± 340 Ma, respectively
 941 (Morgan et al. 2002; Fig. 24). The ages agreed within uncertainty with that of 1850 ± 1 Ma
 942 determined using U-Pb methods by Krogh et al. (1984). Gamma Os values for the McCreedy
 943 West data averaged 346 ± 10 and that from Falconbridge was 375 ± 12 . The $^{187}\text{Os}/^{188}\text{Os}$ values
 944 could be modelled as resulting from mixtures of Proterozoic and Archean country rocks,
 945 However, Morgan et al. (2002) also used $^{186}\text{Os}/^{188}\text{Os}$ ratios to indicate that in addition to
 946 metasedimentary rocks a third component was necessary to explain the Re-Os systematics of the
 947 Falconbridge and McCreedy West samples. The third component was thought to be either mafic
 948 rocks of Archean or Proterozoic age. It is now thought that the Sudbury melt sheet included Ni-
 949 Cu and PGE-bearing sulfides from Proterozoic mafic rocks in the target area (Keays and
 950 Lightfoot 2004). Of particular significance is the conclusion that the Re-Os isotope systematics
 951 of the Sudbury ores can only be explained if a significant portion of Os was derived from crustal
 952 metasedimentary rocks, in agreement with the origin of the SIC as an impact melt sheet.

953 *Ni-Cu-PGE deposits of the Noril'sk region, Siberia.* Walker et al. (1994) and Malitch and
 954 Latypov (2011) have presented Re-Os isotopic data from the Noril'sk, Talnakh, and Kharaelakh
 955 ore-bearing intrusions. Data from both studies provide isochrons that are consistent with the U-
 956 Pb ages of the intrusions (~ 247 Ma) and γ_{Os} values that show slight differences between
 957 intrusions but range from only 0.4 to 12.9 (Figure 25). Both Walker et al. (1994) and Malitch and
 958 Latypov (2011) suggested that the Re-Os isotopic values may be indicative of their mantle
 959 source and in particular deep mantle that had incorporated ancient Re-enriched crust.
 960 Alternatively, the γ_{Os} values could be indicative of very minor amounts of crustal contamination
 961 in the lithosphere. The very low γ_{Os} values do not indicate the extensive interaction with crustal
 962 material that is suggested by the elevated sulfur isotope compositions of the ores (e.g. Grinenko
 963 1966; Ripley et al. 2003; Malitch et al. 2014) and the anomalous Sr isotope compositions
 964 reported by Arndt et al. (2003). This may reflect the derivation of S and Sr from evaporates
 965 which would tend to have low concentrations of Re and Os. Alternatively, Leshner and Burnham
 966 (2001) suggested that due to mass action constraints, Re-Os isotopic values may be "re-set" to
 967 near chondritic values and S isotope values little affected as uncontaminated mantle-derived
 968 magmas exchanged with sulfides in a conduit environment. A similar process has been proposed
 969 to explain the Re-Os isotopic systematics of the Eagle deposit (see below).

970 *The Voisey's Bay Ni-Cu-Co deposit, Labrador.* Lambert et al. (1999b 2000) have utilized the
 971 Re-Os isotope system in the interpretation of the genesis of the Voisey's Bay Ni-Cu-Co deposit.
 972 The deposit is known as a "conduit-type" because of the clear occurrence of sulfide

973 mineralization in dike-like bodies that connect larger intrusions (e.g., Naldrett and Li 2007;
 974 Lightfoot et al 2012). Massive sulfide mineralization occurs in a widened portion of the dike that
 975 connects the western deeps intrusion and the upper Eastern deeps intrusion. Mining of the
 976 massive sulfide, or “Ovoid”, is currently in progress. Lambert et al. (1999b 2000) identified two
 977 scales of Re-Os isotope development, and a multi-stage process of mineralization. Whole rock
 978 samples of the massive sulfide assemblage remained closed over a large spatial interval, and an
 979 imprecise 1323 ± 135 Ma isochron was generated; this age was within error of the 1332.7 ± 1 Ma
 980 badelleyite U-Pb age for the Voisey’s Bay intrusion of Amelin et al. (1999). Of particular
 981 significance is the initial $^{187}\text{Os}/^{188}\text{Os}$ value determined from the isochron plot (Figure 26). This
 982 initial ratio yielded a γ_{Os} value of 1040 ± 200 , signifying extensive contamination with old crustal
 983 material. The Proterozoic Tasiuyak Gneiss was taken to be a likely source, as other petrogenetic
 984 indicators also suggested that assimilation of the Tasiuyak Gneiss had been extensive (e.g., Li
 985 and Naldrett 2000). Archean rocks of the Nain Province could not be entirely eliminated, and
 986 Lambert et al. (2000) suggested that a two-stage process of magma contamination had occurred,
 987 with high-MgO basaltic magmas first contaminated in the lower crust. The results from the study
 988 of the whole rock massive sulfides provide an excellent example of how the Re-Os system may
 989 provide both geochronologic data and information on magma-country rock interaction. In this
 990 case the Re-Os system of the sulfides was homogenized prior to crystallization of the sulfide
 991 assemblage. Lambert et al. (2000) also showed that disseminated sulfide-bearing intrusive rocks
 992 showed a great deal of scatter on an isochron plot, and suggested that variable degrees of mixing
 993 with country rocks were responsible. In addition, sulfide mineral separates from the massive
 994 sulfides defined an isochron with an age of 1004 ± 20 Ma, consistent with re-setting of the sulfide
 995 system on the mineral scale as a result of hydrothermal alteration associated with the Grenville
 996 orogeny.

997 *The Eagle Deposit, Midcontinent Rift System, Michigan.* The Eagle deposit is a newly discovered
 998 Ni-Cu-PGE sulfide deposit in mafic rocks associated with the 1.1 Ga Midcontinent Rift System
 999 of Minnesota, Michigan and Canada. Mineralization occurs within irregularities in a dike-like
 1000 body which is part of the Marquette-Baraga Dike Swarm (Ding et al. 2010). It bears similarities
 1001 to the Voisey’s Bay deposit in terms of its conduit environment. Ding et al. (2012) present Re-Os
 1002 isotopic data from disseminated, net-textured and massive sulfides. Results produced an
 1003 isochron of 1106 ± 34 Ma (Figure 27), in good agreement with the U-Pb age of the intrusion of
 1004 1107 ± 2 Ma reported by Ding et al. (2010). The γ_{Os} value corresponding to the initial $^{187}\text{Os}/^{188}$
 1005 Os ratio of 0.1607 was 34, and could be explained by less than 3% bulk contamination of a
 1006 mantle-derived picritic magma with Proterozoic country rocks. The apparent low degree of
 1007 contamination is contrary to models for ore genesis that favor extensive crustal contamination.
 1008 Ripley and Li (2003) and Ding et al. (2012) showed how exchange reactions in magma conduits
 1009 involving early-formed sulfide and uncontaminated magmas could produce isotopic values
 1010 approaching those of the uncontaminated magma and mask evidence for earlier high degrees of
 1011 contamination (Figure 28).

1012 *The Stillwater Complex, Montana.* As described above, the 2700 Ma Stillwater Complex hosts
 1013 one of the world’s major PGE reef-style deposits. The J-M Reef and host rocks, as well as PGE-
 1014 bearing chromitites in the Ultramafic Series, have been studied using the Re-Os isotope system
 1015 by a number of researchers (e.g., Lambert et al. 1989, 1994; Martin 1989, Marcantonio et al.
 1016 1993; Horan et al 2001). Lambert et al. (1989, 1994), Martin (1989), and Horan et al (2001) have
 1017 all concluded that two sources of Os were involved in the generation of the Complex. Lambert et

1018 al. (1994) reported that PGE-enriched units of the Complex (B chromitite seam and the J-M
 1019 Reef) were isochronous and characterized by elevated γ_{Os} values of 12 to 34. PGE-poor
 1020 chromitites (G and H) were found to be near-chondritic with γ_{Os} values of -2 to +4. The Re-Os
 1021 data were consistent with other petrogenetic data that indicated that two magma types were
 1022 involved – one an ultramafic magma with little sign of crustal contamination but possible
 1023 derivation from the subcontinental lithospheric mantle, and the other a more mafic to anorthositic
 1024 magma that had been contaminated with Archean crust prior to emplacement. The mixing of
 1025 these two magma types was proposed to account for the elevated γ_{Os} values and was thought to
 1026 be instrumental in the formation of the J-M Reef. Horan et al (2001) separated chromite from
 1027 chromite seams and silicate-rich layers of the Ultramafic Series. They found variable γ_{Os} values
 1028 ranging from 2 to 16.4, and also suggested that two magmas were involved in the formation of
 1029 the Ultramafic Series, one which was near-chondritic and the other which was characterized by
 1030 elevated γ_{Os} values and had been contaminated by sedimentary rocks beneath the Complex.
 1031 Martin (1989) concluded that a chondritic mantle melt was contaminated with mafic to
 1032 intermediate crust at the time of the Ultramafic-Banded Series transition and at the time of J-M
 1033 Reef formation. Marcantonio et al. (1993) indicated that chromitites from the Ultramafic Series
 1034 were derived from a mantle magma that had been affected by little or no interaction with
 1035 continental crust. The minor scatter in the chromitite Os isotope values was attributed to
 1036 hydrothermal processes. Molybdenite (Re-rich and Os-poor) was separated from the G-
 1037 chromitite and yielded an age of 2740, in agreement with the accepted age of the Complex.
 1038 Marcantonio et al. (1993) suggested that all elevated γ_{Os} values found in the Complex could have
 1039 resulted from interaction with hydrothermal fluids of the type which produced the molybdenite.

1040 *The Great Dyke, Zimbabwe.* Schoenberg et al. (2003) have studied chromite separates from
 1041 chromitites of the 2576 Ma Great Dyke. Results from their study show that most chromitites
 1042 form an imprecise isochron of 2580 ± 500 Ma (Fig. 29). Mixing calculations involving Archean
 1043 country rocks suggest that from 0 to 33% of the Os in the chromitites may have been of crustal
 1044 origin. When combined with other isotopic and petrologic data the authors concluded that the
 1045 source magmas underwent no interaction with subcontinental lithospheric mantle, and that the
 1046 parent magma of the Great Dyke was plume-derived with a heterogeneous Os isotope signature,
 1047 not unlike some oceanic basalts where the incorporation of recycled oceanic crust has been
 1048 proposed. Significant contamination by Archean granitoid crust was ruled out based on the low
 1049 Os concentrations and unradiogenic Os isotope ratios of representative country rock samples.

1050 *The Bushveld Complex, South Africa.* Re-Os isotope studies of chromitites, pyroxenites, sulfides
 1051 and alloys have been conducted as an aid in evaluating the genesis of PGE enrichment in the
 1052 UG2 chromitite (McCandless and Ruiz 1991; Schoenberg et al. 1999), the Merensky Reef (Hart
 1053 and Kinloch 1989; McCandless and Ruiz 1991; Schoenberg et al. 1999), and the Platreef
 1054 (Reisberg et al. 2011). Results of these studies have been summarized by Reisberg et al. (2011),
 1055 and are shown here in Figure 30. The results from all of these studies indicate that the Bushveld
 1056 parent magmas underwent variable degrees of contamination by crust, in agreement with other
 1057 isotopic indicators of crustal contamination. Schoenberg et al. (1999) note that chromitites show
 1058 increasing $^{187}Os/^{188}Os$ values upward, from near chondritic values in the lower chromitites to
 1059 strongly enriched values in the upper chromitites. The enrichment was thought to be a result of
 1060 enhanced degrees of crustal contamination. Hart and Kinloch (1989) analyzed erlichmanite and
 1061 laurite grains from the Merensky Reef, and found that erlichmanite was near chondritic, with
 1062 $^{187}Os/^{188}Os$ values similar to those of the lower chromitites. Laurite grains were strongly

1063 radiogenic, with $^{187}\text{Os}/^{188}\text{Os}$ values similar to those of sulfides and whole rocks from the Reef
1064 reported by both McCandless and Ruiz (1991) and Schoenberg et al. (1999). McCandless and
1065 Ruiz (1991) suggested that the contaminant was Re-rich black shales that occur below the
1066 Complex. Schoenberg et al. (1999) proposed that primitive mantle-derived magma mixed with
1067 highly contaminated granophyric roof melt near the top of the chamber. In both scenarios the
1068 Merensky Reef records a substantial contribution of crustally derived Os. The chondritic
1069 erlichmanite grains found in the Reef by Hart and Kinloch (1989) suggest that uncontaminated
1070 mantle-derived magma was first emplaced at the level of the Reef, but that highly crustally
1071 contaminated magma followed. It is also possible that the erlichmanite grains represent mantle
1072 xenocrysts and that crustally contaminated magmas from chambers at depth entrained them. The
1073 radiogenic signals from pyroxenites of the Platreef also led Reisberg et al. (2011) to propose that
1074 the Platreef parental magma was crustally contaminated by black shales, and well-mixed prior to
1075 emplacement. They note that the rapid return to less radiogenic Os isotope compositions above
1076 the Merensky Reef cannot mark a change from one magma type to another, but must represent
1077 the input of a large quantity of radiogenic Os at the level of the reef. The spike in $^{187}\text{Os}/^{188}\text{Os}$
1078 values at the level of the Merensky Reef and the Platreef was thought to indicate the
1079 contamination of magma by a crustal lithology unusually rich in radiogenic Os – most likely
1080 black shales. The Reisberg et al. (2011) model differs somewhat from the McCandless and Ruiz
1081 (1991) model in that Reisberg et al. (2011) propose contamination in magma chambers at
1082 intermediate crustal depths, rather than immediately below the current base of the Complex.
1083 Using representative concentrations and $^{187}\text{Os}/^{188}\text{Os}$ ratios Reisberg et al. (2011) determined
1084 that less than 1% bulk assimilation of black shale was necessary to account for the enriched
1085 signals in the Platreef. They also suggested that minor additional crustal contamination may
1086 have occurred at the level of emplacement of the Platreef.

1087 *Summary.* The Re-Os isotope system has obvious utility in the age-dating of magmatic ore
1088 deposits. In addition, the system may be a sensitive indicator of the importance of crustal
1089 contamination in ore formation. Results range from those where there is very little Os isotope
1090 indication of crustal contamination being involved in ore genesis (e.g. Noril'sk, Great Dyke) to
1091 those where the addition of crustal Os is strongly indicated (e.g., Sudbury, Voisey's Bay,
1092 Bushveld). In conduit deposits such as Noril'sk and Eagle where other isotopic systems (e.g. S,
1093 Rb-Sr) support a strong role for crustal contamination, a process such as isotopic exchange and
1094 mixing involving sulfide-rich magma in the conduit and uncontaminated magmatic pulses may
1095 explain the decoupling between the isotopic systems. Another end-member interpretation is that
1096 in some environments country rock contaminants may contain insufficient Re and Os to perturb
1097 the mantle characteristics of the source magma, whereas concentrations and isotopic values are
1098 sufficient to readily perturb other isotopic systems such as S. A third interpretation would be that
1099 in systems where no Os isotope evidence for contamination exists, the magma was derived from
1100 a mantle source that had been modified by the addition of crustal components such as S (e.g.,
1101 addition of altered crust via subduction) and as a result was characterized by anomalous S
1102 isotopic ratios, but the amount of radiogenic Os added was too small to perturb the mantle Os
1103 signal. Subcontinental lithospheric mantle is thought to be Re-depleted and hence melts derived
1104 from that source should be expected to have negative γ_{Os} values. The Re-Os isotopic system will
1105 no doubt continue to be a major tool for the evaluation of the source of Os and the significance
1106 of crustal contamination in magmatic Ni-Cu-PGE deposits. Care must be taken to ensure that
1107 isotope perturbations have not been caused by hydrothermal activity and the mobility of Re and
1108 Os in relatively low-temperature fluids.

1109

1110 **Conclusions**

1111 Most PGE ore deposits are found within or at the contact with mafic-ultramafic intrusions
1112 and are associated with base metal sulfide minerals, pyrrhotite, pentlandite and chalcopyrite.
1113 The PGE are present in pyrrhotite, pentlandite and in PGM found among the BMS and at the
1114 contact between BMS and chromite or silicates. The standard model for the formation of the
1115 deposits is that a mafic to ultramafic magma became saturated in a base metal sulfide liquid and
1116 the PGE partitioned into this sulfide liquid. The PGE content of the liquid is dependent on the
1117 composition of the silicate magma but also on the amount of magma with which it interacted. In
1118 order to form a PGE ore deposit the sulfide liquid must interact with a very large amount of
1119 silicate magma. Some deposits such as the droplet ore of Noril'sk 1 or Merensky reef and Main
1120 sulfide zone may have formed in this manner. Other deposits require additional processes to
1121 explain the variations in PGE content of the ores. Fractional crystallization of the sulfide liquid
1122 is an important process that leads to the formation of an MSS cumulate depleted in Cu but
1123 enriched in Re, Os, Ir, Ru and Rh. The fractionated liquid is enriched in Cu, Pt, Pd, Au and
1124 TABS,. Intermediate solid solution sulfide crystallizes from the fractionated liquid but Pt, Pd
1125 Au and TABS do not partition into ISS and they concentrate into the very last liquid. In most
1126 cases this liquid is trapped with ISS cumulate and as a result the Cu-rich ore is also Pt, Pd and
1127 Au and TABS rich. The variations in PGE contents in some ores such as the McCreedy East
1128 deposit of Sudbury or the Talnakh and Kharaelakh deposits of the Noril'sk area are the result of
1129 this crystal fractionation. The Pt-Pd-,Au-TABS rich liquid would not crystallize until relatively
1130 low temperatures (500-600 °C). Therefore, it is possible that the liquid could be injected into the
1131 fractures around or within the intrusion during some structural disturbance. Also even once
1132 crystallized it could melt at lower amphibolite faces conditions and migrate during
1133 metamorphism. Possibly the low-S-high-Pt-Pd deposits such as the High Grade ore of Lac des
1134 Iles or Broken Hammer of Sudbury formed by mobilization of Pd-Pt-TABS liquid.

1135 Because of the chalcophile nature of both Re and Os the Re-Os isotopic system is widely
1136 applied in the evaluation of ore genesis. The system has wide applicability in the geochronology
1137 of magmatic ore systems. In addition, the long-term enrichment of Re in the crust has made the
1138 system a very sensitive one in the evaluation of the degree of interaction between mantle-derived
1139 magmas and continental crust. Osmium isotope ratios may provide an indication of the source of
1140 Os in an ore deposit, as well as the extent of country rock contamination that may have been
1141 important in the ore-forming process.

1142

1143 **Acknowledgements**

1144 The research of SJB has been supported by Natural Sciences and Engineering Research Council
1145 of Canada for the past 29 years and by the Canada Research Chair in Magmatic Metallogeny for
1146 10 years. Both sources of funds are for fundamental research and the continuity of this support
1147 has been essential to the development of SJB's research program. The research of EMR on the
1148 genesis of magmatic ore deposits has been supported by the United States National Science
1149 Foundation for the past 38 years; appreciation is expressed for both basic research support and
1150 analytical instrumentation. We also thank all those members of the magmatic ore deposits

1151 community who organized and participated in conferences and field trips to the world's Ni and
1152 PGE deposits; seeing these deposits and discussions with colleagues on these occasions greatly
1153 helped to clarify our ideas. We thank the editors Dr. Havey and Day for the invitation to write
1154 this chapter and the reviewers Dr. D. Holwell and ? for their time and effort in helping to
1155 improve the manuscript.
1156

1157

1158

REFERENCES

- 1159 Amelin Y, Li C, Naldrett AJ (1999) Geochronology of the Voisey's Bay intrusion, Labrador,
1160 Canada, by precise U-Pb dating of coexisting baddeleyite, zircon, and apatite. *Lithos*
1161 47:33-51.
- 1162 Ames D, Farrow C (2007) Metallogeny of the Sudbury mining camp, Ontario. *In: Mineral*
1163 *deposits of Canada: a synthesis of major deposit-types, district metallogeny, the evolution*
1164 *of geological provinces, and exploration methods. Geological Association of Canada,*
1165 *Mineral Deposits Division, Special Publication 5, p 329-350.*
- 1166 Andersen JC (2006) Postmagmatic sulphur loss in the Skaergaard intrusion: implications for the
1167 formation of the Platinova Reef. *Lithos* 92:198-221
- 1168 Anikina E, Malitch K, Pushkarev E, Shmelev V (2014) The Nizhny Tagil and Volkovsky
1169 massifs of the Uralian Platinum Belt, and related deposits. Field trip guidebook. 12th
1170 International Platinum Symposium. Yekaterinburg: IGG UB RAS, p 48.
- 1171 Arevalo Jr R, McDonough WF (2010) Chemical variations and regional diversity observed in
1172 MORB. *Chem Geol* 271:70-85
- 1173 Arndt NT, Czamanske, GK, Walker RJ, Chauvel C, Fedorenko VA (2003) Geochemistry and
1174 origin of the intrusive hosts of the Noril'sk-Talnakh Cu-Ni-PGE sulfide deposits. *Econ*
1175 *Geol* 98:495-515.
- 1176 Augé T, Genna A, Legendre O, Ivanov KS, Volchenko YA (2005) Primary platinum
1177 mineralization in the Nizhny Tagil and Kachkanar ultramafic complexes, Urals, Russia: a
1178 genetic model for PGE concentration in chromite-rich zones. *Econ Geol* 100:707-732
- 1179 Barra F, Ruiz J, Mathur R, Titley S (2003) A Re-Os study of sulfide minerals from the Bagdad
1180 porphyry Cu-Mo deposit, northern Arizona, USA. *Miner Deposita* 38:585-596.
- 1181 Ballhaus C, Tredoux M, Spath A (2001) Phase relations in the Fe-Ni-Cu-PGE-S system at
1182 magmatic temperature and application to massive sulphide ores of the Sudbury igneous
1183 complex. *Jour Petrol* 42:1911-1926
- 1184 Ballhaus C, Bockrath C, Wohlgemuth-Ueberwasser C, Laurenz V, Berndt J (2006) Fractionation
1185 of the noble metals by physical processes. *Contrib Mineral Petr* 152:667-684
- 1186 Barnes S-J, Gomwe TS (2011) Pd deposits of the Lac des Iles Complex, Northwestern Ontario.
1187 *In: Reviews in Economic Geology Vol 17. Li. C, Ripley EM, (eds). Society of Economic*
1188 *Geologists p 351-370*
- 1189 Barnes S-J, Lightfoot PC (2005) Formation of Magmatic Nickel-Sulfide Ore Deposits and
1190 Processes Affecting Their Copper and Platinum-Group Element Contents *In: Economic*
1191 *Geology 100th Anniversary Volume. Hendenquist JW, Thompson JFH, Goldfarb RJ,*
1192 *Richards JP, (eds) p 179-214*
- 1193 Barnes S-J, Maier WD (2002a) Platinum-group element distributions in the Rustenberg Layered
1194 Suite of the Bushveld Complex, South Africa. *In: The Geology, Geochemistry,*
1195 *Mineralogy and Mineral Beneficiation of Platinum-Group Elements Special Vol. 54.*
1196 *Cabri LJ (ed) Canadian Institute of Mining, Metallurgy and Petroleum, p 553-580*
- 1197 Barnes S-J, Maier WD (2002b) Platinum-group elements and microstructures of normal
1198 Merensky Reef from Impala Platinum Mines, Bushveld Complex. *Jour Petrol* 43:103-128

- 1199 Barnes S-J, Couture J-F, Sawyer EW, Bouchaib C (1993) Nickel-copper sulfide occurrences in
 1200 Belleterre-Angliers belt of the Pontiac sub-province and the use of Cu/Pd s in interpreting
 1201 platinum-group element distributions. *Econ Geol* 88:1402-1418
- 1202 Barnes S-J, Makovicky E, Makovicky M, Rose-Hansen J, Karup-Moller S (1997a) Partition
 1203 coefficients for Ni, Cu, Pd, Pt, Rh, and Ir between monosulphide solid solution and
 1204 sulphide liquid and the formation of compositionally zoned Ni-Cu sulphide bodies by
 1205 fractional crystallization of sulphide liquid. *Can Jour Earth Sci* 34:366-374
- 1206 Barnes S-J, Zientek ML, Severson MJ (1997b) Ni, Cu, Au, and platinum-group element contents
 1207 of sulphides associated with intraplate magmatism: a synthesis. *Can Jour Earth Sci*
 1208 34:337-351
- 1209 Barnes S-J, Cox RA, Zientek ML (2006) Platinum-group element, Gold, Silver and Base Metal
 1210 distribution in compositionally zoned sulfide droplets from the Medvezky Creek Mine,
 1211 Noril'sk, Russia. *Contrib Mineral Petrol* 152:187-200
- 1212 Barnes S-J, Prichard HM, Cox RA, Fisher PC, Godel B (2008) The location of the chalcophile
 1213 and siderophile elements in platinum-group element ore deposits (a textural, microbeam
 1214 and whole rock geochemical study): Implications for the formation of the deposits. *Chem*
 1215 *Geol* 248:295-317
- 1216 Barnes S-J, Savard D, Bedard LP, Maier WD (2009) Selenium and sulfur concentrations in the
 1217 Bushveld Complex of South Africa and implications for formation of the platinum-group
 1218 element deposits. *Mineral Deposita* 44:647-663
- 1219 Barnes SJ, Maier WD, Curl EA (2010) Composition of the Marginal Rocks and Sills of the
 1220 Rustenburg Layered Suite, Bushveld Complex, South Africa: Implications for the
 1221 Formation of the Platinum-Group Element Deposits. *Econ Geol* 105:1491-1511
- 1222 Barnes SJ, Naldrett AJ (1985) Geochemistry of the JM (Howland) Reef of the Stillwater
 1223 Complex, Minneapolis Adit area; I, Sulfide chemistry and sulfide-olivine equilibrium.
 1224 *Econ Geol* 80: 627-645
- 1225 Bates RL, Jackson JA (1987) *Glossary of Geology*. American Geological Institute, Alexandria
- 1226 Baumgartner J, Dey A, Bomans PH, Le Coadou C, Fratzl P, Sommerdijk NA, Faivre D (2013)
 1227 Nucleation and growth of magnetite from solution. *Nat Mater* 12:310-314.
- 1228 Boudreau A, Mathez E, McCallum I (1986) Halogen geochemistry of the Stillwater and
 1229 Bushveld Complexes: evidence for transport of the platinum-group elements by Cl-rich
 1230 fluids. *J Petrol* 27:967-986
- 1231 Boudreau A, Djon L, Tchalikian A, Corkery J (2014) The Lac Des Iles Palladium deposit,
 1232 Ontario, Canada part I. The effect of variable alteration on the offset zone. *Mineral*
 1233 *Deposita* 49:625-654
- 1234 Brenan JM (2002) Re-Os fractionation in magmatic sulfide melt by monosulfide solid solution.
 1235 *Earth Planet Sci Lett* 199:257-268
- 1236 Brenan JM (2008) Re-Os fractionation by sulfide melt-silicate melt partitioning: a new spin.
 1237 *Chem Geol* 248:140-165
- 1238 Brenan JM (2015) Se-Te fractionation by sulfide-silicate melt partitioning: Implications for the
 1239 composition of mantle-derived magmas and their melting residues. *Earth Planet Sci Lett*
 1240 422:45-57
- 1241 Brenan JM, McDonough WF, Dalpe C (2003) Experimental constraints on the partitioning of
 1242 rhenium and some platinum- group elements between olivine and silicate melt. *Earth*
 1243 *Planet Sci Lett* 212: 135-150

- 1244 Brenan JM, Finnigan CF, McDonough WF, Homolova V (2012) Experimental constraints on the
 1245 partitioning of Ru, Rh, Ir, Pt and Pd between chromite and silicate melt: the importance
 1246 of ferric iron. *Chem Geol* 302:16-32
- 1247 Brenan JM, Bennett N, Zajacz Z (2015) Experimental methods in siderophile and chalcophile
 1248 element geochemistry. *Rev Mineral Geochem* v.81: xxx-xxx.
- 1249 Brüggemann GE, Naldrett AJ, Asif M, Lightfoot PC, Gorbachev NS, Fedorenko VA (1993)
 1250 Siderophile and chalcophile metals as tracers of the evolution of the Siberian Trap in the
 1251 Noril'sk region, Russia. *Geochim Cosmochim Acta* 57:2001-2018
- 1252 Cabri LJ (1992) The distribution of trace precious metals in minerals and mineral products.
 1253 *Mineral Mag* 56:289-308
- 1254 Cabri LJ (2002) The platinum-group minerals. *In: The Geology, Geochemistry, Mineralogy and*
 1255 *Mineral Beneficiation of the Platinum-group elements. Special Volume 54. Cabri LJ, (ed)*
 1256 *Canadian Institute of Mining, Metallurgy and Petroleum, p 13-129*
- 1257 Campbell IH, Naldrett AJ (1979) The influence of silicate: sulphide ratios on the geochemistry
 1258 of magmatic sulphides. *Econ Geol* 74:1503-1505
- 1259 Capobianco CJ, Hervig RL, Drake MJ (1994) Experiments on crystal/liquid partitioning of Ru,
 1260 Rh and Pd for magnetite and hematite solid solutions crystallized from silicate melt.
 1261 *Chem Geol* 113:23-43
- 1262 Carlson RW (2005) Application of the Pt-Re-Os isotopic systems to mantle geochemistry and
 1263 geochronology. *Lithos* 82:249-272
- 1264 Cawthorn RG, Lee CA, Schouwstra RP, Mellowship P (2002) Relationship between PGE and
 1265 PGM in the Bushveld Complex. *Can Mineral* 40:311-328
- 1266 Cawthorn RG, Lee C (1998) Field excursion guide to the Bushveld Complex 8th International
 1267 Platinum Symposium. The Geological Society of the South Africa and The South African
 1268 Institute of Mining and Metallurgy, South Africa.
- 1269 Cowley A (2013) Platinum 2013 Interim Review
 1270 [http://www.platinum.matthey.com/documents/market-review/2013-interim/full-](http://www.platinum.matthey.com/documents/market-review/2013-interim/full-review/english.pdf)
 1271 [review/english.pdf](http://www.platinum.matthey.com/documents/market-review/2013-interim/full-review/english.pdf)
- 1272 Crocket JH, Fleet ME, Stone WE (1992) Experimental partitioning of osmium, iridium and gold
 1273 between basalt melt and sulphide liquid at 1300°C. *Aust J Earth Sci* 39:427-432.
- 1274 Czamanske G, Kuniylov V, Zientek M, Cabri L, Likhachev A, Calk L, Oscarson R (1992) A pro
 1275 ton-microprobe study of magmatic sulphide ores from the Noril'sk-Talnakh district,
 1276 Siberia. *Can. Min.* 30:249-287.
- 1277 Dare SAS, Barnes SJ, Prichard HM (2010) The distribution of platinum group elements (PGE)
 1278 and other chalcophile elements among sulfides from the Creighton Ni-Cu-PGE sulfide
 1279 deposit, Sudbury, Canada, and the origin of palladium in pentlandite. *Mineral Deposita*
 1280 45:765-793
- 1281 Dare SAS, Barnes S-J, Prichard HM, Fisher PC (2011) Chalcophile and platinum-group element
 1282 (PGE) concentrations in the sulfide minerals from the McCreeley East deposit, Sudbury,
 1283 Canada, and the origin of PGE in pyrite. *Mineral Deposita* 46:381-407
- 1284 Dare SAS, Barnes S-J, Prichard HM, Fisher PC (2014) Mineralogy and geochemistry of Cu-Rich
 1285 ores from the McCreeley East Ni-Cu-PGE Deposit (Sudbury, Canada): Implications for
 1286 the behavior of platinum group and chalcophile elements at the end of crystallization of a
 1287 sulfide liquid. *Econ Geol* 109:343-366

- 1288 Dickin A, Richardson J, Crocket J, McNutt R, Peredery W (1992). Osmium isotope evidence for
 1289 a crustal origin of platinum group elements in the Sudbury nickel ore, Ontario, Canada.
 1290 *Geochim Cosmochim Acta* 56:3531-3537
- 1291 Dietz RS (1964) Sudbury structure as an astrobleme. *Journal of Geology* 74: 412-434.
- 1292 Ding X, Li C, Ripley EM, Rossell D, Kamo S (2010) The Eagle and East Eagle sulfide ore-
 1293 bearing mafic-ultramafic intrusions in the Midcontinent Rift System, upper Michigan:
 1294 Geochronology and petrologic evolution. *Geochem Geophys Geosyst* 11:Q03003,
 1295 doi:10.1029/2009GC002546.
- 1296 Ding X, Ripley EM, Shirey SB, Li C (2012) Os, Nd, O and S isotope constraints on country rock
 1297 contamination in the conduit-related Eagle Cu-Ni-(PGE) deposit, Midcontinent Rift
 1298 System, Upper Michigan. *Geochim Cosmochim Acta* 89:10-30.
- 1299 Distler VV, Malevsky AY, Laputina IP (1977) Distribution of platinoids between pyrrhotite and
 1300 pentlandite in crystallization of a sulphide melt. *Geochimica International* 14:30-40 (In
 1301 Russian)
- 1302 Distler VV (1994) Platinum Mineralisation of the Noril'sk Deposits. *In: Proceedings of the*
 1303 *Sudbury-Noril'sk symposium. Vol Special Publication no. 5. Lightfoot PC, Naldrett AJ,*
 1304 *(eds). Ontario Geological Survey, p 243-262*
 1305 www.geologyontario.mndmf.gov.on.ca/mndmfiles/pub/data/imaging/SV05/SV05.pdf
- 1306 Djon MLN, Barnes SJ (2012) Changes in sulfides and platinum-group minerals with the degree
 1307 of alteration in the Roby, Twilight, and High Grade Zones of the Lac des Iles Complex,
 1308 Ontario, Canada. *Mineral Deposita*: 47:875-896
- 1309 Drobe J, Lindsay D, Stein H, Gabites J (2013) Geology, mineralization and geochronological
 1310 constraints of the Mirador Cu-Au porphyry district, southeast Ecuador. *Econ Geol*
 1311 108:11-35.
- 1312 Dutrizac JE (1976) Reactions in cubanite and chalcopyrite: *Can Mineral* 14:172–181
- 1313 Ebel DS, Naldrett AJ (1997) Crystallization of sulfide liquids and the interpretation of ore
 1314 composition. *Can J Earth Sci* 34:352-365.
- 1315 Eckstrand OR (2005) Ni-Cu-Cr-PGE mineralization types: Distribution and classification. *In:*
 1316 *Exploration for Platinum Group Element Deposits* Mungall JE, (ed) Mineralogical
 1317 Association of Canada, Short Course Notes Vol 35, p 487-490
- 1318 Elliott RP (1965) Constitution of binary alloys. 877 p. McGraw-Hill NEW YORK
- 1319 Farrow CEG, Lightfoot PC (2002) Sudbury PGE revisited: Toward an integrated model. *In: The*
 1320 *Geology, Geochemistry, Mineralogy and Mineral Beneficiation of Platinum-Group*
 1321 *Elements. Spec. Vol 54. Cabri LJ, (ed), p 237-297*
- 1322 Fleet ME, Chryssoulis SL, Stone WE, Weisener CG (1993) Partitioning of platinum-group
 1323 elements and Au in the Fe-Ni-Cu-S system: experiments on the fractional crystallization
 1324 of sulphide melt. *Contrib Mineral Petrol* 115:36-44
- 1325 Fleet, M.E., Crocket, J.H., Liu, M., Stone, W.E. (1999) Laboratory partitioning of platinum-
 1326 group elements (PGE) and gold with application of magmatic sulfide -PGE deposits.
 1327 *Lithos* 47:127-142.
- 1328 Fonseca RO, Campbell IH, O'Neill HSC, Allen CM (2009) Solubility of Pt in sulphide mattes:
 1329 implications for the genesis of PGE-rich horizons in layered intrusions. *Geochim*
 1330 *Cosmochim Acta* 73:5764-5777
- 1331 Fonseca RO, Mallmann G, O'Neill HSC, Campbell IH, Laurenz V (2011) Solubility of Os and Ir
 1332 in sulfide melt: Implications for Re/Os fractionation during mantle melting. *Earth Planet*
 1333 *Sci Lett* 311:339-350

- 1334 Fortin M-A, Riddle J, Desjardins-Langlais, Y, Baker DR. (2015), The effect of water on the
 1335 sulfur concentration at sulfide saturation (SCSS) in natural melts. *Geochim Cosmochim*
 1336 *Acta* doi: <http://dx.doi.org/10.1016/j.gca.2015.03.022>
- 1337 Foustoukos DI, Bizimis M, Frisby C, Shirey SB (2015) Redox controls on Ni-Fe-PGE
 1338 mineralization and Re/Os fractionation during serpentinization of abyssal peridotite.
 1339 *Geochim Cosmochim Acta*; in press.
- 1340 Gaetani GA, Grove TL (1997) Partitioning of moderately siderophile elements among olivine,
 1341 silicate melt, and sulfide melt: constraints on core formation in the Earth and Mars.
 1342 *Geochim Cosmochim Acta* 61:1829-1846
- 1343 Godel, B. (2007) Rôle des liquides sulfurés dans la formation des minéralisations riches en
 1344 éléments du groupe du platine: applications au complexe du Bushveld (Afrique du Sud)
 1345 et au Complexe de Stillwater (États-Unis), Ph.D., p. 367. Université du Québec à
 1346 Chicoutimi
- 1347 Godel B, Barnes S-J (2008) Platinum-group elements in sulfide minerals and the whole rock of
 1348 the J-M Reef (Stillwater complex): Implication for the formation of the reef. *Chem Geol*
 1349 248:272-294
- 1350 Godel B, Barnes S-J, Maier WD (2007) Platinum-group elements in sulphide minerals, platinum-
 1351 group minerals, and the whole rocks of the Merensky Reef (Bushveld Complex, South
 1352 Africa): Implication for the Formation of the Reef. *J Petrol* 48:1569-1604
- 1353 Grant RW, Bite A (1984) Sudbury quartz diorite offset dykes. *In: The geology and ore deposits*
 1354 *of the Sudbury Structure. Special Volume 1.* Pye EG, Naldrett AJ, Giblin PE, (eds).
 1355 Ontario Geological Survey, p 275-301
- 1356 Grinenko, LN (1966) Sulphur isotope composition of sulphides of the Talnakh copper–nickel
 1357 deposit (Noril'sk region) in light of its origin. *Geokhimiya* 4:15-30 (in Russian).
- 1358 Grinenko LI (1985) Sources of sulfur of the nickeliferous and barren gabbro-dolerite intrusions
 1359 of the northwestern Siberian platform. *Int Geol Rev* 27:695-708
- 1360 Groves DI, Goldfarb RJ, Gebre-Mariam M, Hagemann, S, Robert F. (1998). Orogenic gold
 1361 deposits: a proposed classification in the context of their crustal distribution and
 1362 relationship to other gold deposit types. *Ore Geol Rev* 13: 7-27
- 1363 Hanley, J.J., Mungall, J.E., Pettke, T., Spooner, E.T.C., and Bray, C.J. (2008) Fluid and halide
 1364 melt inclusions of magmatic origin in the Ultramafic and Lower Banded Series,
 1365 Stillwater Complex, Montana, USA. *J Petrol* 49:1133-1160.
- 1366 Harmer RE, Sharpe MR (1985) Field Relations and Strontium Isotope Systematics of the
 1367 Marginal Rocks of the Eastern Bushveld Complex. *Econ Geol* 80:813-837
- 1368 Harris C, Pronost JJM, Ashwal L.D., Cawthorn RG, (2005) Oxygen and hydrogen isotope
 1369 stratigraphy of the Rustenburg Layered Suite, Bushveld Complex: constraints on crustal
 1370 contamination. *J Petrol* 45:579-601
- 1371 Hart SR, Kinloch ED (1989) Osmium isotope systematics in Witwatersrand and Bushveld ore
 1372 deposits. *Econ Geol* 84:1651-1655
- 1373 Harvey J, Warren JM, Shirey SB (2015) Mantle sulfides and their role in Re-Os-Pb
 1374 geochronology. *Rev Mineral Geochem* v.81: xxx-xxx.
- 1375 Hauri EH (2002) Osmium isotopes and mantle convection. *Philos Trans R Soc Lond A* 360:371-
 1376 2382
- 1377 Helmy HM, Ballhaus C, Wohlgemuth-Ueberwasser C, Fonseca RO, Laurenz V (2010)
 1378 Partitioning of Se, As, Sb, Te and Bi between monosulfide solid solution and sulfide
 1379 melt–Application to magmatic sulfide deposits. *Geochim Cosmochim Acta* 74:6174-6179

- 1380 Helmy HM, Ballhaus C, Fonseca RO, Wirth R, Nagel T, Tredoux M (2013a) Noble metal
 1381 nanoclusters and nanoparticles precede mineral formation in magmatic sulphide melts.
 1382 *Nat Commun* 4. doi:10.1038/ncomms3405
- 1383 Helmy HM, Ballhaus C, Fonseca RO, Nagel TJ (2013b) Fractionation of platinum, palladium,
 1384 nickel, and copper in sulfide–arsenide systems at magmatic temperature. *Contrib Mineral
 1385 Petrol* 166:1725-1737
- 1386 Helz, RT (1995) The Stillwater Complex, Montana; a subvolcanic magma chamber? *Am Mineral
 1387* 80: 1343-1346
- 1388 Henrique-Pinto R, Barnes S-J, Savard DD, Mehdi S (2015) Quantification of Metals and Semi-
 1389 Metals in Carbon-Rich Rocks: A New Sequential Protocol Including Extraction from
 1390 Humic Substances. *Geostandards and Geoanalytical Research* doi:10.1111/j.1751-
 1391 908X.2015.00340.x
- 1392 Hinchey JG, Hattori KH (2005) Magmatic mineralization and hydrothermal enrichment of the
 1393 High Grade Zone at the Lac des Iles Palladium mine, northern Ontario, Canada. *Mineral.
 1394 Deposita* 40:13-23
- 1395 Hoffman E, MacLean WH (1976) Phase relations of michenerite and merenskyite in the Pd-Bi-
 1396 Te system. *Econ Geol* 71:1461-1468
- 1397 Holwell DA, Keays RR (2014) The formation of low-volume, high-tenor magmatic PGE-Au
 1398 sulfide mineralization in closed systems: Evidence from precious and base metal
 1399 geochemistry of the Platinova Reef, Skaergaard intrusion, East Greenland. *Econ Geol
 1400* 109:387-406
- 1401 Holwell D, McDonald I, (2007) Distribution of platinum-group elements in the Platreef at
 1402 Overysel, northern Bushveld Complex: a combined PGM and LA-ICP-MS study. *Contrib
 1403 Mineral Petrol* 154:171-190.
- 1404 Holwell D, Boyce A, McDonald I, (2007) Sulfur isotope variations within the Platreef Ni-Cu-
 1405 PGE deposit: Genetic implications for the origin of sulfide mineralization. *Econ Geol
 1406* 102:1091-1110.
- 1407 Horan MF, Morgan JW, Grauch RI, Coveney JB Jr, Murowchick JB, Hulbert LJ (1994)
 1408 Rhenium and osmium isotopes in black shales and Ni-Mo-PGE –rich sulfide layers,
 1409 Yukon Territory, Canada, and Hunan and Guizhou provinces, China. *Geochim
 1410 Cosmochim Acta* 58: 257-265
- 1411 Horan MF, Morgan JW, Walker RJ, Cooper RW (2001) Re-Os isotopic constraints on magma
 1412 mixing in the Peridotite Zone of the Stillwater Complex, Montana USA. *Contrib Mineral
 1413 Petrol* 141: 446-457
- 1414 Hutchinson D, Kinnaird JA (2005) Complex multistage genesis for the Ni–Cu–PGE
 1415 mineralisation in the southern region of the Platreef, Bushveld Complex, South Africa.
 1416 *Trans Inst Min Metall* 114:208-224
- 1417 Junge M, Oberthür T, Melcher F (2014) Cryptic variation of chromite chemistry, platinum group
 1418 element and platinum group mineral distribution in the UG-2 chromitite: An example
 1419 from the Karee Mine, western Bushveld Complex, South Africa. *Econ Geol* 109:795-810
- 1420 Keays RR, Lightfoot PC (2004) Formation of Ni–Cu–Platinum Group Element sulfide
 1421 mineralization in the Sudbury impact melt sheet. *Mineral Petr* 82: 217-258
- 1422 Kerr A, Leitch AM (2005) Self-destructive sulfide segregation systems and the formation of
 1423 high-grade magmatic ore deposits. *Econ Geol* 100:311-332
- 1424 Ketris M, Yudovich YE (2009) Estimations of Clarkes for Carbonaceous biolithes: World
 1425 averages for trace element contents in black shales and coals. *Int J Coal Geol* 78:135-148

- 1426 Kinloch ED (1982) Regional trends in the platinum-group mineralogy of the Critical Zone of the
1427 Bushveld Complex, South Africa. *Econ Geol* 77:1328-1347
- 1428 Kinnaird JA (2005). Geochemical evidence for multiphase emplacement in the southern Platereef.
1429 *Trans Inst Min Metall* 114, 225-242.
- 1430 Kiseeva ES, Wood BJ (2013) A simple model for chalcophile element partitioning between
1431 sulphide and silicate liquids with geochemical applications. *Earth Planet Sci Lett* 383:68-
1432 81
- 1433 Klöck W, Palme H, Tobschall H (1986) Trace elements in natural metallic iron from Disko
1434 Island, Greenland. *Contrib Mineral Petrol* 93:273-282
- 1435 Kozyrev SM, Komarova MZ, Emelina LN, Oleshkevich OI, Yakovleva OA, Lyalinov DV,
1436 Maximov VI (2002) The Mineralogy and Behaviour of PGM During Processing of
1437 the Noril'sk-Talnakh PGE-Cu-Ni Ores. *In: Geology, Geochemistry, Mineralogy and*
1438 *Mineral Beneficiation of Platinum Group Elements* Cabri LJ, (ed) Canadian Institute of
1439 Mining, Metallurgy and Petroleum, Spec. Vol 54: 757-791
- 1440 Krough TE, Davis DW, Corfu F (1984) precise U-Pb zircon and baddeleyite ages from the
1441 Sudbury area. *In The Geology and ore deposits of the Sudbury Structure*, Pye EG,
1442 Naldrett AJ, Giblin PE (eds) Ontario Geological Survey Spec Vol 1: 431-447.
- 1443 Kruger FJ (1994) The Sr-isotopic stratigraphy of the western Bushveld Complex. *South Afr J*
1444 *Geol* 97:393-398
- 1445 Kullerud G, Yund RA, Moh GH, (1969) Phase relations in the Cu-Fe-S, Cu-Ni-S and Fe-Ni-S
1446 systems. *Econ Geol Monograph* 4:323-343
- 1447 Lambert DD, Morgan JW, Walker RJ, Shirey SB, Carlson RW, Zientek ML, Koski MS (1989)
1448 Re-Os and Sm-Nd isotope systematics of the Stillwater Complex. *Science* 244:1169-1174
- 1449 Lambert DD, Walker RJ, Morgan JW, Shirey SB, Carlson RW, Zientek ML, Lipin BR, Koski
1450 MS, Cooper RW (1994) Re-Os and Sm-Nd isotopic geochemistry of the Stillwater
1451 Complex, Montana: Implications for the petrogenesis of the J-M Reef. *J Petrol* 35: 1717-
1452 1753
- 1453 Lambert DD, Foster JG, Frick LR, Ripley EM, Zientek ML (1998a) Geodynamics of magmatic
1454 Cu-Ni-PGE deposits: New insights from the Re-Os isotope system. *Econ Geol* 93: 121-
1455 136
- 1456 Lambert DD, Foster JC, Frick LM, Hoatson DM, Purvis, AC (1998b) Application of the Re-Os
1457 isotopic system to the study of Precambrian magmatic sulfide deposits of Western
1458 Australia. *Aust J Earth Sci* 45:265-284
- 1459 Lambert DD, Foster JG, Frick LR, Ripley EM (1999a) Re-Os isotope geochemistry of magmatic
1460 sulfide ore systems. *Rev in Econ Geol* 12:29-58
- 1461 Lambert DD, Frick LR, Foster JG, Li C, Naldrett AJ (1999b) Re-Os isotope systematics of the
1462 Voisey's Bay Ni-Cu-Co magmatic ore system, Labrador, Canada. *Lithos* 47: 69-88
- 1463 Lambert DD, Frick LR, Foster JG, Li C, Naldrett AJ (2000) Re-Os isotope systematics of the
1464 Voisey's Bay Ni-Cu-Co magmatic sulfide system, Labrador, Canada:II. Implications for
1465 parental magma chemistry, ore genesis, and metal redistribution. *Econ Geol* 95:867-888
- 1466 Laurenz V, Fonseca RO, Ballhaus C, Jochum KP, Heuser A, Sylvester PJ, (2013) The solubility
1467 of palladium and ruthenium in picritic melts: 2. The effect of sulfur. *Geochim*
1468 *Cosmochim Acta* 108:172-183
- 1469 Lavigne MJ, Michaud MJ (2001) Geology of North American Palladium Ltd's Roby Zone
1470 Deposit, Lac des Iles. *Explor Min Geol* 10:1-17

- 1471 Leshner CM, Burnham OM (2001) Multicomponent elemental and isotopic mixing in Ni-Cu-
1472 (PGE) ores at Kambalda, Western Australia. *Can Mineral* 39:421-446
- 1473 Li C, Naldrett AJ (2000) Melting reactions of gneissic inclusions with enclosing magma at
1474 Voisey's Bay, Labrador, Canada: Implications with respect to ore genesis. *Econ Geol*
1475 95:801-814.
- 1476 Li C, Ripley EM (2009) Sulfur contents at sulfide-liquid or anhydrite saturation in silicate melts:
1477 empirical equations and example applications. *Econ Geol* 104:405-412
- 1478 Li C, Barnes SJ, Makovicky E, Karup-Moller S, Makovicky M, Rose-Hansen J (1996)
1479 Partitioning of Ni, Cu, Ir, Rh, Pt and Pd between monosulfide solid solution and sulfide
1480 liquid: effects of composition and temperature. *Geochim Cosmochim Acta* 60:1231-1238
- 1481 Li C, Ripley EM, Merino E, Maier WD, 2004. Replacement of base metal sulfides by actinolite,
1482 epidote, calcite, and magnetite in the UG2 and Merensky Reef of the Bushveld Complex,
1483 South Africa. *Econ Geol* 99:0173-0184.
- 1484 Li Y, Audétat A (2012) Partitioning of V, Mn, Co, Ni, Cu, Zn, As, Mo, Ag, Sn, Sb, W, Au, Pb,
1485 and Bi between sulfide phases and hydrous basanite melt at upper mantle conditions.
1486 *Earth Planet Sci Lett* 355:327-340
- 1487 Li Y, Audétat A (2013) Gold solubility and partitioning between sulfide liquid, monosulfide
1488 solid solution and hydrous mantle melts: Implications for the formation of Au-rich
1489 magmas and crust–mantle differentiation. *Geochim Cosmochim Acta* 118:247-262
- 1490 Lightfoot PC, Keays RR (2005) Siderophile and chalcophile metal variations in flood basalts
1491 from the Siberian trap, Noril'sk region: Implications for the origin of the Ni-Cu-PGE
1492 sulfide ores. *Econ Geol* 100:439-462
- 1493 Lightfoot PC, Keays RR, Morrison GG, Bite A, Farrel K (1997) Geochemical relationships in
1494 the Sudbury igneous complex: Origin of the main mass and offset dikes. *Econ Geol*
1495 92:289-307
- 1496 Lightfoot PC, Keays RR, Evans-Lambwood D, Wheeler R (2012) S saturation history of Nain
1497 Plutonic Suite mafic intrusions: origin of the Voisey's Bay Ni–Cu–Co sulfide deposit,
1498 Labrador, Canada. *Mineral Deposita* 47:23-50
- 1499 Liu Y, Brenan J (2015) Partitioning of platinum-group elements (PGE) and chalcogens (Se, Te,
1500 As, Sb, Bi) between monosulfide-solid solution (MSS), intermediate solid solution (ISS)
1501 and sulfide liquid at controlled fO₂–fS₂ conditions. *Geochim Cosmochim Acta*
1502 159:139-161
- 1503 Locmelis M, Pearson NJ, Barnes SJ, Fiorentini ML (2011) Ruthenium in komatiitic chromite.
1504 *Geochim Cosmochim Acta* 75:3645-3661
- 1505 Lyubetskaya T, Korenaga J (2007) Chemical composition of Earth's primitive mantle and its
1506 variance: 1. Method and results. *J Geophys Res B: Solid Earth* 112 B03211,
1507 doi:10.1029/2005JB00422
- 1508 McCandless TE, Ruiz J (1991) Osmium isotopes and crustal sources for platinum-group
1509 mineralization in the Bushveld Complex, South Africa. *Geology* 19:1225-1228
- 1510 McDonald I, Holwell DA, (2007) Did lower zone magma conduits store PGE-rich sulphides that
1511 were later supplied to the Platreef? *South African Jour. Geology* 110:611-616.
- 1512 McDonald I, Holwell D (2011) Geology of the northern Bushveld Complex and the setting and
1513 genesis of the Platreef Ni-Cu-PGE deposit: *Rev in Econ Geol* 17:297-327.
- 1514 McDonald I, Holwell DA, Armitage PE (2005) Geochemistry and mineralogy of the Platreef and
1515 “Critical Zone” of the northern lobe of the Bushveld Complex, South Africa: implications

- 1516 for Bushveld stratigraphy and the development of PGE mineralisation. *Mineral Deposita*
 1517 40: 526-549.
- 1518 McLaren CH, De Villiers JP (1982) The platinum-group chemistry and mineralogy of the UG2
 1519 chromitite layer of the Bushveld Complex. *Econ Geol*77:1348-1366
- 1520 Maier WD, Barnes S-J (2008) Platinum-group elements in the UG1 and UG2 chromitites, and
 1521 the Bastard reef, at Impala platinum mine, western Bushveld Complex, South Africa:
 1522 Evidence for late magmatic cumulate instability and reef constitution. *South Afr J Geol*
 1523 111:159-176
- 1524 Maier WD, de Klerk L, Blaine J, Manyeruke T, Barnes SJ, Stevens MVA, Mavrogenes JA
 1525 (2008) Petrogenesis of contact-style PGE mineralization in the northern lobe of the
 1526 Bushveld Complex: comparison of data from the farms Rooipoort, Townlands, Drenthe
 1527 and Nonnenwerth. *Mineral Deposita* 43:255-280
- 1528 Maier WD, Barnes SJ, Campbell IH, Fiorentini ML, Peltonen P, Barnes SJ, Smithies RH (2009)
 1529 Progressive mixing of meteoritic veneer into the early Earth's deep mantle. *Nature*
 1530 460:620-623.
- 1531 Maier W, Barnes S-J, Groves D (2013) The Bushveld Complex, South Africa: formation of
 1532 platinum–palladium, chrome-and vanadium-rich layers via hydrodynamic sorting of a
 1533 mobilized cumulate slurry in a large, relatively slowly cooling, subsiding magma
 1534 chamber. *Mineral Deposita* 48:1-56
- 1535 Makovicky E (2002) Ternary and quaternary phase systems in PGE. *In: The Geology,*
 1536 *Geochemistry, Mineralogy and Mineral Beneficiation of the Platinum-group elements.*
 1537 Cabri LJ, (ed) Canadian Institute of Mining, Metallurgy and Petroleum, Special Volume
 1538 54,p 131-175
- 1539 Makovicky M, Makovicky, E. and Rose-Hansen, J. (1986) Experimental studies on the solubility
 1540 and distribution of platinum-goup elements in base metal sulfides in platinum deposits.
 1541 *In: Metallogeny of Basic and Ultrabasic Rocks.* Gallagher MJ, (Ed) Institute Mining and
 1542 Metallurgy
- 1543 Malitch KN, Latypov RM (2011) Re–Os and S isotope constraints on timing and source
 1544 heterogeneity of PGE-Cu-Ni sulfide ores: A case study at the Talnakh ore junction,
 1545 Noril'sk Province, Russia. *Can Mineral* 43:1653-1677
- 1546 Malitch KN, Latypov RN, Badinina IU, SluzhenekinSF (2014) Insights into ore genesis of Ni-
 1547 Cu-PGE sulfide deposits of the Noril'sk Province (Russia): Evidence from copper and
 1548 sulfur isotopes. *Lithos* 204: 172-187.
- 1549 Mallmann G, O'Neill HStC, (2007) the effect of oxygen fugacity on the partitioning of rhenium
 1550 between crystals and silicate melt during mantle melting. *Geochim Cosmochim Acta*
 1551 71:2837-2857
- 1552 Marcantonio F, Zindler A, Reisberg L, Mathez EA (1993) Re-Os systematics in chromitites from
 1553 the Stillwater Complex, Montana, USA. *Geochim Cosmochim Acta* 57:4029-4037.
- 1554 Martin CE (1989) Re-Os isotopic investigation of the Stillwater Complex, Montana. *Earth and*
 1555 *Planet Sci Lett* 93; 336-344
- 1556 Mathez E, Mey J (2005) Character of the UG2 chromitite and host rocks and petrogenesis of its
 1557 pegmatoidal footwall, northeastern Bushveld Complex. *Econ Geol*100, 1617-1630.
- 1558 Mavrogenes JA, O'Neill HSC (1999) The relative effects of pressure, temperature and oxygen
 1559 fugacity on the solubility of sulphide in mafic magma. *Geochim Cosmochim Acta*
 1560 63:1173-1180.

- 1561 Merkle RKW (1992) Platinum-group minerals in the middle group of chromitite layers at
 1562 Marikana, western Bushveld Complex: indications for collection mechanisms and
 1563 postmagmatic modification. *Can J Earth Sci* 29:209-221
- 1564 Moffatt WG (1979a) The handbook of binary phase diagrams, 3 vol.: Schenectady, New York,
 1565 Genium Publishing Corp.
- 1566 Moffatt WG (1979b) The index to binary phase collections, 1st ed.: Schenectady, New
 1567 York, General Electric Company.
- 1568 Morgan JW, Wandless GA, Petrie RK, Irving AJ (1981) Composition of the Earth's upper
 1569 mantle-I. Siderophile trace elements in ultramafic nodules. *Tectonophysics* 75:47-67
- 1570 Morgan JW, Walker RL, Horan MF, Beary ES, Naldrett AJ (2002) ^{190}Pt - ^{186}Os and ^{187}Re - ^{187}Os
 1571 systematics of the Sudbury Igneous Complex, Ontario. *Geochim Cosmochim Acta*
 1572 66:273-290
- 1573 Mudd GM (2012) Key trends in the resource sustainability of platinum group elements. *Ore Geol*
 1574 *Rev* 46:106-117
- 1575 Mungall JE, Brenan J (2014) Partitioning of platinum-group elements and Au between sulfide
 1576 liquid and basalt and the origins of mantle-crust fractionation of the chalcophile elements.
 1577 *Geochim Cosmochim Acta* 125:265-289
- 1578 Mungall JE, Andrews DRA, Cabri LJ, Sylvester PJ, Tubrett M (2005) Partitioning of Cu, Ni, An,
 1579 and platinum-group elements between monosulfide solid solution and sulfide melt under
 1580 controlled oxygen and sulfur fugacities. *Geochim Cosmochim Acta* 69:4349-4360
- 1581 Naldrett AJ (2004) Magmatic sulfide deposits, geology, geochemistry and exploration. Springer,
 1582 Berlin
- 1583 Naldrett AJ (2011) Fundamentals of magmatic sulfide deposit. *In: Magmatic Ni-Cu and PGE*
 1584 *deposits: Geology, Geochemistry, and Genesis. Rev in Econ Geol Vol 17. Li C, Ripley*
 1585 *EM, (eds). Society of Economic Geologists, Lillteton, p 1-50*
- 1586 Naldrett AJ, Li C (2007) The Voisey's Bay deposit, Labrador, Canada. *In: Mineral deposits of*
 1587 *Canada: a synthesis of major deposit-types, district metallogeny, the evolution of*
 1588 *geological provinces, and exploration methods. Goodfellow WD (ed) Geol Assoc of*
 1589 *Canada, Mineral Deposits Division, Spec Pub 5, 387-407*
- 1590 Naldrett AJ, Gasparrini E, Barnes SJ, Von Gruenewaldt G, Sharpe M (1986) The Upper Critical
 1591 Zone of the Bushveld Complex and the origin of Merensky-type ores. *Econ Geol*
 1592 81:1105-1117
- 1593 Naldrett A, Kinnaird J, Wilson A, Yudovskaya M, Chunnnett G (2011) Genesis of the PGE-
 1594 enriched Merensky reef and chromitite seams of the Bushveld Complex. *Rev in Econ*
 1595 *Geol* 17:235-296
- 1596 Oberthür T (2002) Platinum-group element mineralization of the Great Dyke, Zimbabwe. *In:*
 1597 *The Geology, Geochemistry, Mineralogy and Mineral Beneficiation of Platinum-Group*
 1598 *Elements. Cabri LJ (ed.) Canadian Institute of Mining, Metallurgy and Petroleum,*
 1599 *Special Vol 54, p 483-506*
- 1600 Oberthür T, Cabri LJ, Weiser TW, McMahon G, Müller P (1997) Pt, Pd and other trace elements
 1601 in sulfides of the main sulfide zone, Great Dyke, Zimbabwe: a reconnaissance study. *Can*
 1602 *Mineral* 35:597-609
- 1603 O'Driscoll B, Gonzáles Jiménez JM (2015) Platinum group minerals. *Rev Mineral Geochem*
 1604 v.81: xxx-xxx
- 1605 Pagé P, Barnes S-J, Bédard JH, Zientek ML (2012) In situ determination of Os, Ir, and Ru in
 1606 chromites formed from komatiite, tholeiite and boninite magmas: implications for

- 1607 chromite control of Os, Ir and Ru during partial melting and crystal fractionation. *Chem*
 1608 *Geol* 302:3-15
- 1609 Pagé P and Barnes S-J (2013) [Improved in-situ determination of PGE concentration of chromite](#)
 1610 [by LA-ICP-MS: Towards a better understanding](#). *In: Mineral Deposits Research for a*
 1611 *High Tech World 12th Biennial SGA Meeting* p. 1050-1053
- 1612 Park J-W, Campbell I.H., Eggins S.M. (2012) Enrichment of Rh, Ru, Ir and Os in Cr spinels
 1613 from oxidized magmas: evidence from the Ambae volcano, Vanuatu. *Geochim*
 1614 *Cosmochim Acta* 78:28-50
- 1615 Pasava J, Oszczepalski S, Du A (2010) Re–Os age of non-mineralized black shale from the
 1616 Kupferschiefer, Poland, and implications for metal enrichment. *Mineral Deposita* 45:189-
 1617 199
- 1618 Patten C, Barnes SJ, Mathez EA (2012) Textural variations in MORB sulfide droplets due to
 1619 differences in crystallization history. *Can Mineral* 50:675-692
- 1620 Patten C, Barnes S-J, Mathez EA, Jenner FE (2013) Partition coefficients of chalcophile
 1621 elements between sulfide and silicate melts and the early crystallization history of sulfide
 1622 liquid: LA-ICP-MS analysis of MORB sulfide droplets. *Chem Geol* 358:170-188
- 1623 Peach CL, Mathez EA, Keays RR (1990) Sulfide melt-silicate melt distribution coefficients for
 1624 noble metals and other chalcophile elements as deduced from MORB: implications for
 1625 partial melting. *Geochim Cosmochim Acta* 54:3379-3389
- 1626 Penberthy C, Oosthuyzen E, Merkle R (2000) The recovery of platinum-group elements from the
 1627 UG-2 chromitite, Bushveld Complex—a mineralogical perspective. *Miner Petrol* 68:213-
 1628 222
- 1629 Penniston-Dorland SC, Wing BA, Nex PA, Kinnaird JA, Farquhar J, Brown M,
 1630 Sharman ER (2008) Multiple sulfur isotopes reveal a magmatic origin for the Platreef
 1631 platinum group element deposit, Bushveld Complex, South Africa. *Geology* 36:979-982
- 1632 Pentek A, Molnar F, Watkinson DH, Jones PC (2008) Footwall-type Cu-Ni-PGE Mineralization
 1633 in the Broken Hammer Area, Wisner Township, North Range, Sudbury Structure. *Econ*
 1634 *Geol* 103:1005-1028
- 1635 Prendergast MD, Wilson AH (1989) The Great Dyke of Zimbabwe II: mineralisation and
 1636 mineral deposits. *In: Magmatic sulphides the Zimbabwe volume* Prendergast MD, Jones
 1637 MJ, (eds). Institution of Mining and Metallurgy, London, p 21-42
- 1638 Prichard HM, Barnes S-J, Maier WD, Fisher PC (2004) Variations in the nature of the platinum-
 1639 group minerals in a cross-section through the Merensky Reef at Impala Platinum:
 1640 Implications for the mode of formation of the reef. *Can Mineral* 42:423-437
- 1641 Pruseth K, Palme H (2004) The solubility of Pt in liquid Fe-sulfides. *Chem Geol* 208:233-245
- 1642 Queffurus M, Barnes S-J (2014) Selenium and sulfur concentrations in country rocks from the
 1643 Duluth Complex Minnesota, USA: Implications for formation of the Cu-Ni_PGE
 1644 sulfides. *Econ Geol* 109:785-794
- 1645 Reisberg R, Tredoux M, Harris C, Coftier A, Chaumba J (2011) Re and Os distribution and Os
 1646 isotope composition of the Platreef at the Sandsloot-Mogolakwena mine, Bushveld
 1647 Complex, South Africa. *Chem Geol* 281:352-363
- 1648 Rice A, Moore J (2001) Physical modeling of the formation of komatiite-hosted nickel deposits
 1649 and a review of the thermal erosion paradigm. *Can Mineral* 39:491-503
- 1650 Richardson SH, Shirey SB (2008) Continental mantle signature of Bushveld magmas and coeval
 1651 diamonds. *Nature* 453:910-913
- 1652 Righter K, Hauri EH (1998) Compatibility of rhenium in garnet during mantle melting and
 magma genesis. *Science* 280:1737-1741

- 1653 Righter K, Campbell AJ, Humayun M, Hervig RL (2004) Partitioning of Ru, Rh, Pd, Re, Ir and
 1654 Au between Cr-bearing spinel, olivine, pyroxene and silicate melts. *Geochim Cosmochim*
 1655 *Acta* 68:867-880
- 1656 Ripley EM, Al-Jassar TJ (1987) Sulfur and oxygen isotope studies of melt - country rock
 1657 interaction, Babbitt Cu-Ni deposit, Duluth Complex, Minnesota. *Econ Geol* 82:87-107
- 1658 Ripley EM, Li C (2003) Sulfur isotope exchange and metal enrichment in the formation of
 1659 magmatic Cu-Ni-(PGE) deposits. *Econ Geol* 98:635-641
- 1660 Ripley EM, Li C (2013) Sulfur isotope exchange and metal enrichment in the formation of
 1661 magmatic Cu-Ni-(PGE) deposits. *Econ Geol* 98:635-641
- 1662 Ripley EM, Brophy JG, Li C (2002) Copper solubility in a basaltic melt and sulfide
 1663 liquid/silicate melt partition coefficients of Cu and Fe. *Geochim Cosmochim Acta*
 1664 66:2791-2800
- 1665 Ripley EM, Lightfoot PC, Li C, Elswick ER (2003) Sulfur isotopic studies of continental basalts
 1666 in the Noril'sk region: implications for the association between lavas and ore-bearing
 1667 intrusions. *Geochim Cosmochim Acta* 67: 2805-2817
- 1668 Rose, D., Viljoen, F., Knoper, M., and Rajesh, H. (2011) Detailed assessment of platinum-group
 1669 minerals associated with chromitite stringers in the Merensky Reef of the eastern
 1670 Bushveld Complex, South Africa. *Can Mineral* 49:1385-1396.
- 1671 Roy-Barman M, Wasserburg GJ, Papanastasiou DA, Chaussidon M (1998) Osmium isotopic
 1672 compositions and Re-Os concentrations in sulfide globules from basaltic glasses. *Earth*
 1673 *Planet Sci Lett* 154:331-347
- 1674 Savitsky E, Polyakova V, Gorina N, and Roshan N (1978) Physical metallurgy of platinum
 1675 minerals (translated from revised 1975 Russian edition by I.V. Savin): Moscow, MIR
 1676 Publishers, p. 395.
- 1677 Schoenberg R, Kruger FJ, Nagler TF, Meisel T, Kramers, JD (1999) PGE enrichment in
 1678 chromitite layers and the Merensky Reef of the western Bushveld Complex; a Re-Os and
 1679 Rb-Sr isotope study. *Earth Planet Sci Lett* 172: 49-64.
- 1680 Schoenberg R, Nagler TF, Gnos E, Kramers JD, Kamber, BS (2003) The source of the Great
 1681 Dyke, Zimbabwe, and its tectonic significance: Evidence from Re-Os isotopes. *J Geol*
 1682 565-578
- 1683 Seat Z, Beresford SW, Grguric BA, Gee MM, Grassineau NV (2009) Reevaluation of the role of
 1684 external sulfur addition in the genesis of Ni-Cu-PGE deposits: Evidence from the Nebo-
 1685 Babel Ni-Cu-PGE deposit, West Musgrave, Western Australia. *Econ Geol* 104:521-538
- 1686 Selby D, Zhao XF (2012) The Early Cretaceous Yangzhaiyu Lode Gold Deposit, North China
 1687 Craton: A link between carton reactivation and gold veining. *Econ Geol* 107:43-79
- 1688 Sharpe MR, Hulbert LJ (1985) Ultramafic sills beneath the eastern Bushveld Complex:
 1689 Mobilized suspensions of early lower zone cumulates in a parental magma with boninitic
 1690 affinities. *Econ Geol* 80:849-871
- 1691 Shirey SB, Walker RJ (1998) The Re-Os isotope system in cosmochemistry and high-
 1692 temperature geochemistry. *Annu Rev Earth Planet Sci* 26:423-500
- 1693 Sinyakova E, Kosyakov V (2007) Experimental modeling of zoning in copper-nickel sulfide
 1694 ores. *Dokl Earth Sci* 417:1380-1385
- 1695 Sinyakova E, Kosyakov V (2009) Experimental modeling of zonality of copper-rich sulfide ores
 1696 in copper-nickel deposits. *Dokl Earth Sci* 427:787-792

- 1697 Sinyakova E, Kosyakov V (2012) The behavior of noble-metal admixtures during fractional
1698 crystallization of As- and Co-containing Cu–Fe–Ni sulfide melts. *Russ Geol Geophys*
1699 53:1055-1076
- 1700 Sinyakova E, Kosyakov V (2014) The polythermal section of the Cu–Fe–Ni–S phase diagram
1701 constructed using directional crystallization and thermal analysis. *J Therm Anal Calorim*
1702 117:1085-1089
- 1703 Sluzhenikin S (2011) Platinum-copper-nickel and platinum ores of Noril'sk Region and their ore
1704 mineralization. *Russ J Gen Chem* 81:1288-1301
- 1705 Sluzhenikin SF, Krivolutskaya NA, Rad'ko VA, Malitch KN, Distler VA, Fedorenko VA (2014)
1706 Ultramafic-mafic intrusions, volcanic rocks and PGE-Cu-Ni sulfide deposits of the
1707 Noril'sk Province, Polar Siberia. Field trip guidebook. 12th International Platinum
1708 Symposium IGG UB RAS, Yekaterinburg
- 1709 Smith J, Holwell DA, McDonald I (2014) Precious and base metal geochemistry and mineralogy
1710 of the Grasvalley Norite–Pyroxenite–Anorthosite (GNPA) member, northern Bushveld
1711 Complex, South Africa: implications for a multistage emplacement. *Mineral Deposita*
1712 49:667-692
- 1713 Steele TW, Levin J, Copelwitz I (1975) Preparation and certification of a reference sample of a
1714 precious metal ore. National Institute for Metallurgy, p 1696-1975
- 1715 Stein H, Markey R, Morgan J, Hannah J, Scherstén A (2001) The remarkable Re–Os
1716 chronometer in molybdenite: how and why it works. *Terra Nova* 13:479-486
- 1717 Stone WE, Crocket JH, Fleet ME (1990) Partitioning of palladium, iridium, platinum and gold
1718 between sulfide liquid and basalt melt at 1200°C. *Geochim Cosmochim Acta* 54:2341-
1719 2344
- 1720 Teng HH 2013. How ions and molecules organize to form crystals. *Elements* 9:189-194.
- 1721 Thériault R, Barnes SJ (1998) Compositional variations in Cu-Ni-PGE sulfides of the Dunka
1722 Road deposit, Duluth Complex, Minnesota: the importance of combined assimilation and
1723 magmatic processes. *Can Mineral* 36:869-886
- 1724 Tolstykh ND, Sidorov EG, Kozlov AP (2004) Platinum-group minerals in lode and placer
1725 deposits associated with the Ural-Alaskan-type Gal'moënan complex, Koryak–
1726 Kamchatka platinum belt, Russia. *Can Mineral* 42:619-630
- 1727 Torgashin AS (1994) Geology of the massive and copper ores of the western part of the
1728 Oktyabr'sky deposit. *In: Proceedings of the Sudbury Noril'sk Symposium*. Lightfoot P.C.,
1729 Naldrett AJ, (eds). Ontario Geological Survey, Spec vol 5, Toronto, p 231-241
- 1730 Tredoux M, Lindsay NM, Davies G, McDonald I (1995) The fractionation of platinum-group
1731 elements in magmatic systems, with the suggestion of a novel causal mechanism. *South*
1732 *Afr J Geol* 98:157-167
- 1733 Tuba G, Molnár F, Ames DE, Péntek A, Watkinson DH, Jones PC (2014) Multi-stage
1734 hydrothermal processes involved in “low-sulfide” Cu (–Ni)–PGE mineralization in the
1735 footwall of the Sudbury Igneous Complex (Canada): Amy Lake PGE zone, East Range.
1736 *Mineral Deposita* 49:7-47
- 1737 Viljoen MJ (1999) The nature and origin of the Merensky Reef of the western Bushveld
1738 Complex based on geological facies and geophysical data. *South Afr J Geol* 102:221-239
- 1739 Walker, R.J. (2009) Highly siderophile elements in the Earth, Moon and Mars: update and
1740 implications for planetary accretion and differentiation. *Chem Erde-Geochem* 69(2):101-
1741 125.

- 1742 Walker R, Morgan J, Naldrett A, Li C, Fassett J (1991) Re-Os isotope systematics of Ni-Cu
1743 sulfide ores, Sudbury Igneous Complex, Ontario: evidence for a major crustal
1744 component. *Earth Planet Sci Lett* 105:416-429
- 1745 Walker RJ, Morgan JW, Horan MF, Czamanske GK, Krogstad EJ, Fedorenko VA, Kunilov EJ
1746 (1994) Re-Os isotopic evidence for an enriched-mantle source for the Noril'sk-type, ore-
1747 bearing intrusions, Siberia. *Geochim Cosmochim Acta* 58:4179-4197
- 1748 Weiser T (2002) Platinum-group minerals (PGM) in placer deposits. *In: Geology, Geochemistry,
1749 Mineralogy and Mineral Beneficiation of Platinum Group Elements*. Cabri LJ (ed)
1750 Canadian Institute of Mining, Metallurgy and Petroleum, Spec. Vol. 54, p. 721-756
- 1751 Wilson AH, Brown RT (2005) Exploration and mining perspective of the Main Sulfide Zone of
1752 the Great Dyke, Zimbabwe—case study of the Hartley Platinum Mine. *In: Exploration
1753 for Platinum Group Element Deposits* Mungall JE, (ed) Mineralogical Association of
1754 Canada, Short Course Notes Vol 35, p 409-429
- 1755 Wirth R, Reid D, Schreiber A (2013) Nanometer-sized platinum-group minerals (PGM) in base
1756 metal sulfides: New evidence for an orthomagmatic origin of the Merensky Reef PGE ore
1757 deposit, Bushveld Complex, South Africa. *Can Mineral* 51:143-155
- 1758 Xiong Y, Wood SA (2001) Hydrothermal transport and deposition of rhenium under subcritical
1759 conditions (up to 200° C) in light of experimental studies. *Econ Geol* 96: 1429-1444.
- 1760 Zientek ML (2012) Magmatic ore deposits in layered intrusions - Descriptive model for reef-type
1761 PGE and contact-type Cu-Ni-PGE deposits. U.S. Geological Survey Open File, 2012-
1762 1010 <http://pubs.usgs.gov/of/2012/1010/contents/OF12-1010.pdf>
- 1763 Zientek ML, Foose MP, Mei L (1986) Palladium, platinum, and rhodium contents of rocks near
1764 the lower margin of the Stillwater Complex, Montana. *Econ Geol* 81:1169-1178
- 1765 Zientek ML, Fries T, Vian R (1990) As, Bi, Hg, S, Sb, Sn and Te geochemistry of the JM Reef,
1766 Stillwater Complex, Montana: constraints on the origin of PGE-enriched sulfides in
1767 layered intrusions. *J Geochem Explor.* 37:51-73
- 1768 Zientek ML, Likhachev AP, Kunilov VE, Barnes S-J, Meier AL, Carlson RR, Briggs PH, Fries
1769 TL, Adrian BM (1994) Cumulus processes and the composition of magmatic ore
1770 deposits: examples from the Talnakh District, Russia. *In: Proceedings of the Sudbury-
1771 Noril'sk Symposium* Lightfoot PC, Naldrett AJ, (eds). Ontario Geological Survey, Spec.
1772 Publ. 5, p 373-392
- 1773 Zientek ML, Cooper RW, Corson SR, Geraghty EP (2002) Platinum-group element
1774 mineralization in the Stillwater Complex, Montana. *In: Geology, Geochemistry,
1775 Mineralogy and Mineral Beneficiation of Platinum Group Elements*. Cabri LJ (ed)
1776 Canadian Institute of Mining, Metallurgy and Petroleum, Spec. Vol. 54, p. 459 – 481
1777

Figure captions

- 1780 **Figure 1** Main producers of Pt and Pd in 2013, calculated from Cowley (2013)
- 1781 **Figure 2** Geology of the Bushveld Complex showing the location of the 3 main deposits,
1782 Platreef, Merensky reef and UG2 reef. (modified after Barnes and Maier 2002a)
- 1783 **Figure 3** Geology of the Noril'sk-Talnakh area showing the location of the Noril'sk 1, Talnakh
1784 and Kharaelakh intrusions. Modified after Zientek et al. (1994)

- 1785 **Figure 4** Simplified geology of Zimbabwe showing the location of the Great Dyke. Modified
1786 after Prendergast and Wilson (1989)
- 1787 **Figure 5** Geology of the Stillwater Complex showing the position of the JM reef. Modified after
1788 Godel and Barnes (2008)
- 1789 **Figure 6** Geology of the Lac des Iles Complex modified after Djon and Barnes (2012)
- 1790 **Figure 7** Geology of Sudbury Igneous Complex showing location of the McCreey East deposit,
1791 modified after Dare et al. (2014).
- 1792 **Figure 8** Stratigraphic columns of Bushveld, Great Dyke and Stillwater showing the positions of
1793 the reefs. MR= Merensky, MSZ=Main sulphide zone, modified from figures of Barnes and
1794 Maier (2002a) Prendergast and Wilson (1989) Zientek et al. (2002)
- 1795 **Figure 9** Cross sections of the a) Noril'sk 1 and b) Oktrabr'sky deposits redrawn and simplified
1796 from figures in Torgashin (1994) and Sluzhenikin et al. (2014)
- 1797 **Figure 10** Zoned sulfide droplet from Noril'sk 1 (this work). Distribution of Fe, Cu, Ni
1798 determined by micro-XRF. Distribution of PGE determined by laser ablation ICP-MS. ^{108}Pd has
1799 been corrected for Cd and Zn interferences. ^{103}Rh has been corrected for Cu interference. ^{101}Ru
1800 has been corrected to Ni interference. Cb = Cubanite, Cp = Chalcopyrite. Pn = Pentlandite, Po =
1801 pyrrhotite.
- 1802 **Figure 11** Mantle normalized concentrations in pentlandite, pyrrhotite, chalcopyrite and pyrite
1803 data sources listed in Table 3.
- 1804 **Figure 12** Mantle normalized whole rock metal patterns for Noril'sk and Sudbury data sources
1805 listed in Table 4.
- 1806 **Figure 13** Results of mass balance calculations showing that pentlandite hosts Re and all the
1807 PGE except Pt, pyrrhotite hosts Re and all the PGE except Pd and Pt, pyrite also hosts Re and
1808 most PGE except Pd and Pt. Chalcopyrite is not a significant host of any of the PGE. Data from;
1809 Barnes et al. (2006); Godel et al. (2007); Barnes et al. (2008); Godel and Barnes (2008); Dare et
1810 al. (2011); Djon and Barnes (2012)
- 1811 **Figure 14** Mantle normalized whole rock metal patterns for PGE-dominated deposits. Data
1812 sources shown in Table 4
- 1813 **Figure 15** Concentrations of Sn, Sb, As, Bi, Te normalized to mantle values and plotted in order
1814 of compatibility with sulfide liquid. a) MORB, Upper Continental Crust and Black Shale; b)
1815 PGE dominated deposits; c) Cu-rich massive sulfides; d) Cu-poor massive sulfides. The mantle
1816 normalized concentrations of the elements in the ores increases from Sn to Te. The PGE-
1817 dominated deposits have low concentrations of these elements. The Ni-sulfide deposits are
1818 systematically richer in all the elements and the Cu-rich sulfides are richer than the Fe-rich
1819 sulfides. Data sources in Table 5.

1820 **Figure 16** a,b,c Plot of Pd vs Pt concentrations for basalts and komatiites from the literature
 1821 (grey circles, rocks with >30 wt % MgO or >1500 ppm S), compared with; a) the compositions
 1822 of the Noril'sk basalts (Lightfoot and Keays 2005), b) Bushveld chills (Barnes et al. 2010), c)
 1823 Stillwater chills, cross (Zientek et al. 1986), d) Plot of Ir vs MgO for basalts and komatiites from
 1824 the literature. Note that the Noril'sk basalts and Stillwater chills have similar Pt and Pd contents
 1825 to unmineralized basalts and komatiites. The Bushveld chills have similar Pd values to
 1826 unmineralized basalts and komatiites, but appear slightly richer in Pt than most of the basalts
 1827 from the literature. Literature data from Maier et al. (2009)

1828 **Figure 17** Plot of enrichment factors (Cs/Cl) vs R-factor for elements with partition coefficients
 1829 between 10 and 100 000. The enrichment factors of Pd for Talnakh and Kharaelakh (T&K)
 1830 indicate lower R-factors ~3 000 than those of Noril'sk 1 ~ 20 000.

1831 **Figure 18** Plot of Cu/Pd vs Pd for PGE-dominated deposits. Solid lines show the mixing lines
 1832 between sulfides formed at R-factors of 100, 1000 and 10 000 100 000 with cumulate consisting
 1833 of 90% cumulate and 10 % trapped liquid fraction. Solid dots indicated 100 %, 10 %, 1 % and
 1834 0.1 % sulfides present in the rocks. Data from sources in Table 4

1835 **Figure 19** PGE Plot of Cu/Pd vs Pd for the Noril'sk basalts, the deposits in the Kharaelakh,
 1836 Talnakh and Noril'sk 1 intrusions The dashed line shows the modelled composition of the basalt
 1837 if a sulfide liquid is removed in co-tectic proportions, dots represent 0.1, 0.2 and 0.3 %
 1838 crystallization. Note that many of the basalts plot along this line which suggests they have
 1839 segregated a sulfide liquid. Also the sulfides found in the Noril'sk 1 intrusion require higher R-
 1840 factors (~10 000) than the sulfides found in the Kharaelakh and Talnakh intrusions (~1 000) data
 1841 from Zientek et al. (1994) and Lightfoot and Keays (2005).

1842 **Figure 20** Photomicrographs of sulfide droplets found in MORB glass (modified after Patten et
 1843 al. 2012) a) Droplet that crystallized rapidly showing MSS and ISS intergrowth with Ni-rich
 1844 phase between the two phases. b) A droplet that crystallized slightly more slowly resulting in
 1845 solid MSS at the base and quenched textured ISS in the top left hand corner. c) A droplet that
 1846 crystallized slowly with MSS at the margins and solid ISS in the center.

1847 **Figure 21** Back scatter electron images of PGM: a) and b) PGM that have crystallized from the
 1848 fractionated interstitial liquid (modified from Dare et al. 2014); c) CuPtRhS exsolution in
 1849 pyrrhotite and pentlandite from the Merensky reef (modified from Prichard et al. 2004); c)
 1850 Residual PGM after the replacement of pentlandite, Lac des Iles (modified from Djon and
 1851 Barnes 2012); e) Remobilized Pd bismuthotelluride, (modified from Dare et al. 2010)

1852 **Figure 22.** $^{187}\text{Os}/^{188}\text{Os}$ versus $^{187}\text{Re}/^{188}\text{Os}$ isochron diagram illustrating mixing at 1.1 Ga
 1853 between an uncontaminated mantle magma and a Re-rich sedimentary rock that had evolved
 1854 between 1.85 Ga and 1.1 Ga. The contaminated magma (M) crystallizes at ~ 1.1 Ga and evolves
 1855 to the position of the contaminated bulk rock, far above the $^{187}\text{Os}/^{188}\text{Os}$ value that the
 1856 uncontaminated rock would have attained. Minerals A and B may crystallize from the
 1857 contaminated magma, and together with the bulk rock value define an isochron with an elevated
 1858 $\gamma_{\text{Os}(i)}$ value.

1859 **Figure 23.** Isochron diagram illustrating the potential effects of Re loss/gain and Os loss/gain on
 1860 today's isotope ratios. In this example a rock derived from a mantle-derived magma at 1.1 Ga
 1861 evolves to 0.5 Ga and then the system is opened via interaction with a fluid. In the case of Re
 1862 loss/Os gain, the $^{187}\text{Re}/^{188}\text{Os}$ values are reduced and the resultant values may evolve to $^{187}\text{Os}/^{188}\text{Os}$
 1863 Os values that lie above the expected isochron for unperturbed samples, and may be difficult to
 1864 distinguish from samples with elevated γ_{Os} values due to crustal contamination. In the case of
 1865 relative Re gain/Os loss the resultant values are below those produced from uncontaminated
 1866 magma and are characterized by negative γ_{Os} values.

1867 **Figure 24.** Isochron diagram for samples from the McCreedy West mine, Sudbury (modified
 1868 from Morgan et al., 2002).

1869 **Figure 25.** Isochron diagram for samples from the Noril'sk 1 and Talnakh intrusions (modified
 1870 from Walker et al. 1994).

1871 **Figure 26.** Isochron diagram for samples from the Voisey's Bay deposit (modified from Lambert
 1872 et al...1999b).

1873 **Figure 27.** Isochron diagram for samples from the Eagle deposit (modified from Ding et al.
 1874 Figure captions 2012).

1875 **Figure 28.** Plot showing the decrease in Os and S isotope ratios due to exchange between sulfide
 1876 in a conduit system and batches of uncontaminated, mantle derived magma. The equation of
 1877 Ripley and Li (2003) was used to calculate the trends: $\delta^{34}\text{S}_{\text{sil,exchanged}} = (\delta^{34}\text{S}_{\text{sil,initial}} + R^*(\delta^{34}\text{S}_{\text{sil,initial}} + \Delta))/1+R^*$. For Os the $^{187}\text{Os}/^{188}\text{Os}$ ratio is used rather than the $\delta^{34}\text{S}$ value. In this example
 1878 the initial $^{187}\text{Os}/^{188}\text{Os}$ ratio of the sulfide was set at 1, the $^{187}\text{Os}/^{188}\text{Os}$ ratio of the mantle-derived
 1879 magma was 0.15, the concentration of Os in the silicate magma was set at 1ppb, the $\delta^{34}\text{S}$ values
 1880 of the magma and sulfide were 0 and 12 ‰, and the concentrations of S in the sulfide and
 1881 magma were 30 wt. % and 1000 ppm, respectively. R^* is $(C_{\text{sil}}/C_{\text{sulf}})*R$, where concentrations are
 1882 S or Os and R is the silicate liquid/sulfide liquid mass ratio. N is the integrated silicate/sulfide
 1883 mass ratio where in this example each pass of uncontaminated magma interacted with an equal
 1884 mass of sulfide ($R=1$). Δ is the isotopic difference between sulfur or osmium in the sulfide mass
 1885 and that in the silicate melt (at magmatic temperatures this value is ~ 0). If the R value for each
 1886 increment of exchange is larger, then the rate of S or Os isotope decline is greater.
 1887
 1888

1889 **Figure 29.** Isochron diagram for samples from the Great Dyke (modified from Schoenberg et al.
 1890 2003).

1891 **Figure 30.** $^{187}\text{Os}/^{188}\text{Os}$ values from the Bushveld Complex (modified from Reisberg et al.,
 1892 2011). The Sandsloot pyroxenites are from the Platreef and have values very similar to those of
 1893 the Merensky Reef (Reisberg et al. 2011).

1894

1895

1896

1897

1786

1787

1788

1789

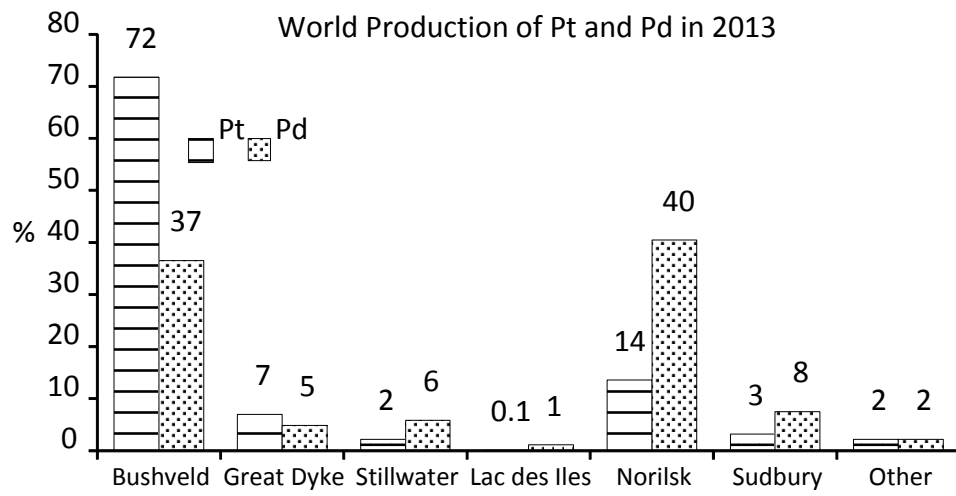










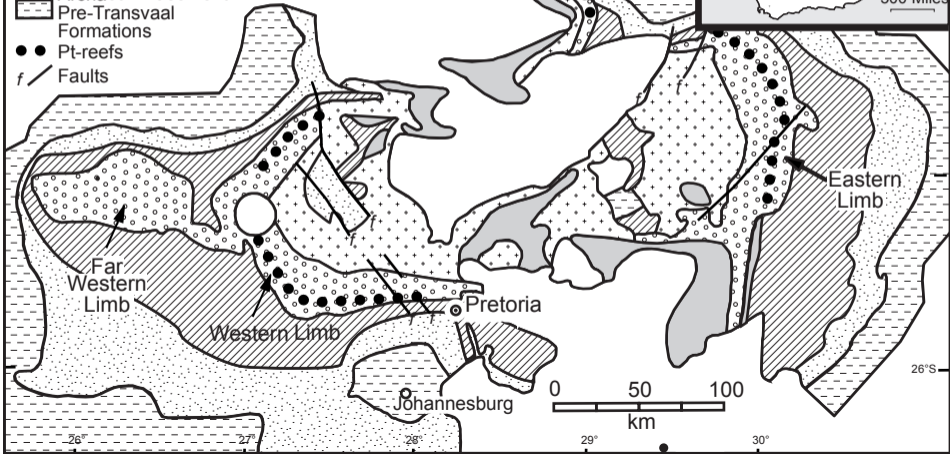
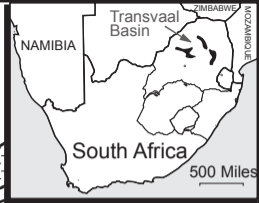


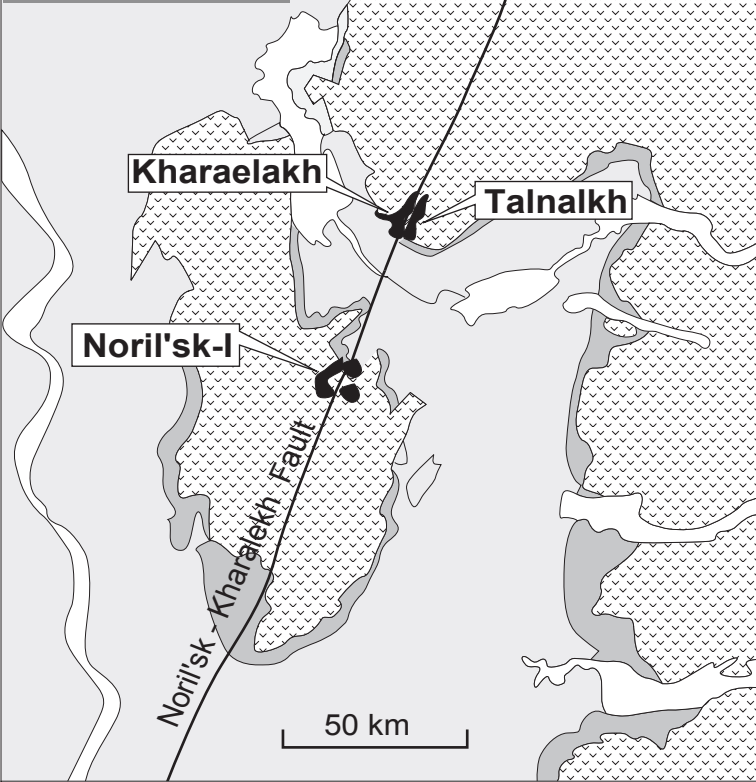
Fig. 1

-  Younger Sedimentary Cover & Intrusions
-  Granophyres + Granites
-  Rustenburg Layered Suite
-  Rooiberg Group
-  Pretoria Group
-  Chuniseport Group
-  Archaean Basement
-  Pre-Transvaal Formations
-  Pt-reefs
-  Faults

} Bushveld Complex

} Transvaal Supergroup





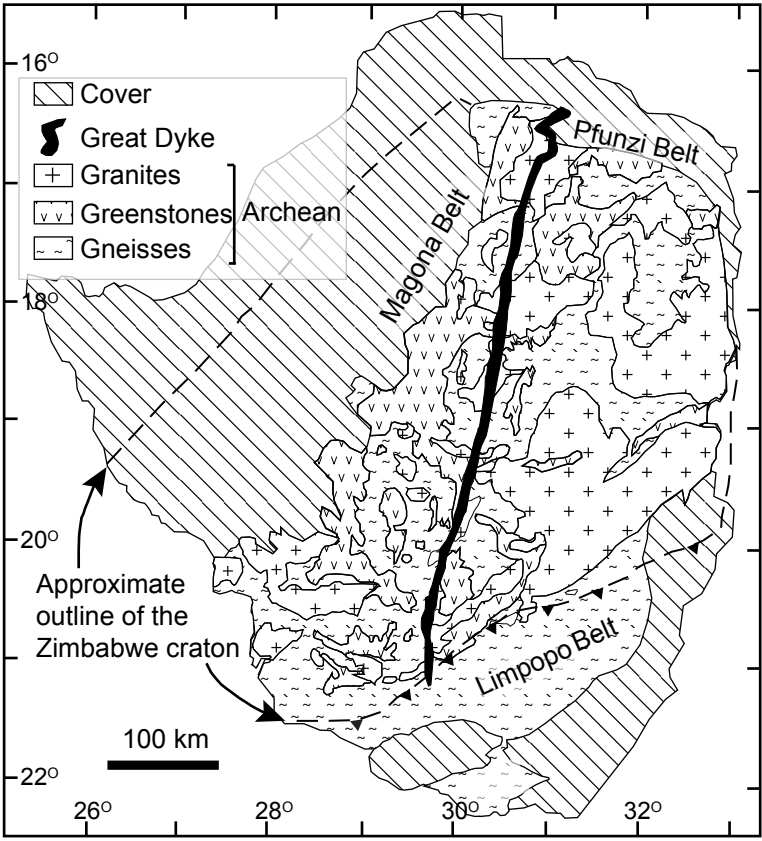
Flood basalts (*Triassic-Permian*)



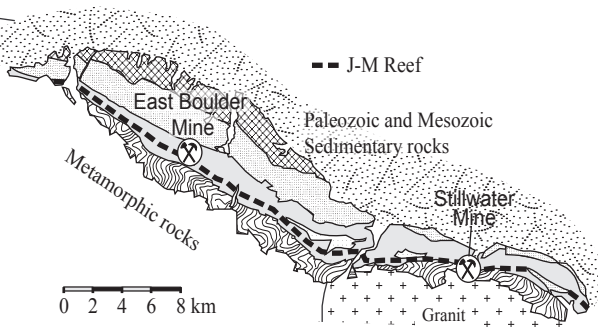
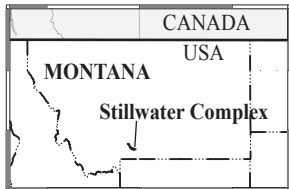
Clastics (*Permian-Carboniferous*)



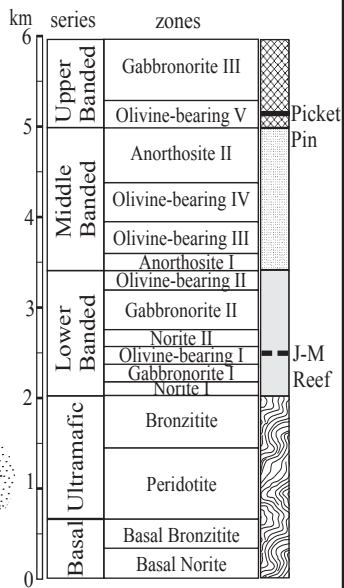
Carbonates + Evaporites (*Paleozoic*)








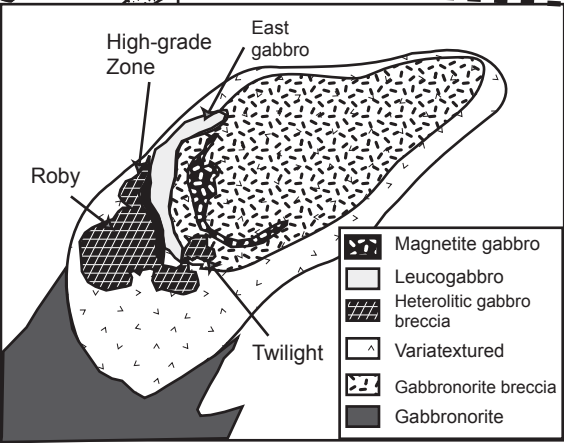
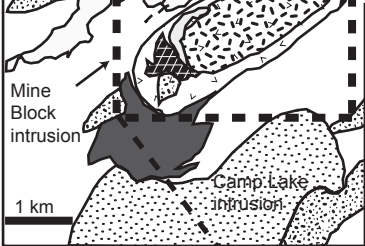
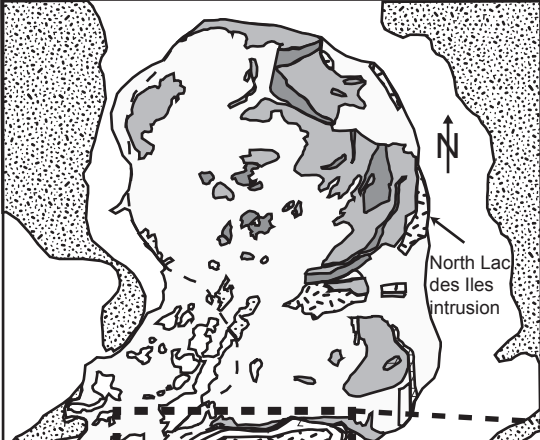
(a)



(b)



-  Diabase
-  Felsic intrusive
-  Hornblende gabbro
-  Pyroxénite
-  Websterite



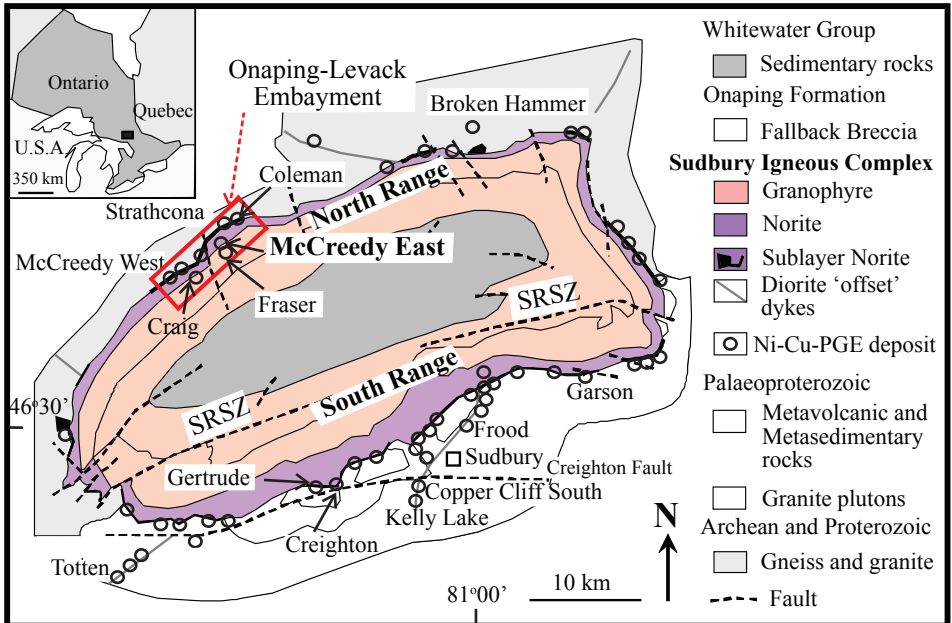
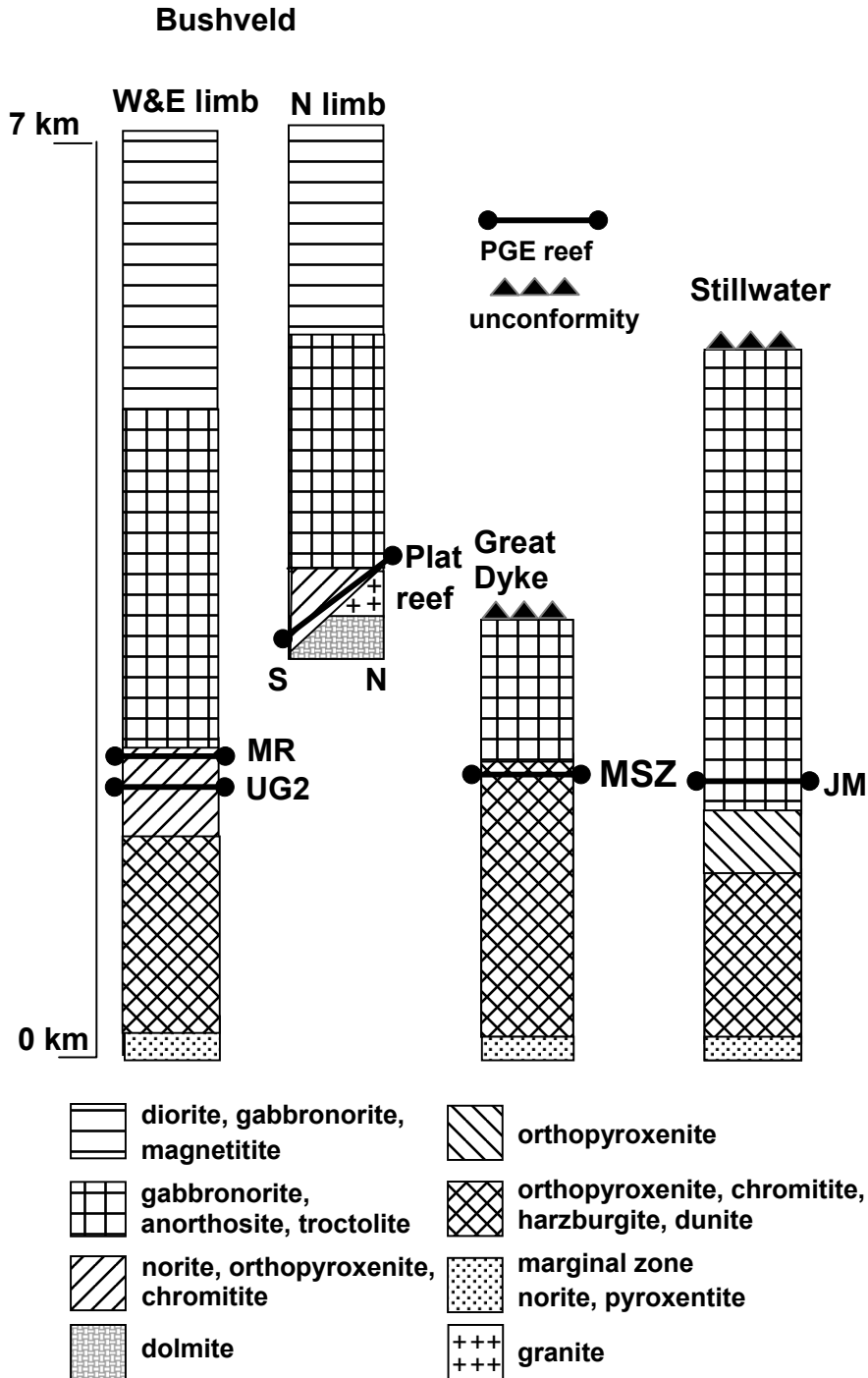
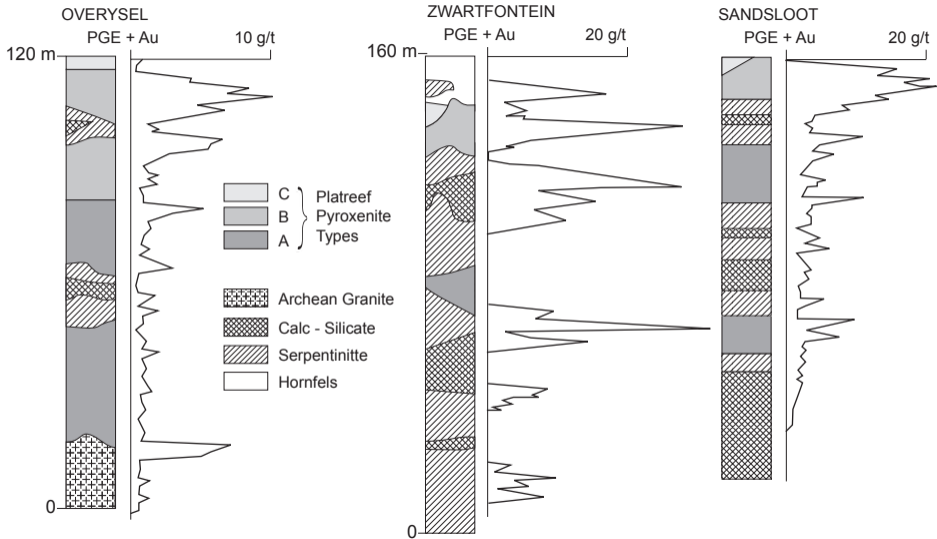


Fig. 8





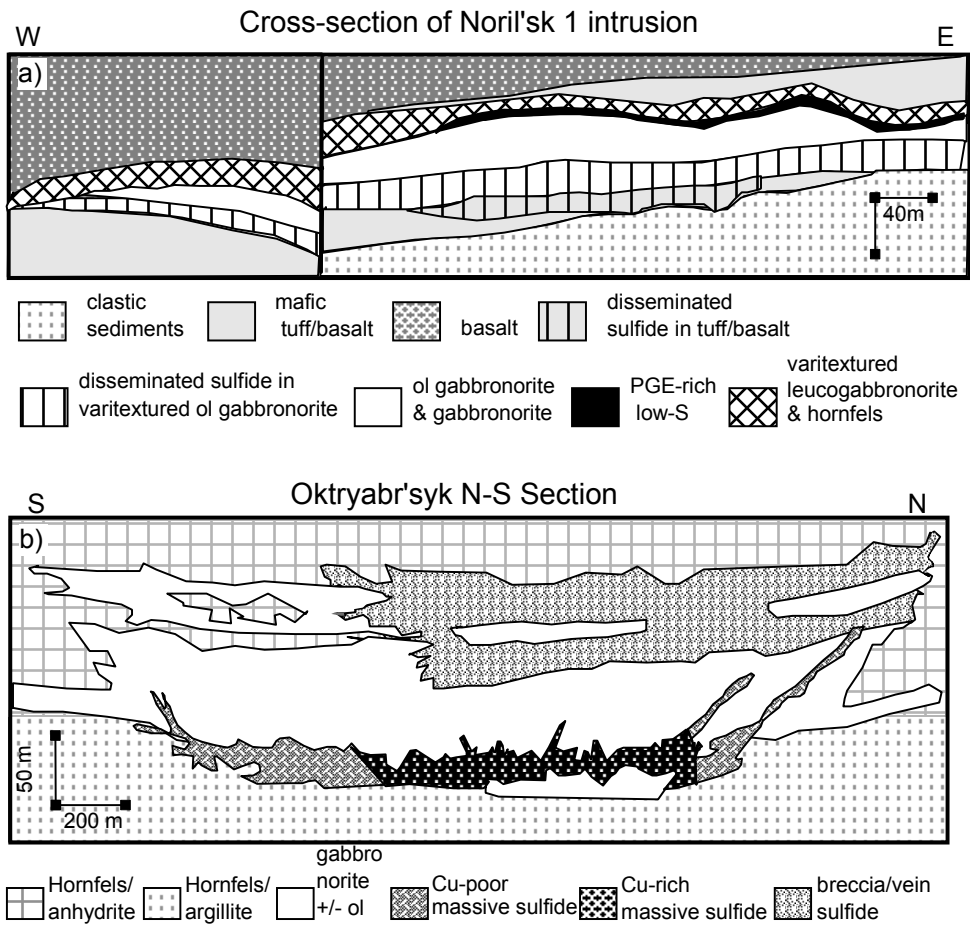


Fig. 10

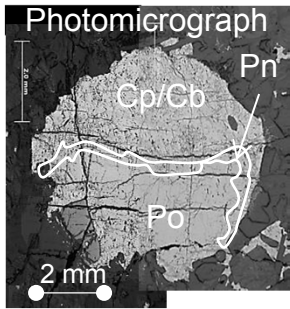
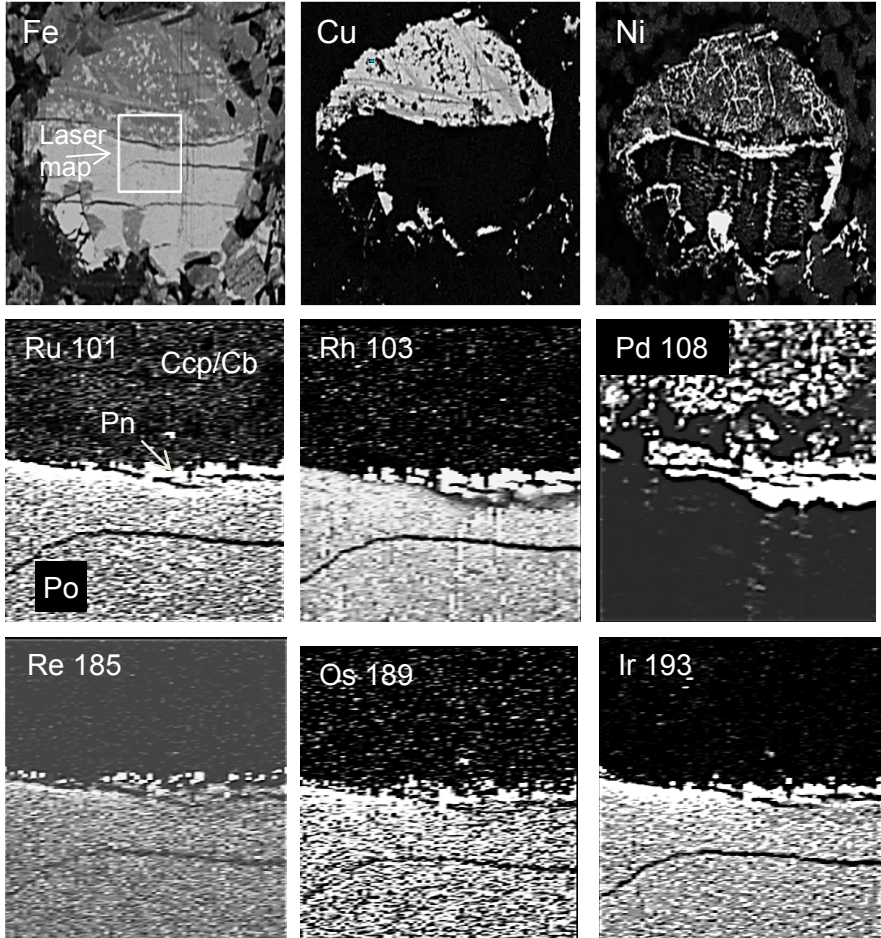


Fig. 11 Sulfide droplet from Noril'sk 1. Distribution of Fe, Cu, Ni determined by micro-XRF; Distribution of PGE determined by laser ablation ICP-MS. 108 Pd has been corrected for Cd and Zn interferences. Rh has been corrected for Cu interference. Ru has been corrected to Ni interference



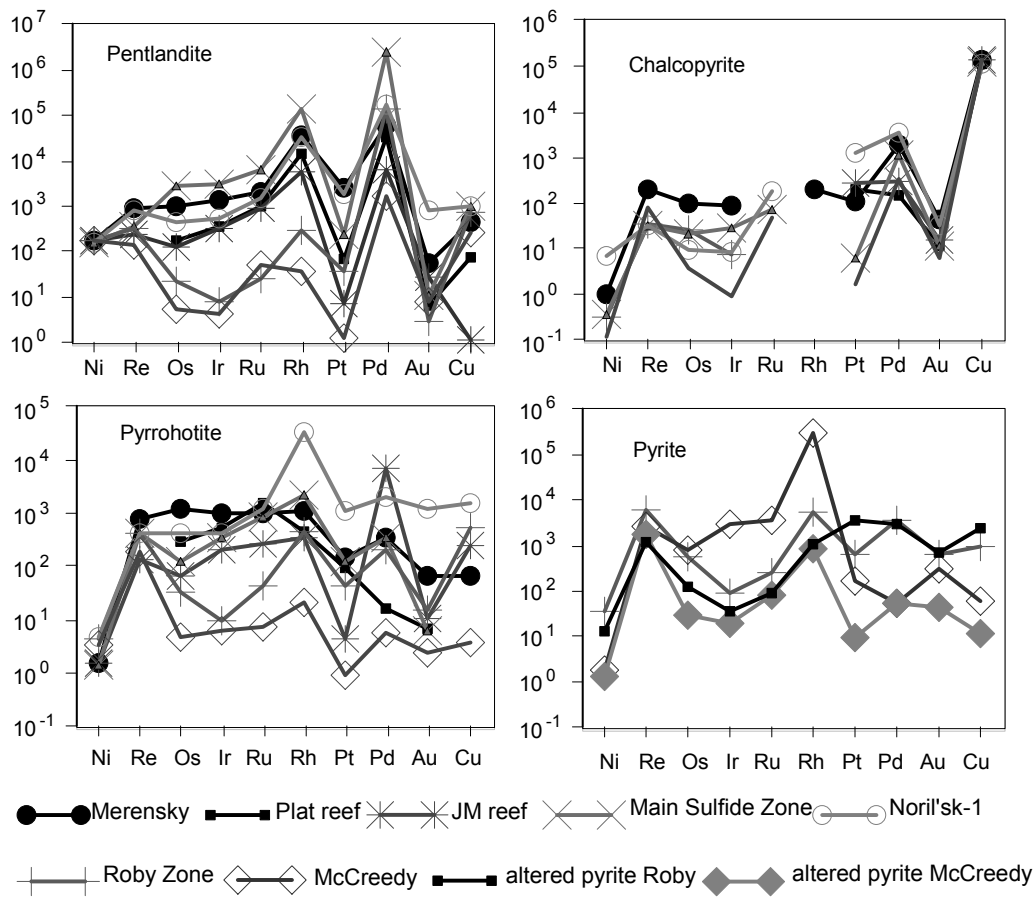


Fig. 12

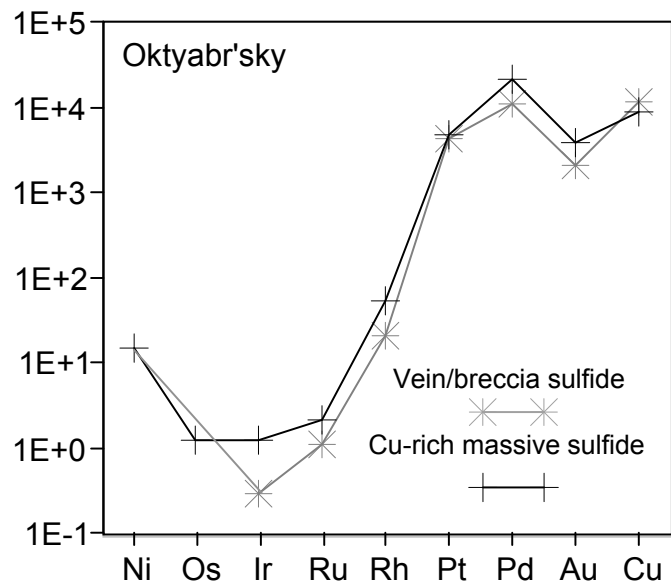
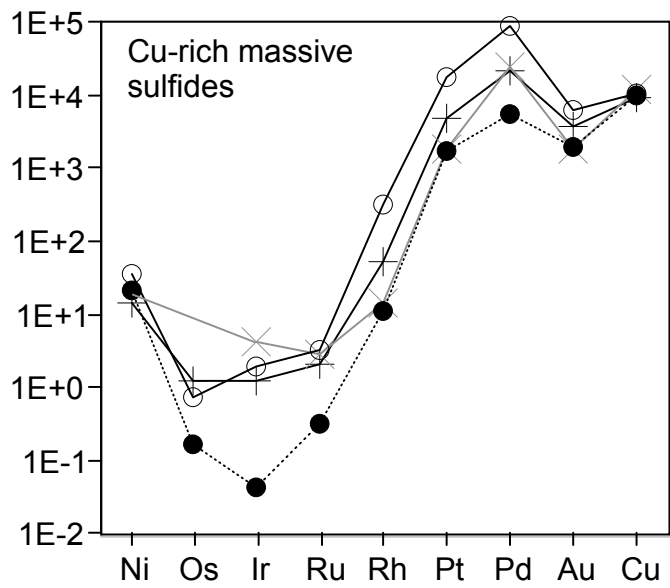
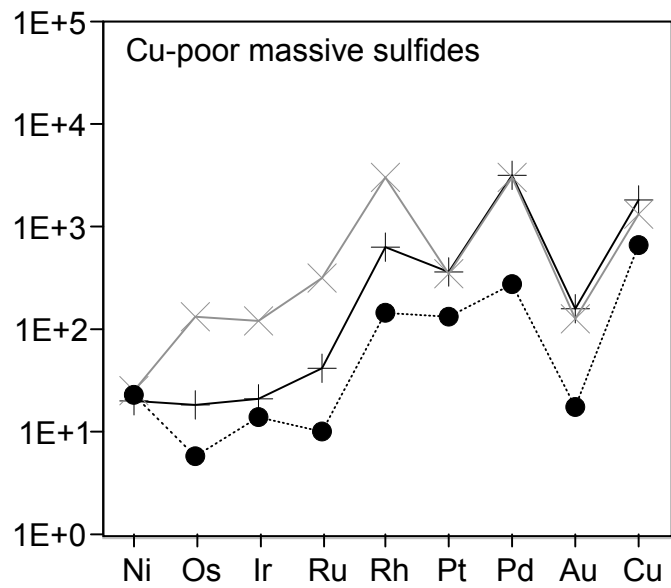
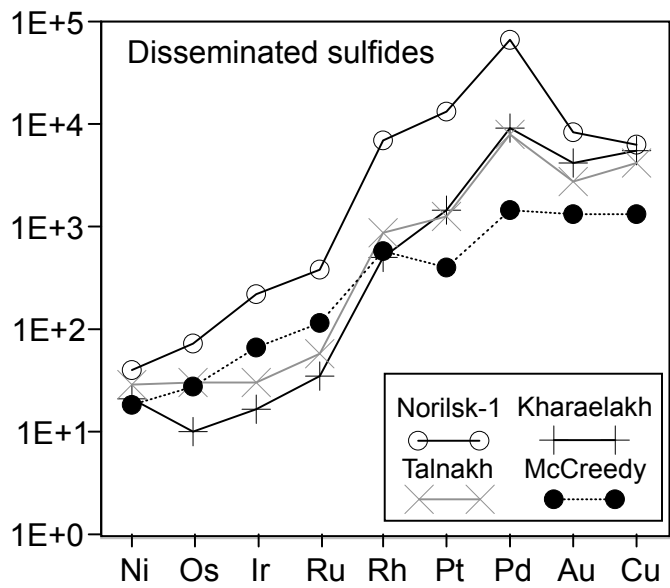
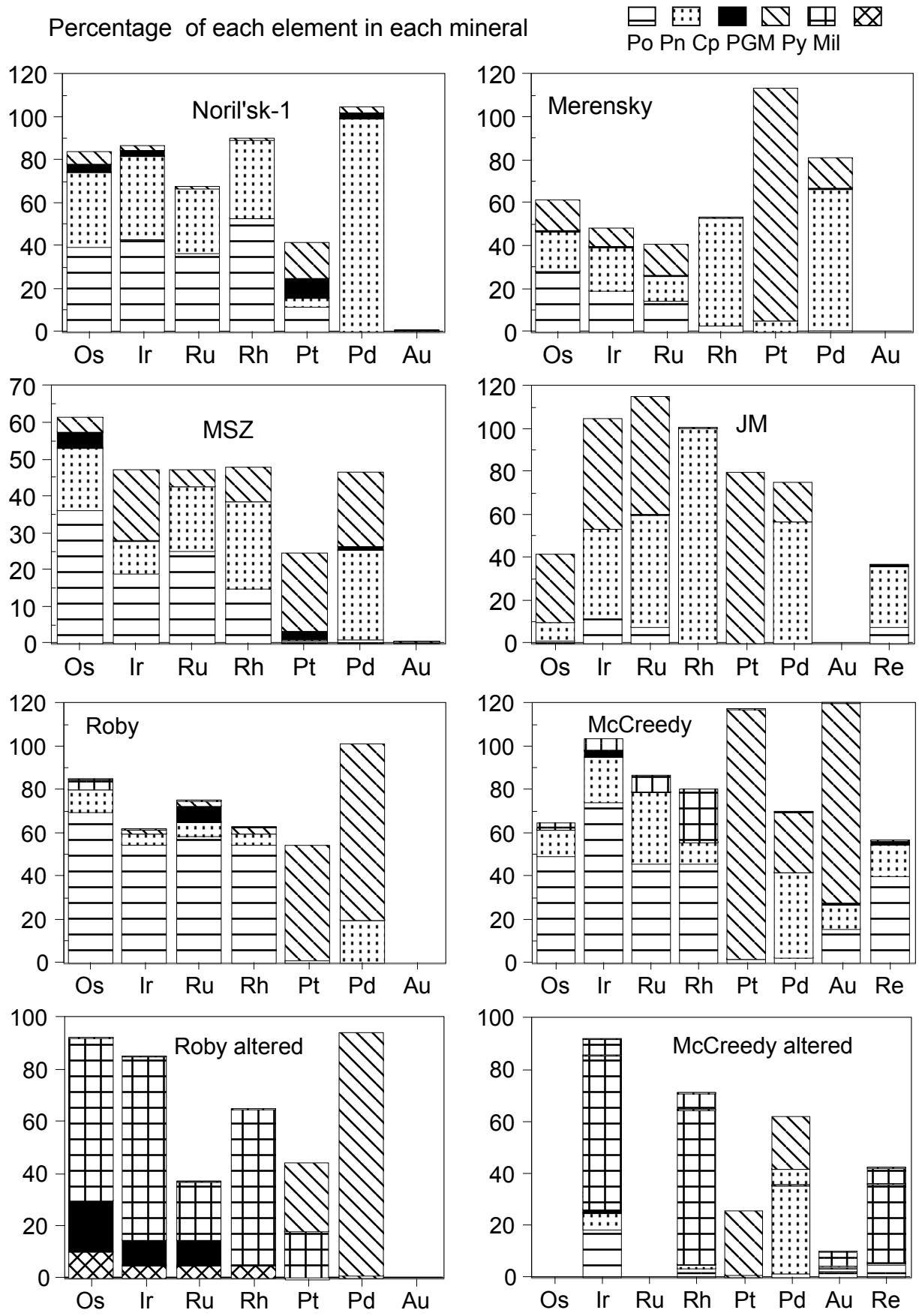


Fig. 13

Fig. 14



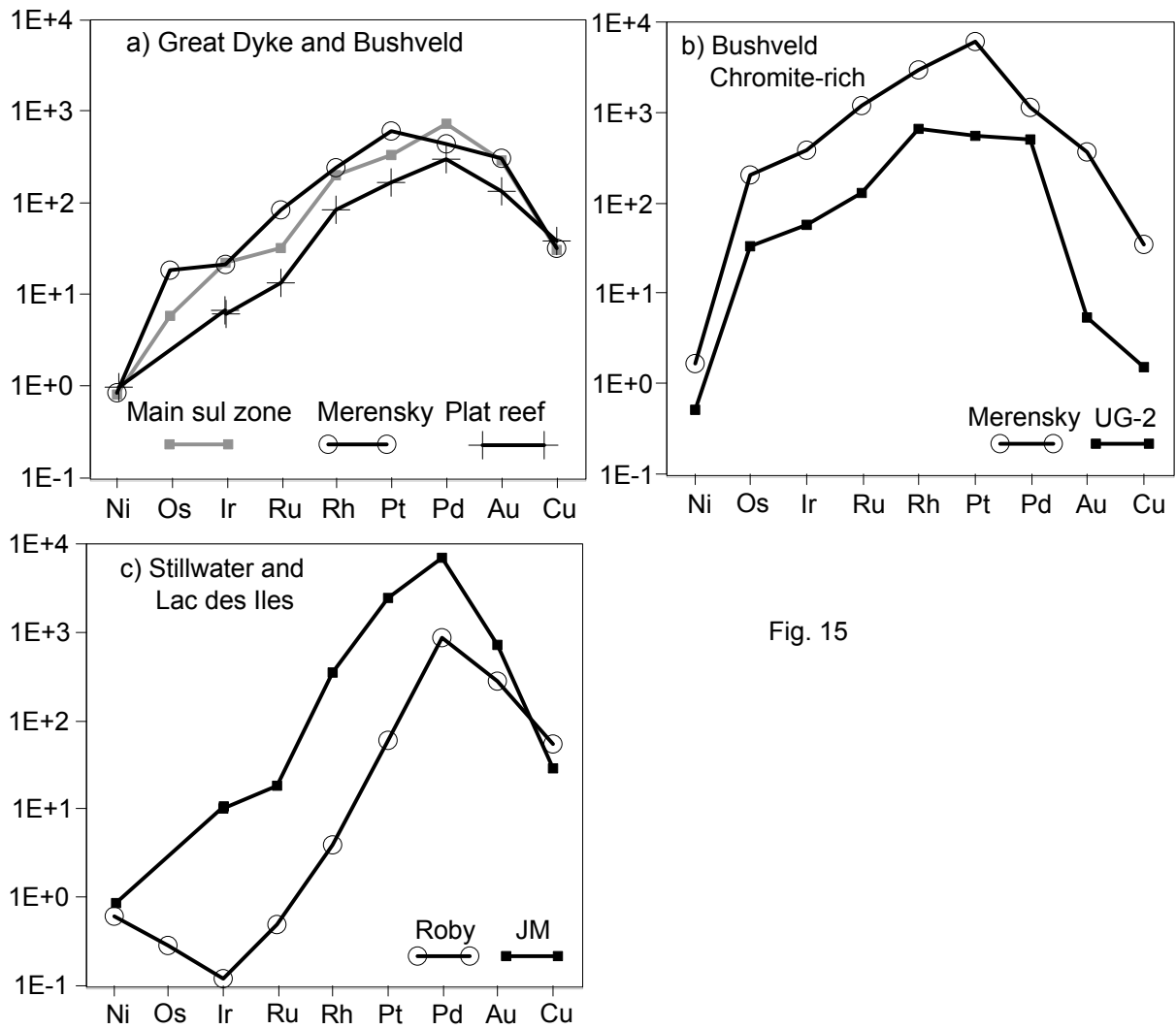


Fig. 15

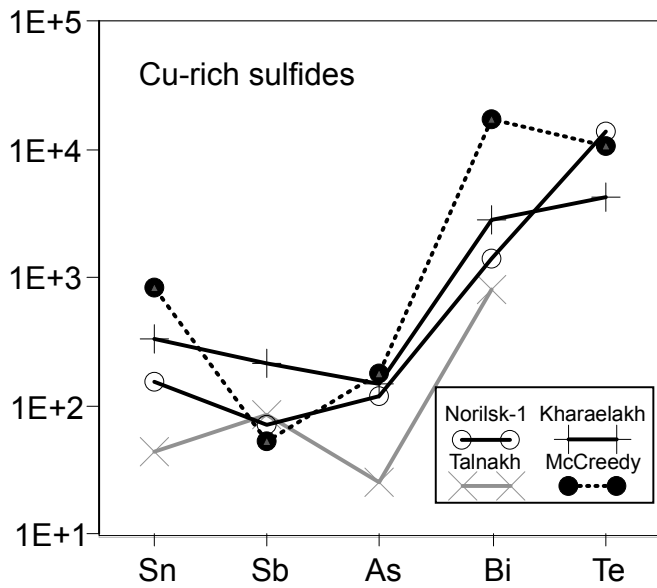
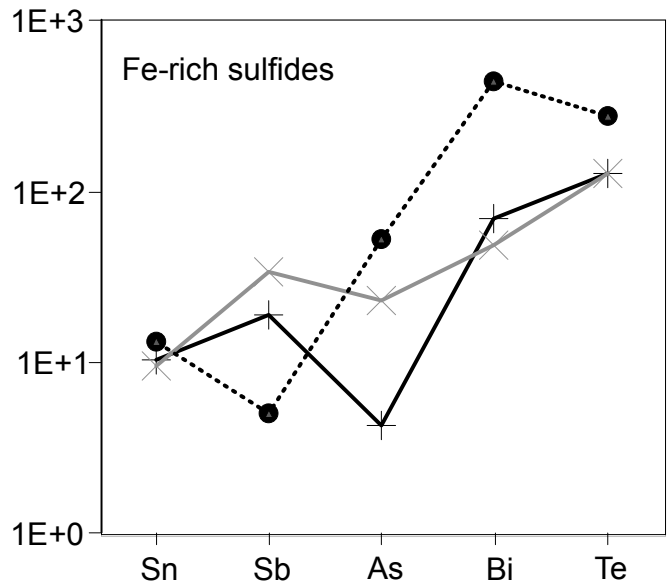
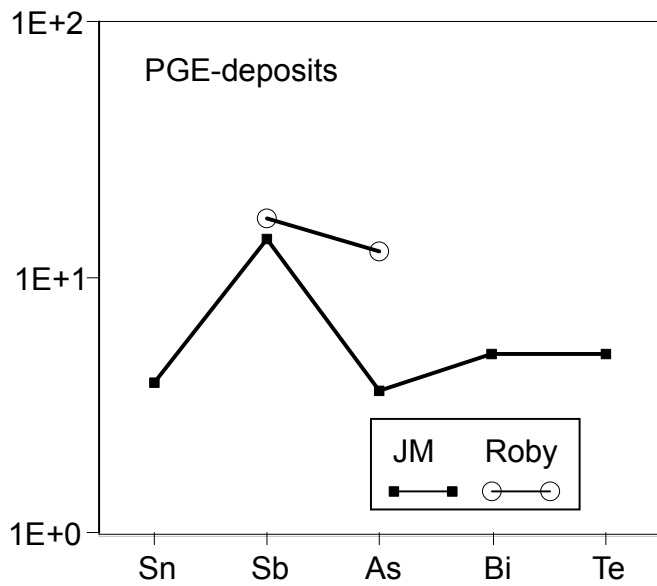


Fig. 16 Concentrations of the metalloids commonly found in platinum-group minerals normalized to mantle values and plotted in order of compatibility. The PGE-dominated deposits have very low concentrations of these elements. The Ni-sulfide deposits are systematically richer in all the elements and the Cu-rich sulfides are richer than the Fe-rich sulfides

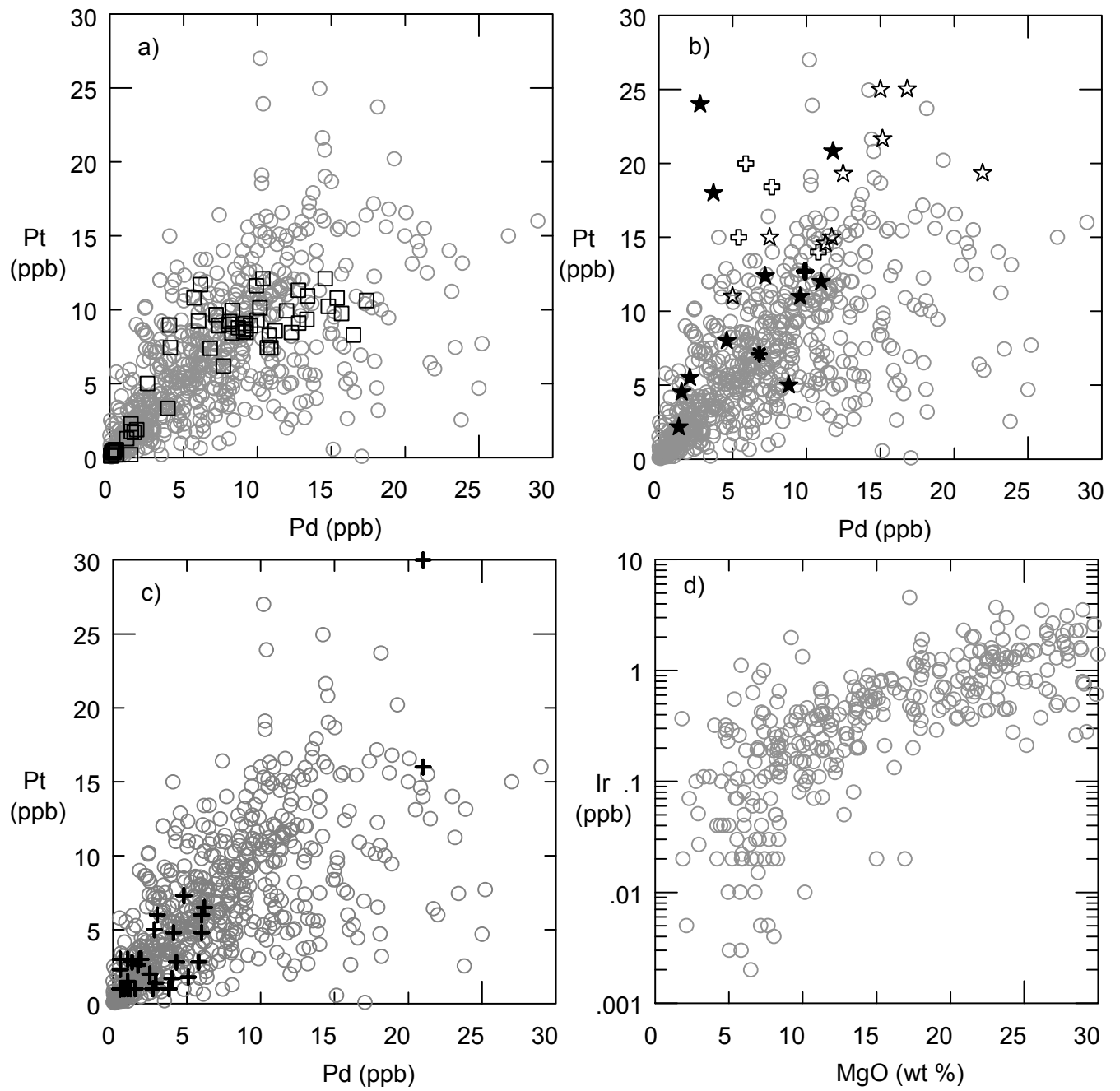
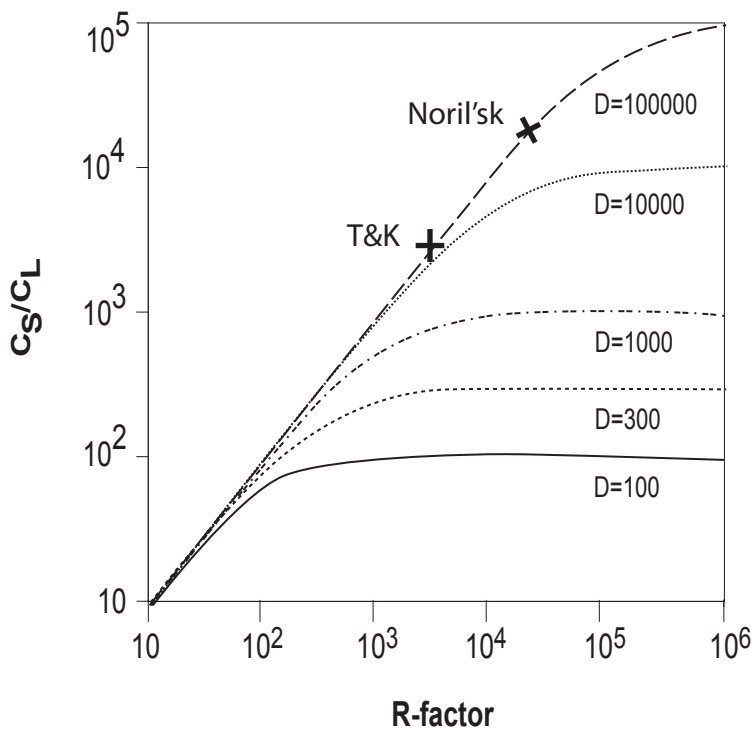


Fig. 17



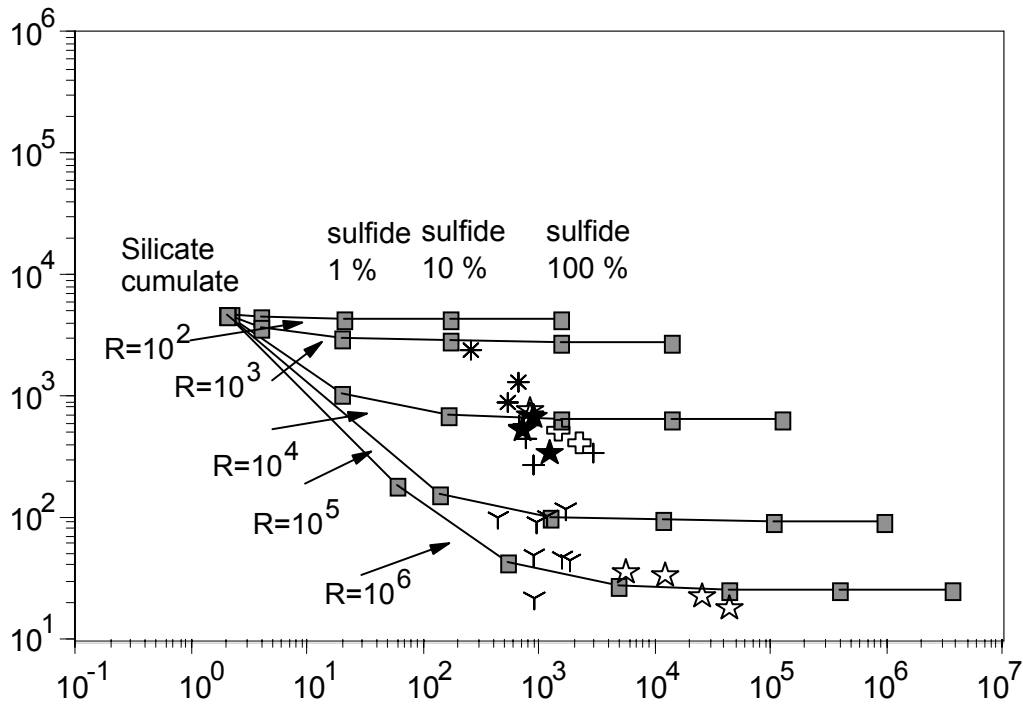


Fig. 19 Plot of Cu/Pd vs Pd for the PGE-dominated deposits, open stars, JM reef, Y UG-2, + Merensky, close stars Main Sulfide Zone, open crosses Roby Zone, asterisk Platreef. Solid lines show the mixing lines between sulfides formed at different R-factors and a silicate or oxide cumulate with 10% trapped liquid of Bushveld chill composition. Solid squares indicated 100 %, 10 %, 1 % , 0.1 % and 0.01 % sulfides present in the rocks.

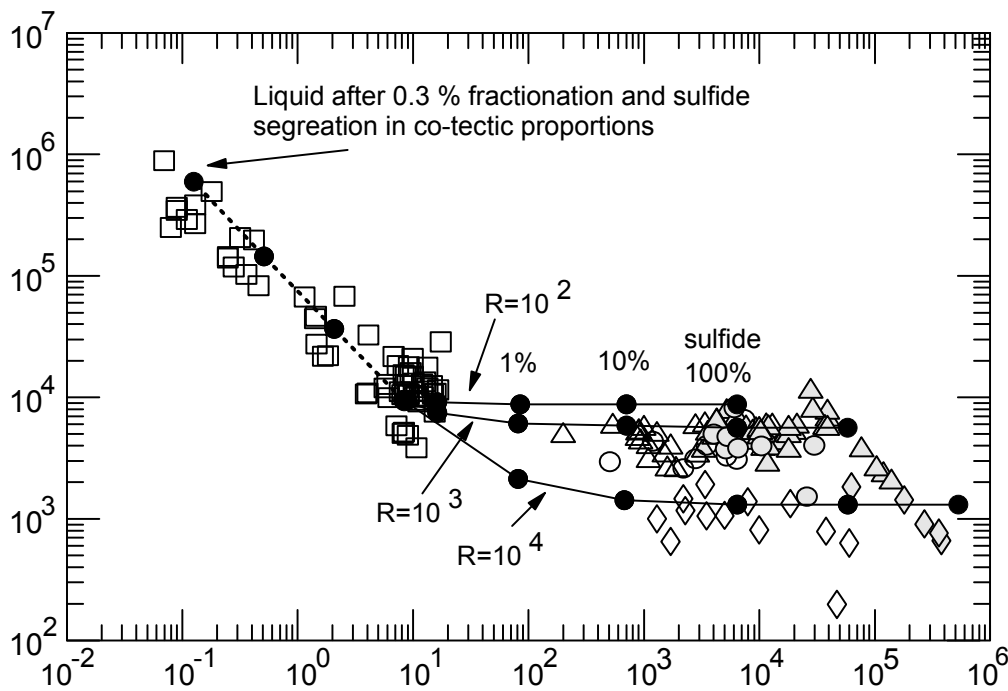


Fig. 20 Plot of Cu/Pd vs Pd for the Noril'sk basalts, squares, the deposits in the Khaeralak (triangles), Talkalh (circles) and Noril'sk-1(diamonds) intrusions. Open symbols disseminated sulfides, closed symbols massive sulfides. Solid lines show the mixing lines between sulfides formed at R-factors of 100, 1000 and 10 000 with basalt. Solid dots indicated 100 %, 10 %, 1 % and 0.1 % sulfides present in the rocks. The dashed line shows the modelled composition of the basalt if a sulfide liquid is removed in co-tectic proportions, dots represent 0.1, 0.2 and 0.3 % crystallization. Note that many of the basalts plot along this line which suggests they have segregated a sulfide liquid. Also the sulfides found in the Noril'sk 1 intrusion require R-factors 10 000 than the sulfides found in the Kharaelakh and Talkalh intrusions (1 000).

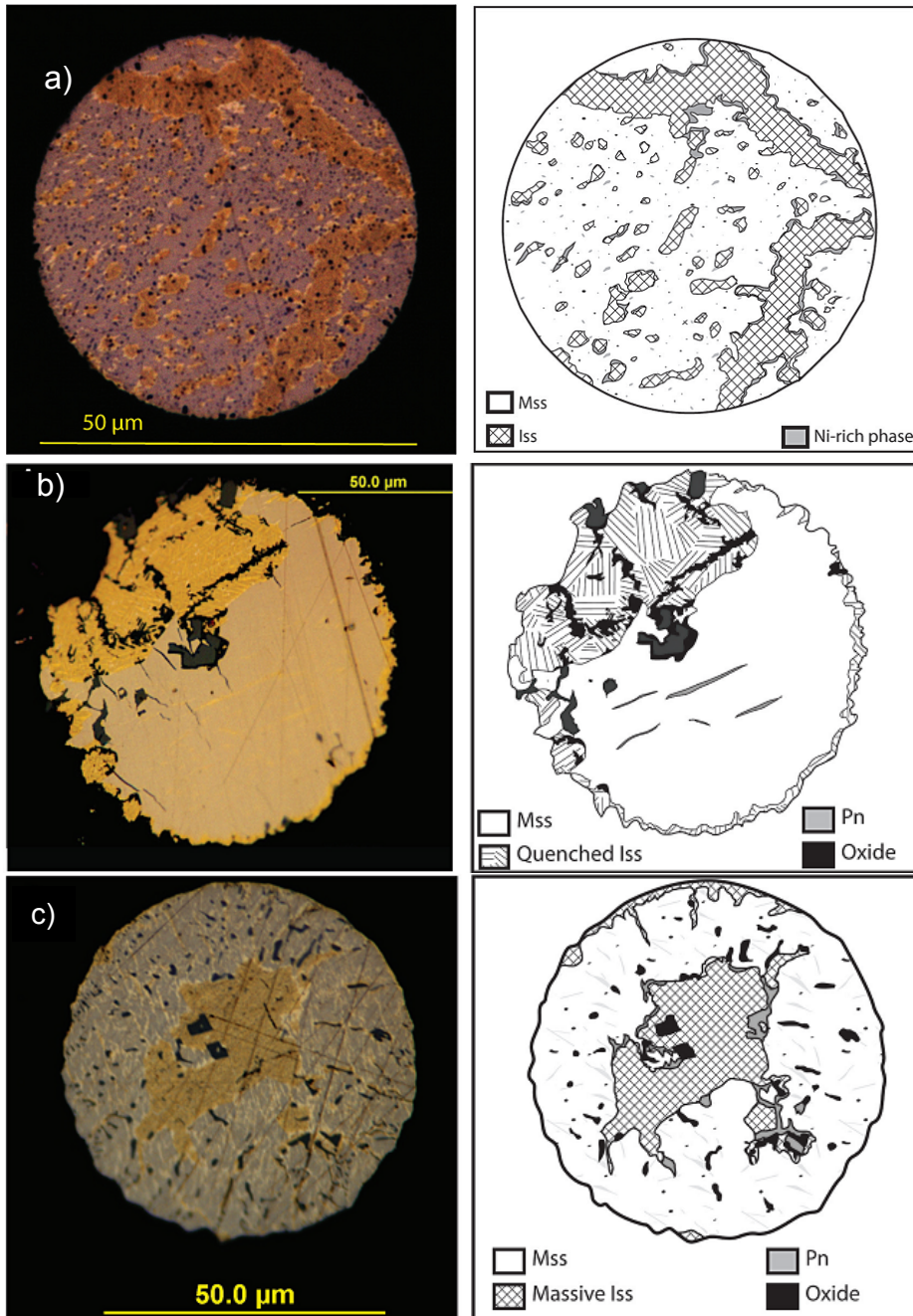


Fig. 21 Photomicrographs of sulfide droplets found in MORB glass (Patten et al. 2012). a) A droplet that crystallized rapidly showing mss and iss intergrowth with Ni-rich phase between the two phases. b) A droplet that crystallized slightly more slowly resulting in solid mss at the base and quenched textured iss in the top left hand corner. c) A droplet that crystallized slowly with mss at the margins and solid iss in the center.

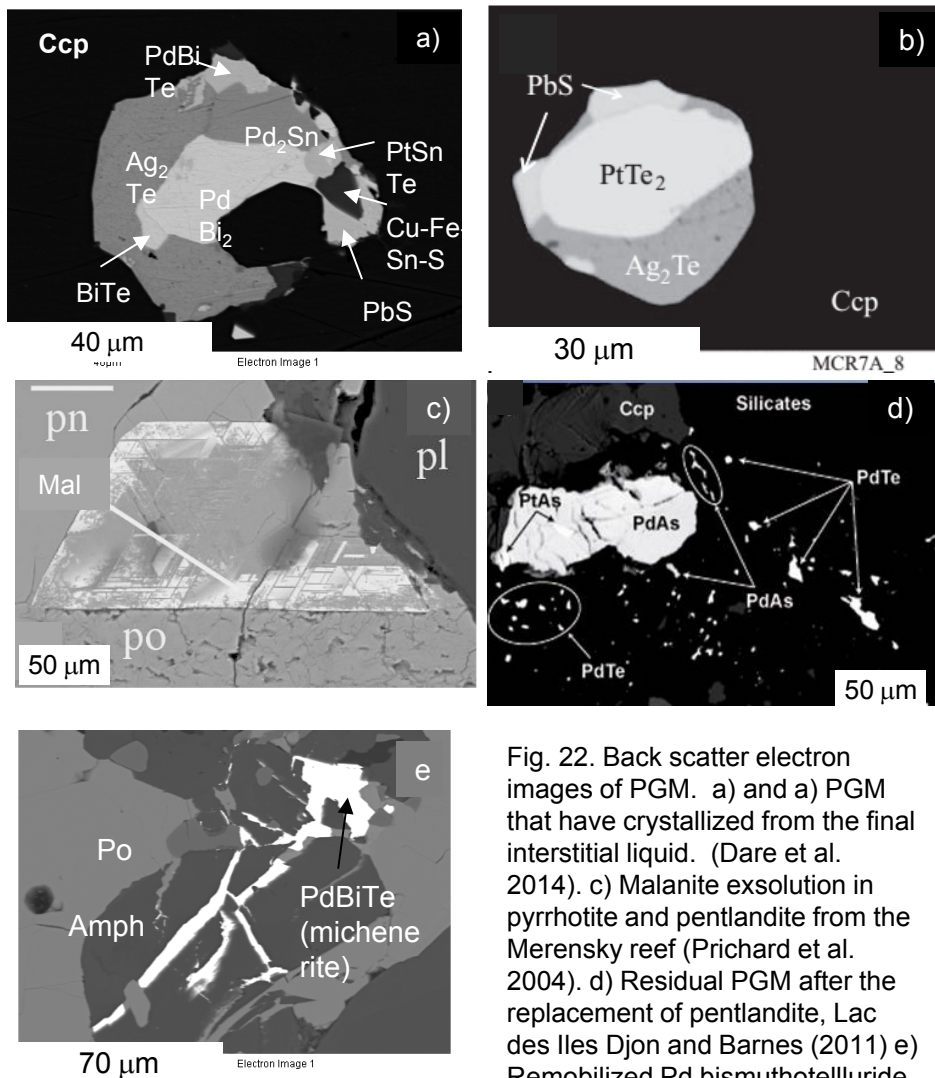
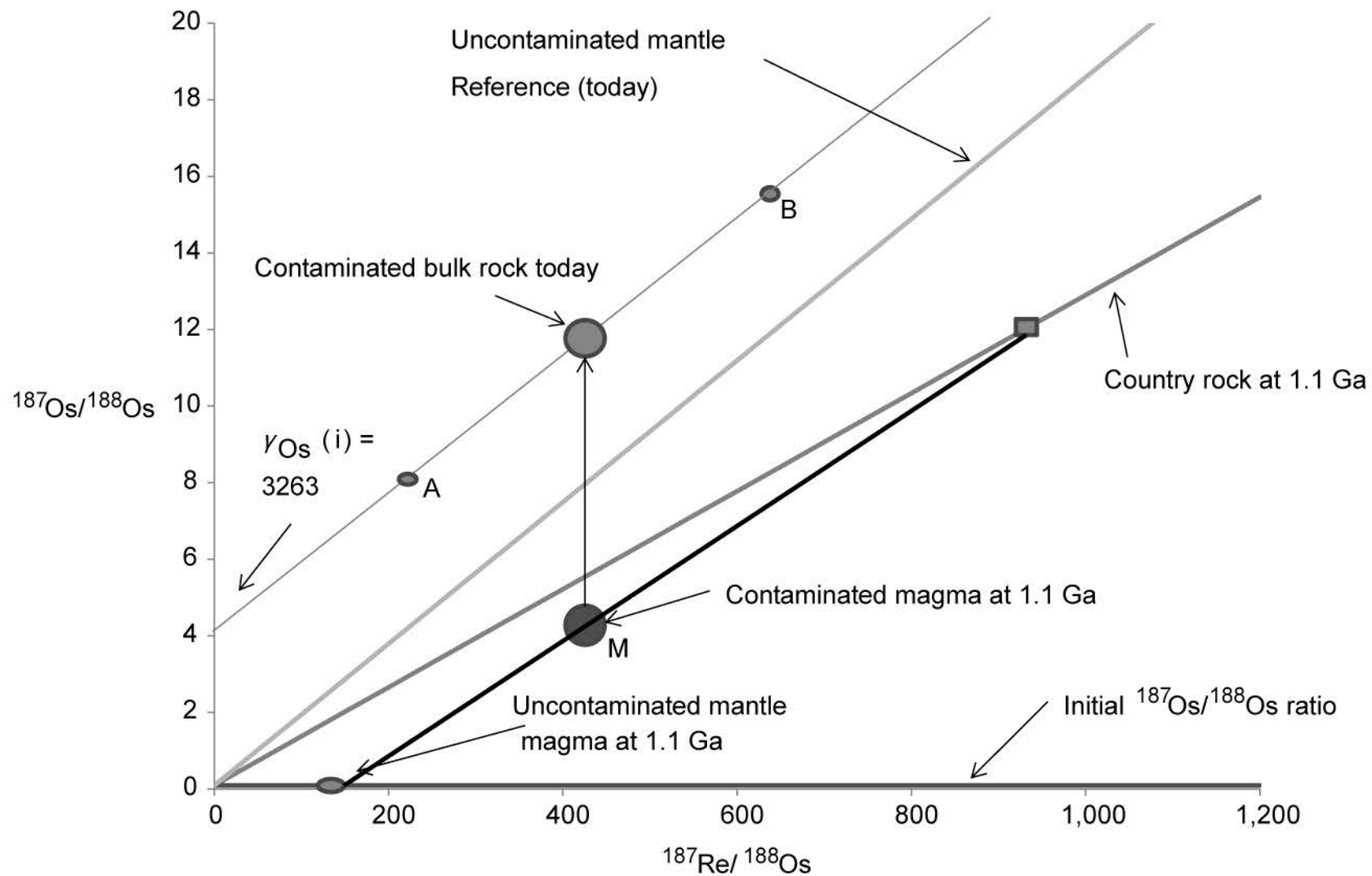
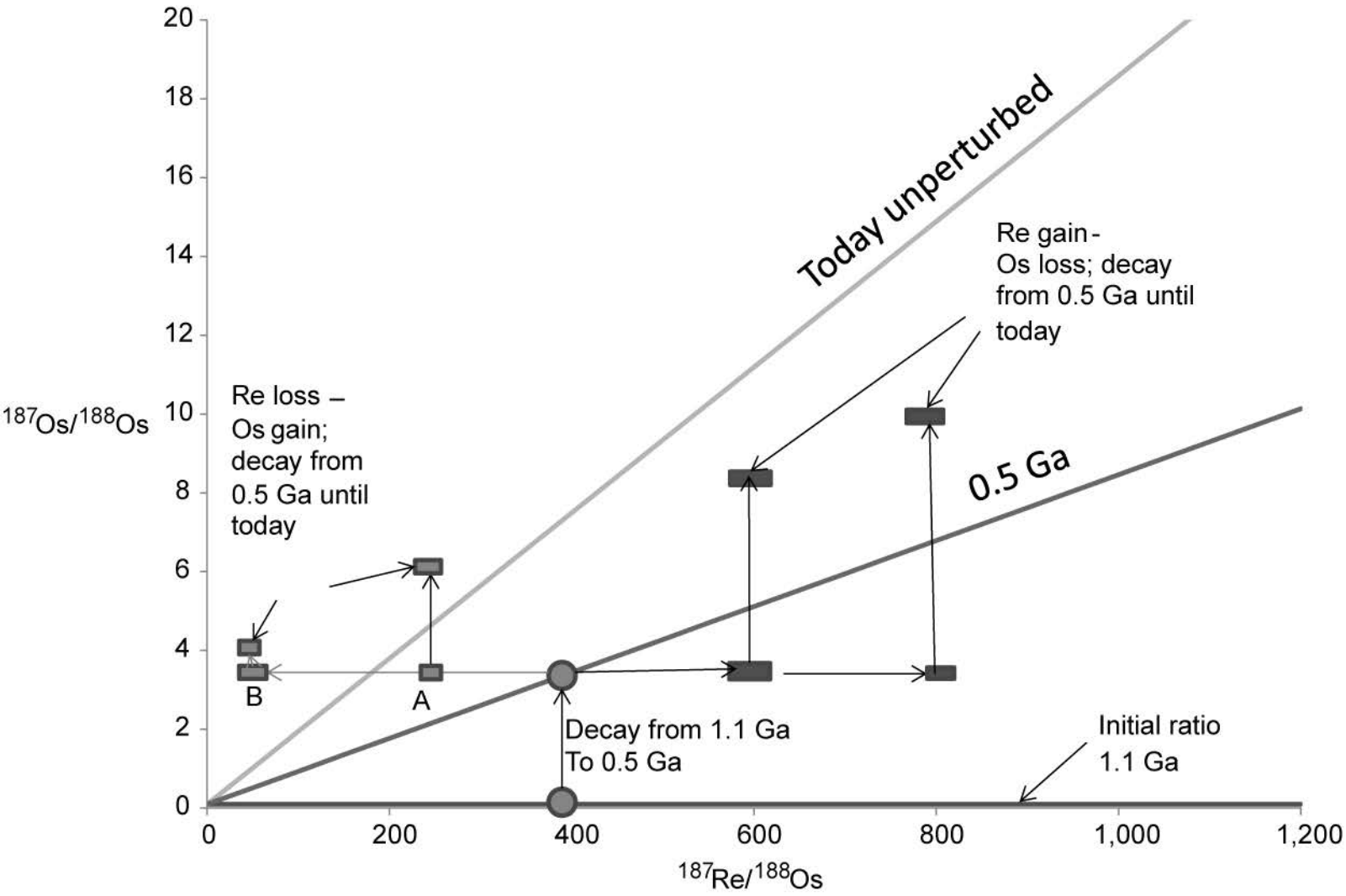
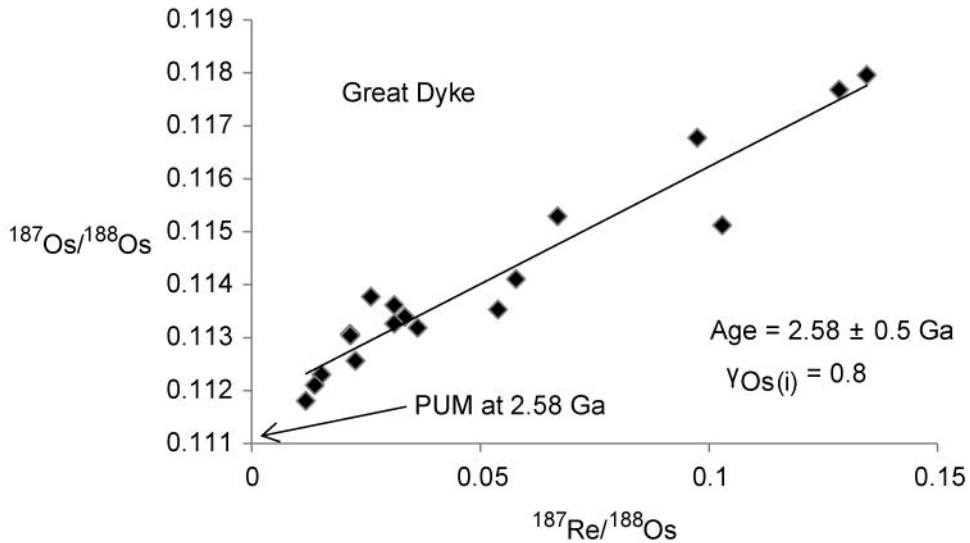
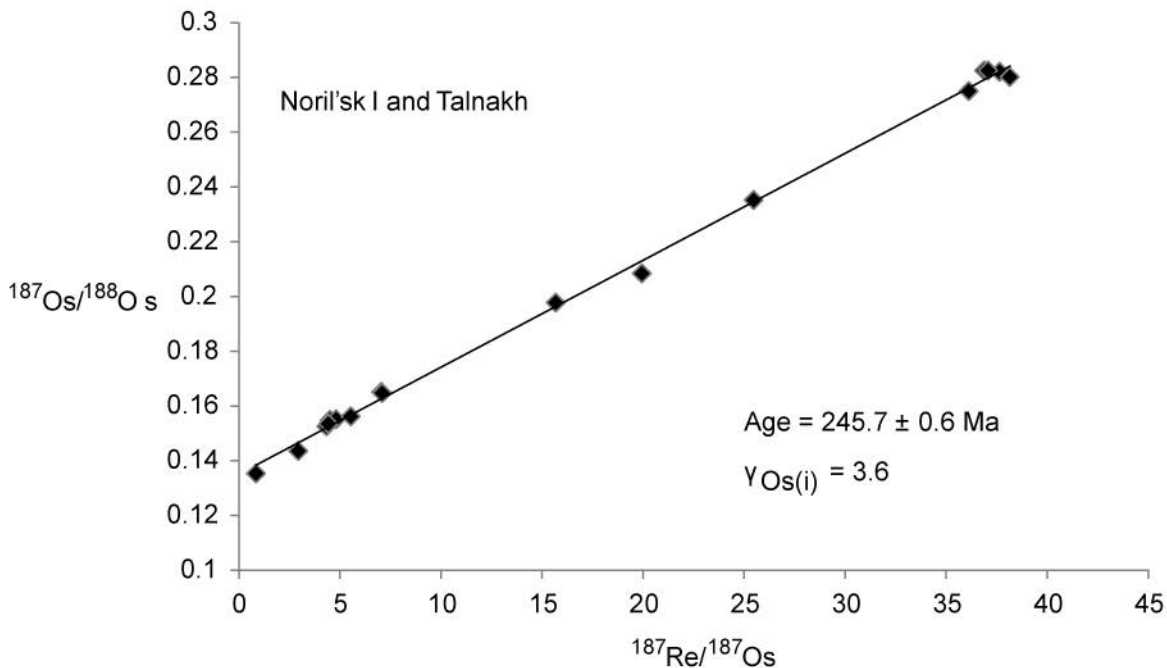


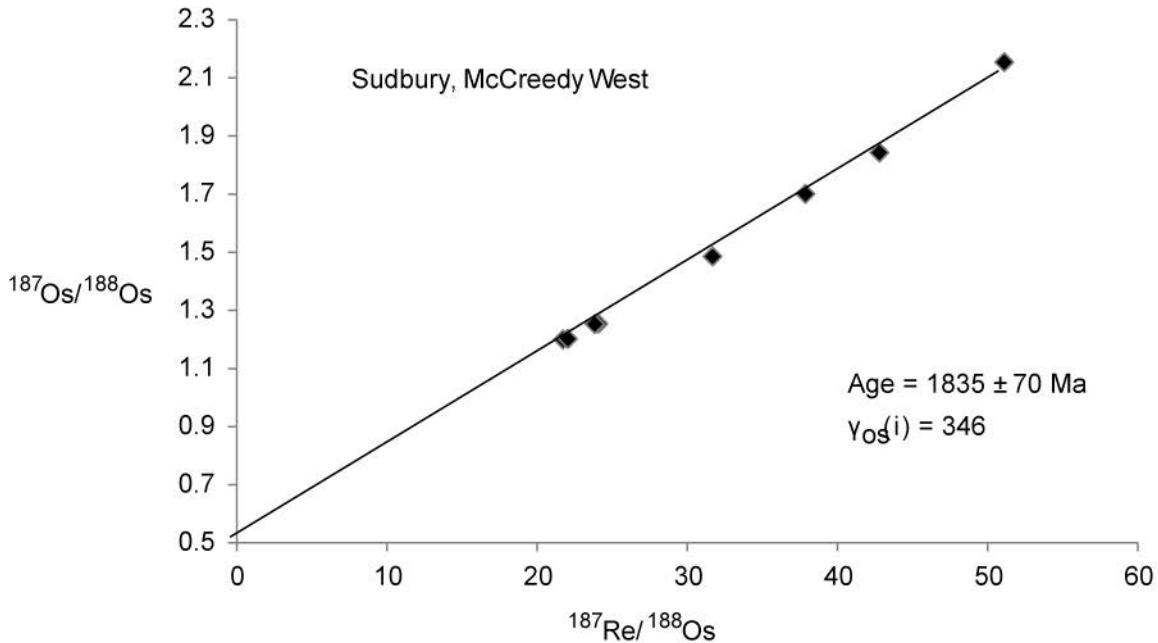
Fig. 22. Back scatter electron images of PGM. a) and a) PGM that have crystallized from the final interstitial liquid. (Dare et al. 2014). c) Malanite exsolution in pyrrhotite and pentlandite from the Merensky reef (Prichard et al. 2004). d) Residual PGM after the replacement of pentlandite, Lac des Iles Djon and Barnes (2011) e) Remobilized Pd bismuthotelluride, (Dare et al. 2010)

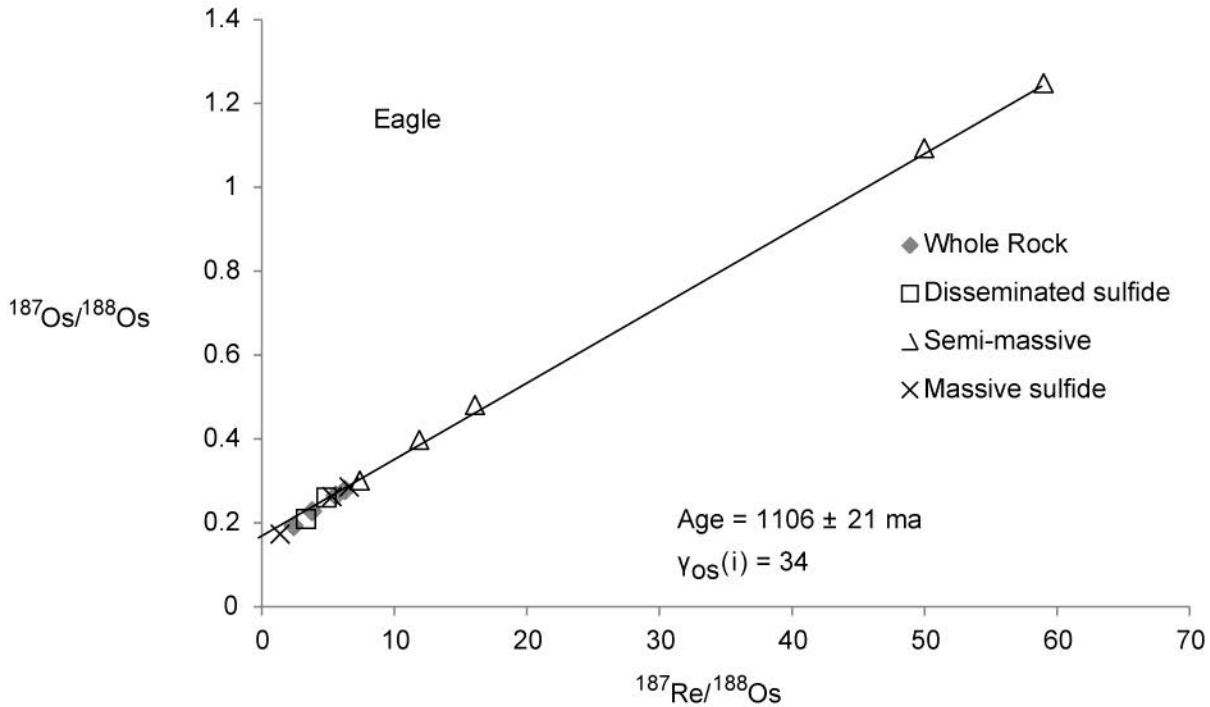


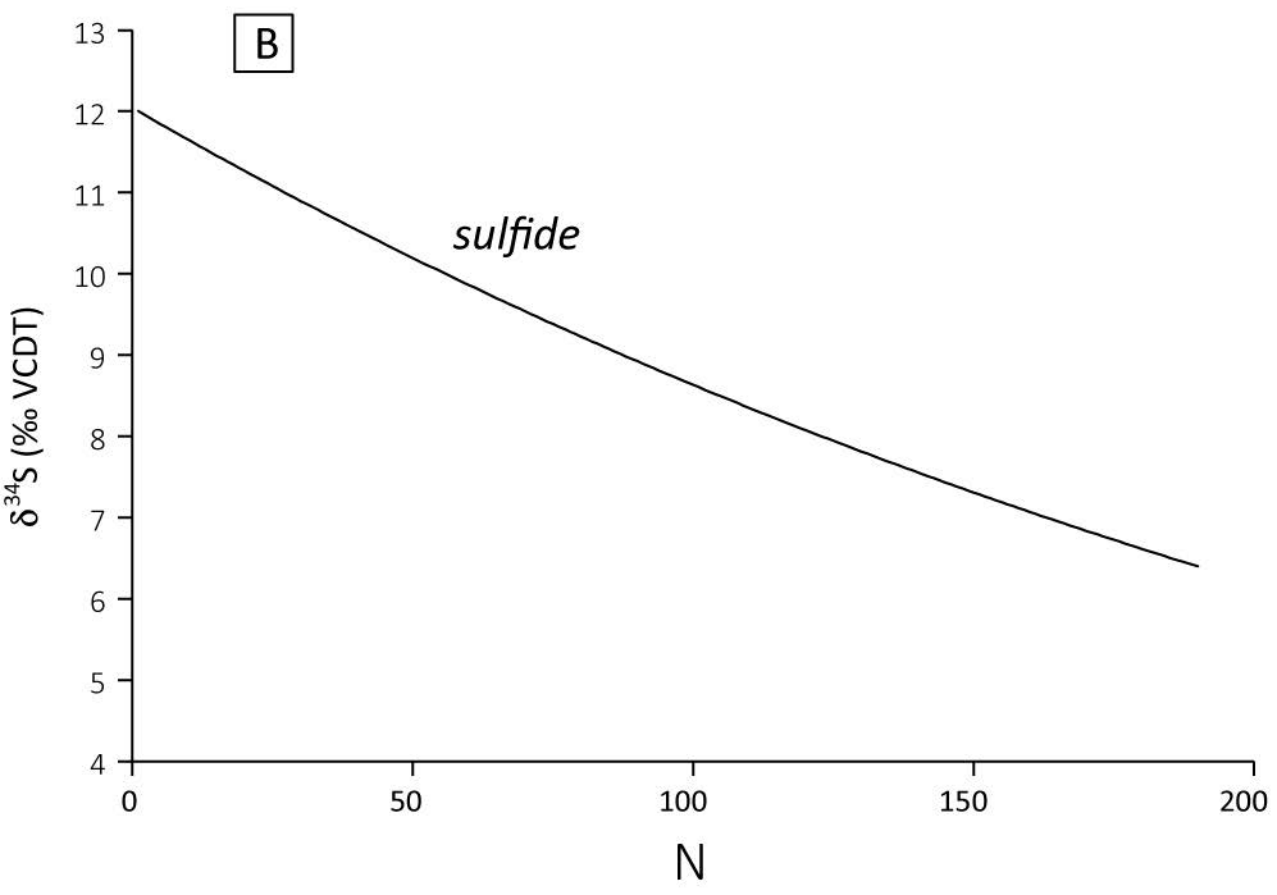
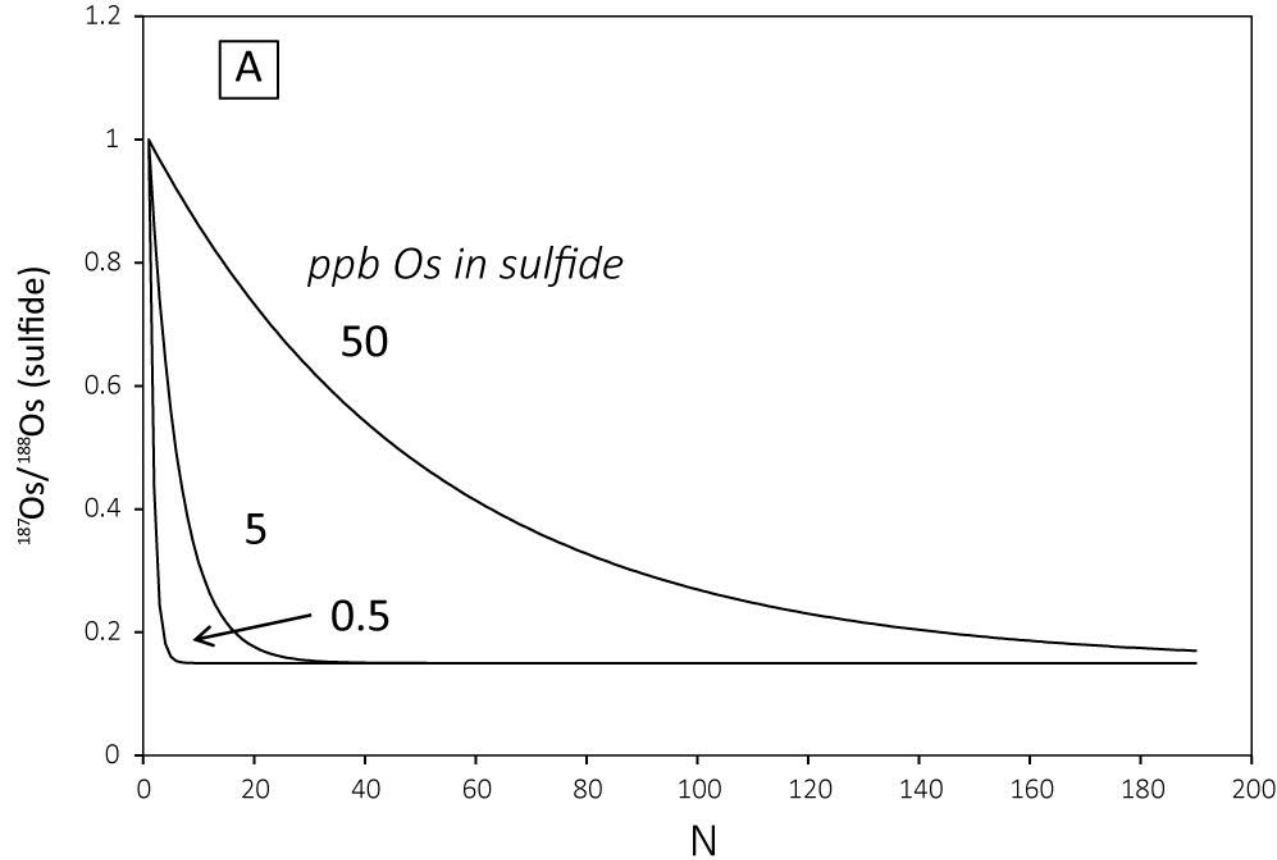


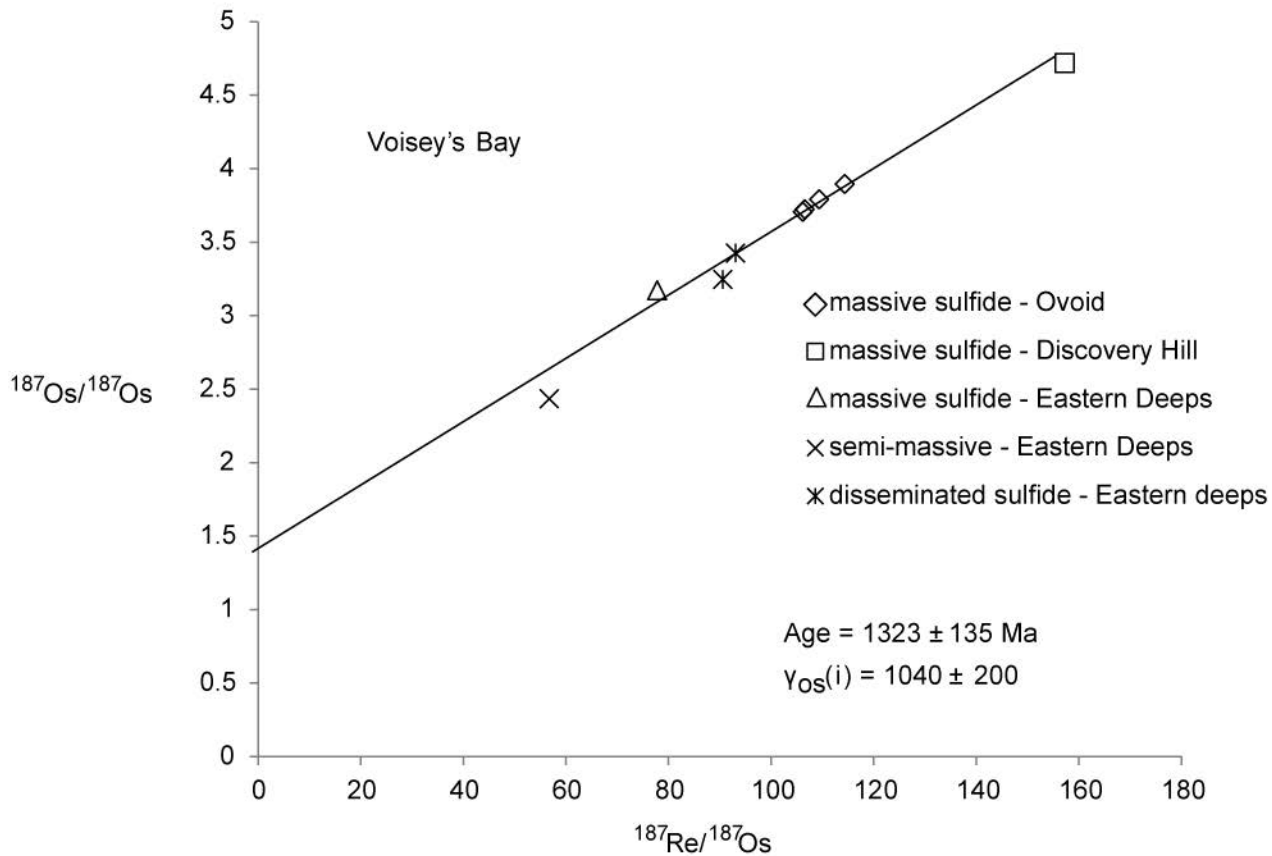




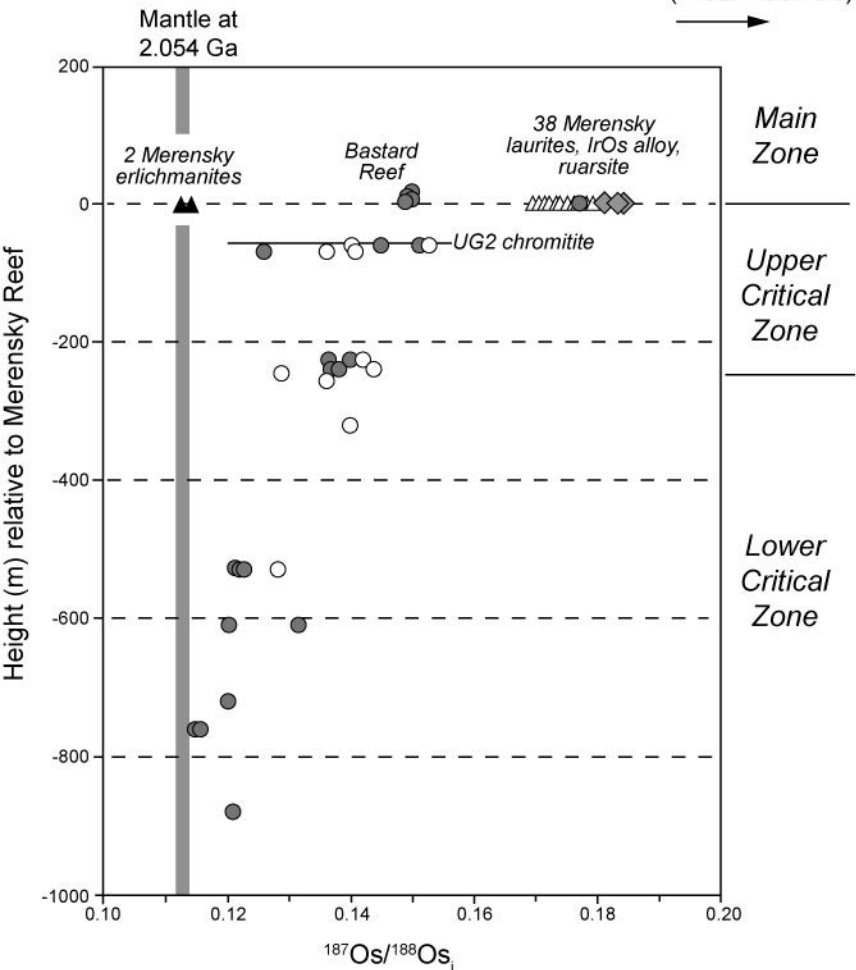








Crust at 2.054 Ga
($^{187}\text{Os}/^{188}\text{Os} \sim 0.5$)



△ Hart & Kinloch (1989) - laurite

▲ Hart & Kinloch (1989) - erlichmanite

● Schoenberg et al. (1999)

○ McCandless et al. (1999)

◆ Sandsloot pyroxenites-Platreef; Riesberg et al. (2011)

Table 1. Partition Coefficients

Element	<i>sulfide/silicate liquid</i>			<i>MSS/sulfide liquid</i>			<i>ISS/sulfide liquid</i>		<i>Refs</i>
	Experimental		Empirical	Experimental		Empirical	Experimental		
	min	max	MORB	min	max		min	max	
Ag	300	970	1138	0.01	0.11	0.38	0.19	1.2	1,2,10,11,24,25
As	0.3	15	25	0.02	0.5		0.11	0.24	1,10,11,24,25
Au	2360	11200	967	0.0038	0.09	0.1	0.21	1	1,2,3,4, 10,24,25
Bi	130	1130	316	0.003	0.0074		0.026	0.13	1,10, 11, 12, 24, 25
Cd	60	112	107			0.3-0.5			2,25
Co	20	114	45	0.92	1.6	1.6			1,2,10,17,22,25
Cu	330	2130	1334	0.06	0.36	0.07	1.00	2	1,2,4,9,10,12,15,16,17,18,19,20,21,23,24
Ir	48000	1900000	<i>11600</i>	2.3	14.7	3.8-13	0.05	0.22	4,5,10,11,15,16,18,19,20,21,22,24,25
Mo	0.1	3.46	1.2	2.1	2.9			1	
Ni	250	1700	776	0.36	1.72	1.1	0.1	0.9	1,2, 10,15, 16, 17, 18,19,20, 21,22,23,24
Os	10000	1140000	<i>24800</i>	2	23	3.4-11	0.06	0.53	4,5,10,11,16,23,24,25
Pb	10	93	57	0.001	0.049		0.05		1,2,9,10,11
Pd	57000	536000	<i>16735</i>	0.06	0.24	0.13	0.3	0.7	10, 11, 15, 16, 21, 22, 23
Pt	4830	3450000	<i>37300</i>	0.04	0.03	0.004	0.125	0.487	4,6,7,10,11, 15, 16, 21, 22,23
Re	20	200000	<i>870</i>	1.6	8.5	4.3-9	0.054	0.11	4, 8,10,11,22
Rh	25000	591000	24300	1	11	2.7-8.3	0.055	0.15	4, 10, 11, 15, 16, 21, 22, 23
Ru	97700	485000	<i>15500</i>	1	19	0.96	0.083	0.84	4, 10,11, 15, 16, 21, 22,23
Sb	1.4	67	3.6	0.002	0.017		0.029	0.142	1,2, 9, 10,11,12
Se	226	2339	345	0.5	0.75	0.4	0.83	1.2	9,10, 11,12, 23
Sn	2.7	8.6	11	<0.03	0.009		0.16		1, 10, 11
Te	1005	8789	4478	0.015	0.07		0.31	0.822	9, 10,11,12
Zn			3.5	0.36	0.62	0.02	3.9		10, 11

1. Li and Audéat (2012); 2 Kiseeva and Wood (2013); 3. Li and Audéat (2013); 4 Mungall and Brenan (2014); 5 Fonseca et al. (2011); 6. Fonseca (2009); 7. Prusest and Palme (2004); 8. Brenan (2008); 9 Brenan (2015); 10 Patten et al. (2013); 11. Liu and Brenan (2015); 12. Helmy et al. (2010); 13. Helmy et al. (2013a); 14. Helmy et al. (2013b); 15. Mungall et al. (2005); 16. Fleet et al. (1993); 17. Sinyakova and Kosyakov (2012); 18. Sinyakova and Kosyakov (2007); 19. Sinyakova and Kosyakov (2009) 20. Sinyakova and Kosyakov (2014); 21. Barnes et al. (1997a); 22. Ballhaus et al. (2001); 23. Brenan (2002); 24. Thériault and Barnes. (1997); 25. Barnes et al. (2006). Bold type indicates coefficients calculated using average MORB to estimate the silicate liquid composition because the concentrations in the glass were less than detection limit. Italics minimum partition coefficients, calculated using whole rock values to estimate the silicate liquid composition.

Table 2. The World's Major Platinum-group Element Resources

Host Intrusion	Deposit Name	Tons X 10 ⁶	Ni %	Cu %	Pt ppm	Pd ppm	Rh ppm	Au ppm	Type	Ref
<i>PGE dominated deposits</i>										
Bushveld	Merensky	3733	~0.2	~0.1	2.9	1.4	0.2	0.26	1	7
Bushveld	UG2	6636	~0.1	~0.01- 0.05	2.7	1.8	0.5	0.06	1	7
Bushveld	Platreef	3418	0.18	0.11	2.8	3.4			1	8
Great Dyke	Main Sulfide Zone	2136	~0.12	0.11	2.7	1.8	0.49	0.06	1	7
Sillwater	JM reef	149	0.1	0.07	3.7	12.9			2	9
Sillwater	JM reef	46			2.6	10.7			3	10
Lac des Iles	Roby+Offset	58	0.08	0.06	0.21	2.1		0.15	4	11
Lac des Iles	Roby+Offset	16	0.07	0.07	0.18	2.8		0.18	5	11
<i>Ni-Cu deposit with PGE by-product</i>										
Noril'sk- Talnakh	All deposits	1665	0.73	1.36	1.36	3.6		0.21	4	12
Noril'sk- Talnakh	All deposits	458	0.89	1.84	1	4.4		0.26	5	12
Sudbury	All deposits	1648	1.2	1.08	0.5	0.58	0.05	0.18	6	13

1. Measured, indicated and inferred; 2. Reserves and mineralized material; 3. Measured; 4. Measured and indicated; 5. Inferred; 6. Mined and reserves; 7. PGE+Au form D. Causey as quoted in Zientek (2012); Ni, Cu from Mudd (2012); 8. Mudd (2012); 9. Abott et al. as quoted in Zientek (2012); 10. Calculated using Sillwater web page www.stillwatermining.com - Investor presentation May 2015; 11. NAP web page Dec 2013 www.napalladium.com; 12. Norilsk Nickel web page for Dec 2013 www.nornick.ru; 13. Naldrett (2011)

Table 3. Metal Concentrations in the Base Metal Sulfide Minerals

Deposit	Ni %	Cu %	Re ppm	Os ppm	Ir ppm	Ru ppm	Rh ppm	Pt ppm	Pd ppm	Au ppm	Ref
<i>Pentlandite</i>											
Merensky	32.41	0.11	0.27	3.11	4.66	10.80	38.03	16.25	223	0.05	1
Platreef	34.40	0.02		0.59	1.20	5.16	15.00	0.45	119	0.01	2
MSZ	34.00	0.00	0.07	0.44	1.09	4.39	5.72	0.05	24	0.02	3
JM	29.56	0.25	0.11	8.69	10.31	33.64	134.2	1.54	8782	0.01	4
Roby & Twilight	34.28	0.20	0.10	0.08	0.03	0.12	0.29	0.25	522	0.00	5
Noril'sk 1	31.20	0.05	0.27	0.82	2.52	8.50	28.55	11.88	296	0.50	6
McCreedy	34.32	0.07	0.05	0.02	0.02	0.25	0.04	0.01	6	0.01	7
<i>Pyrrhotite</i>											
Merensky	0.30	0.02	0.23	3.82	3.34	5.21	1.13	0.98	1.33	0.06	1
Platreef	0.51	0.00		0.93	1.80	7.81	0.45	0.61	0.06	0.01	2
MSZ	0.28	0.00	0.13	0.39	1.22	4.14	2.25	0.86	1.24	0.01	3
JM	0.29	0.06	0.04	0.21	0.72	1.32	0.36	0.03	24.04	0.01	4
Roby & Twilight	0.82	0.14	0.12	0.11	0.03	0.23	0.45	0.28	0.78	0.01	5
Noril'sk1	0.14	0.00	0.40	1.26	4.08	11.30	46.91	10.24	0.36	0.06	6
McCreedy	0.66	0.00	0.06	0.02	0.02	0.04	0.02	0.01	0.02	0.00	7
<i>Chalcopyrite/Cubanite</i>											
Merensky	0.19	33.84	0.06	0.30	0.30	<0.2	0.21	0.70	6.51	0.04	1
Platreef	0.06	28.20						1.31	0.54	0.01	2
JM	0.06	33.00	0.01	0.08	0.03	0.00		1.74	1.04	0.01	3
MSZ	0.07	30.26	0.01	0.07	0.10	0.36	0.17	0.04	4.24	0.01	4
Roby & Twilight	0.01	34.50	<0.02	<0.02	<0.01	0.06	<13	<0.01	0.17	<0.01	5
Noril'sk 1	0.11	28.09	0.01	<.01	<0.01	0.25	<13	0.30	4.30	0.02	6
McCreedy	0.02	35.07	0.02	0.01	0.003	0.24	<10	0.01	1.15	0.01	7
<i>Pyrite</i>											
Roby primary	0.66	0.01	0.17	0.10	0.03	0.20	0.52	0.45	1.15	0.07	5
Roby altered	0.35	0.04	0.05	0.04	0.01	0.06	0.14	2.16	1.86	0.09	5
McCreedy primary	0.04	0.002	0.08	0.26	1.07	1.80	31.76	0.12	0.02	0.03	7
McCreedy altered	0.03	0.000	0.06	<0.01	0.01	0.04	0.09	<0.01	<0.02	0.004	7

1. Godel et al. (2007); 2. Holwell and McDonald (2007); 3. Godel and Barnes (2008); 4. Barnes et al. (2008); 5. Djon and Barnes (2012); 6. This work ;7. Dare et al. (2011)

MSZ = Main sulfide zone

Table 4. Metal Concentrations in Platinum-group Element Deposits

		S	Ni	Cu	Os	Ir	Ru	Rh	Pt	Pd	Au	Ref
		%	%	%	ppb	ppb	ppb	ppb	ppb	ppb	ppb	
<i>Intrusion</i>	<i>Deposit</i>	<i>PGE-dominated deposits</i>										
Bushveld	Merensky	0.42	0.17	0.09	63	74	430	240	3740	1530	310	1
Bushveld	Merensky chromite	0.41	0.34	0.09	715	1264	6140	2665	37320	4173	339	2
Bushveld	UG2	0.05	0.10	0.004	114	185	673	600	3397	1882	5	3
Bushveld	Platreef	0.47	0.18	0.10	20	20	67	76	1000	1166	120	4
Stillwater	JM	0.29	0.17	0.07	na	25	72	190	6800	22000	600	5
Great Dyke	MSZ	0.52	0.18	0.11	23	78	165	198	2079	1912	273	6
Lac des Iles	Roby& Twilight	0.53	0.12	0.16	0.98	0.41	2.48	4	365	3031	290	7
<i>Intrusion</i>	<i>Sulfide type</i>	<i>Ni-Cu sulfide deposits</i>										
Karaelakh	Disseminated	2.97	0.35	1.32	2.9	5.0	15	44	758	2716	364	8
Karaelakh	Cu-poor	34.51	4.08	5.20	61.5	70.6	215	647	2195	10950	158	8
Karaelakh	Cu-rich	32.47	2.75	23.78	3.8	3.9	10	51	27275	71583	3622	8
Karaelakh	Vein./ breccia	30.59	2.34	28.40	nd	0.9	5	18	23079	33500	1838	8
Karaelakh	Hornfels	7.41	0.84	4.00	nd	0.3	1	4	2300	9100	500	8
Karaelakh	Upper	0.26	0.04	0.06	nd	3.6	10	29	250	555		8
Talnakh	Disseminated	3.27	0.55	1.11	10.0	9.7	27	85	736	2668	260	8
Talnakh	Cu-poor	30.38	4.43	3.22	391	361	1376	2700	1858	9403	110	8
Talnakh	Cu-rich	12.00	0.99	12.00	nd	5.0	5	5	3900	30000	630	8
Talnakh	Hornfels	17.80	2.54	2.00	nd	237	797	1570	740	4030	100	8
Talnakh	Vein	9.28	0.79	2.38	80.0	20.0	290	40	1880	6830	490	8
Noril'sk 1	Dissminated	2.09	0.48	1.06	15.2	45.7	115	431	4741	14381	519	8
Noril'sk 1	Cu-rich	32.81	6.82	25.70	2.4	6.0	16	282	103000	297500	5231	8
Noril'sk 1	Upper	0.45	0.06	0.13	0.8	9.3	28	110	280	1300	nd	8
Sudbury	Dissminated	1.03	0.11	0.11	2.8	6.8	17	17	73	153	40	9
Sudbury	McCreedy Cu-poor	31.60	4.36	1.63	14.2	34.7	37	106	883	1152	19	9
Sudbury	McCreedy Cu-rich	31.50	3.84	25.00	0.5	0.1	1	10	9491	17988	1823	9

1. SARM-7 Steele et al. (1975); 2. Barnes and Maier (2002b); 3. Maier and Barnes (2008); 4. Calculated form grade at Mogalakena mine [www.angloplatinum.com/pdf/Reserves and Resources 2011.pdf](http://www.angloplatinum.com/pdf/Reserves%20and%20Resources%202011.pdf); 5. Zientek pers. com.; 6. Oberthür (2002); 7. Barnes and Gomwe (2011); 8. Zientek et al. (1994) and Barnes et al. (1997b); 9. Dare et al. (2011), (2014)

Table 5. Concentrations of As, Bi, Sb, Sn and Te in the Deposits

	As	Bi	Sb	Sn	Te	Ref
	ppm	ppm	ppm	ppm	ppm	
<i>PGE-dominated Deposits</i>						
Merensky n=19	0.30	0.39	0.02	n.a.	0.60	1
UG2 n=13	<0.5	n.a.	<0.02	n.a.	n.a.	2
JM reef n=6	0.34	0.26	0.04	0.20	2.40	3
Lac des Iles n=27	0.30	0.20	0.12	n.a.	0.72	4
<i>Ni-Cu Sulfide Deposits</i>						
Type of sulfide	Karaelakh Intrusion					
Diss n=21	0.57	2.07	0.35	4.70	2.28	5
Cu-poor n=29	0.21	0.28	0.13	1.07	1.01	5
Cu-rich n=8	7.36	11.31	1.51	35.01	33.73	5
Vein n=2	4.10	3.94	0.73	22.35	14.00	5
Hornfels n=1	0.44	1.50	0.33	5.60	2.20	5
Talnakh Intrusion						
Diss n=11	0.52	1.21	0.27	2.45	2.10	5
Cu-poor n=7	1.15	0.19	0.24	0.99	1.03	5
Cu-rich n=1	1.30	3.30	0.60	4.50	n.a.	5
Hornfels n=1	0.45	0.27	0.18	0.87	0.99	5
Noril'sk 1						
Diss n=14	0.49	1.46	0.25	1.35	1.50	5
Cu-poor n=1	1.90	1.10	0.12	2.20	11	5
Cu-rich n=4	5.95	5.70	0.51	16.04	113	5
McCreedy East						
Diss n=1	2.20	0.95	10.00	19.10	0.35	6
Cu-poor n=5	2.40	1.70	<0.06	1.50	2.10	6
Cu-rich n=9	9.20	68.70	0.37	87.70	87	6
<i>Reference</i>						
Black Shale	45	0.4	1.6	3.5	0.19	7
MORB	0.11	0.01	0.014	1.00	0.005	8

1. Average of Rustenburg and Impala Mines samples from Barnes and Maier (2002b), Godel et al. (2007); 2. Maier and Barnes (2008); 3. Average of East Boulder and Sillwater mine samples from Godel and Barnes (2008); 4. Average of Roby and Twilight Zone samples from Barnes and Gomwe (2011) and Hinchey and Hartori (2005); 5. Zientek et al. (1994); 6. Dare et al. (2011), (2014); 7. Henrique-Pinto; 8. Arevalo and McDonough (2010)